

# Pre-inflation & CMB Power Loss



[arXiv: 1309.3413]

[arXiv: 1404.xxxx]

## Francisco Gil Pedro



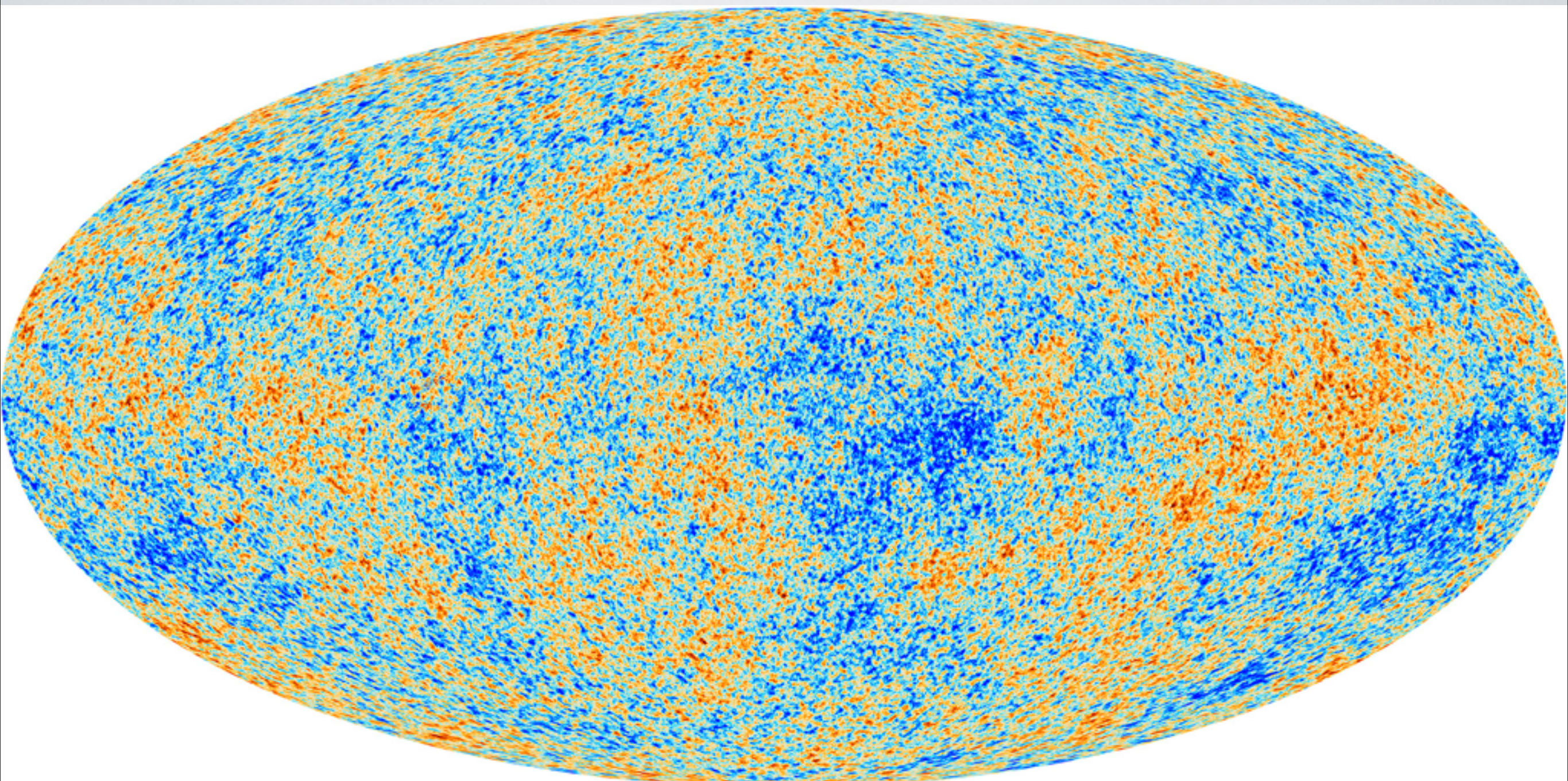
in collaboration with:  
Michele Cicoli, Bhaskar Dutta,  
Sean Downes, and Alexander Westphal

# Outline:

- ▶ Inflation in 2014
- ▶ The standard inflationary picture
- ▶ The spectrum of slow-roll inflation
- ▶ Observational hints for power loss
- ▶ Slow-roll steepening
- ▶ Pre-inflation
- ▶ Universality in power loss
- ▶ Summary

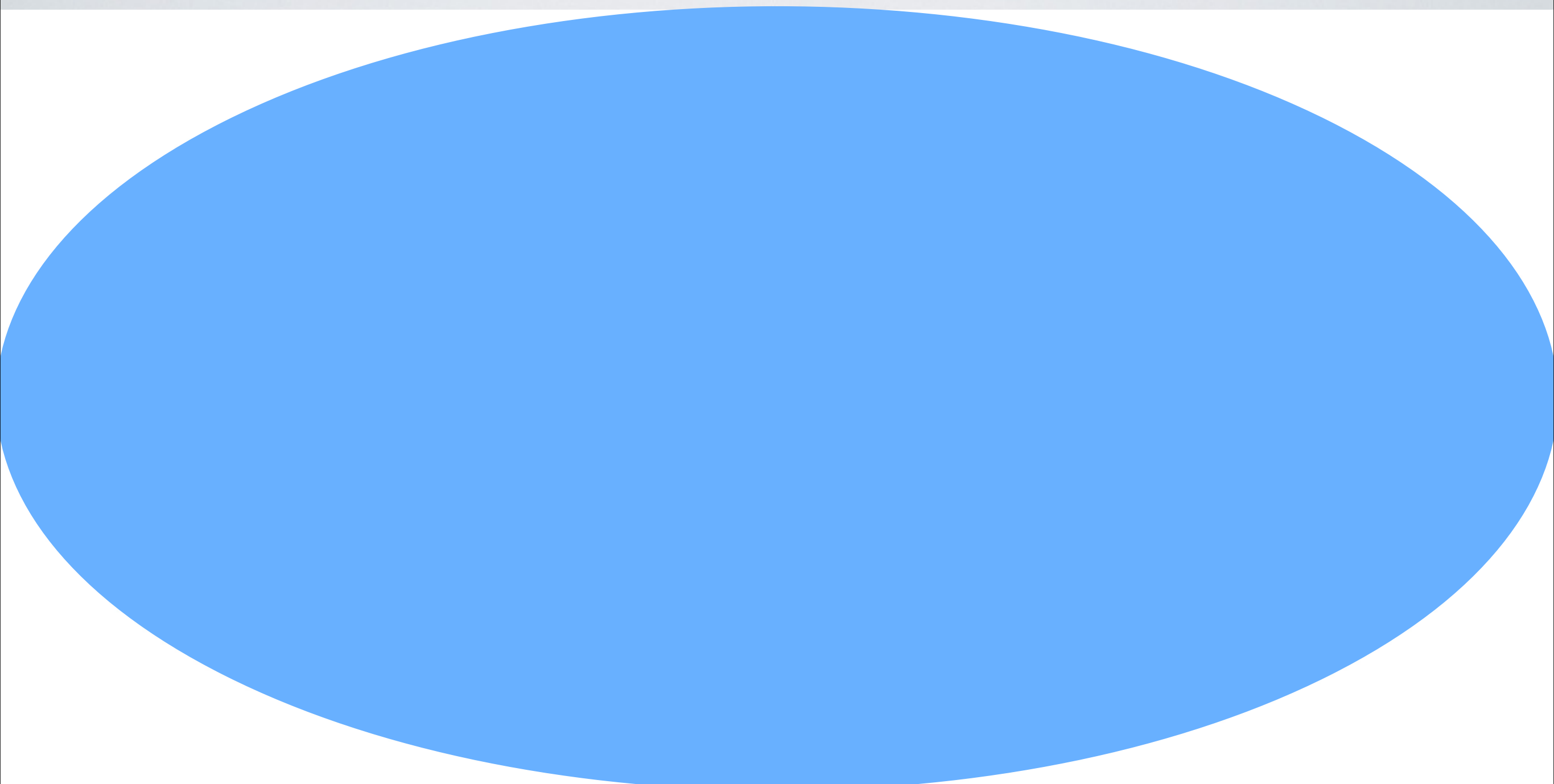
# Inflation in 2014

Planck 2013



# Inflation in 2014

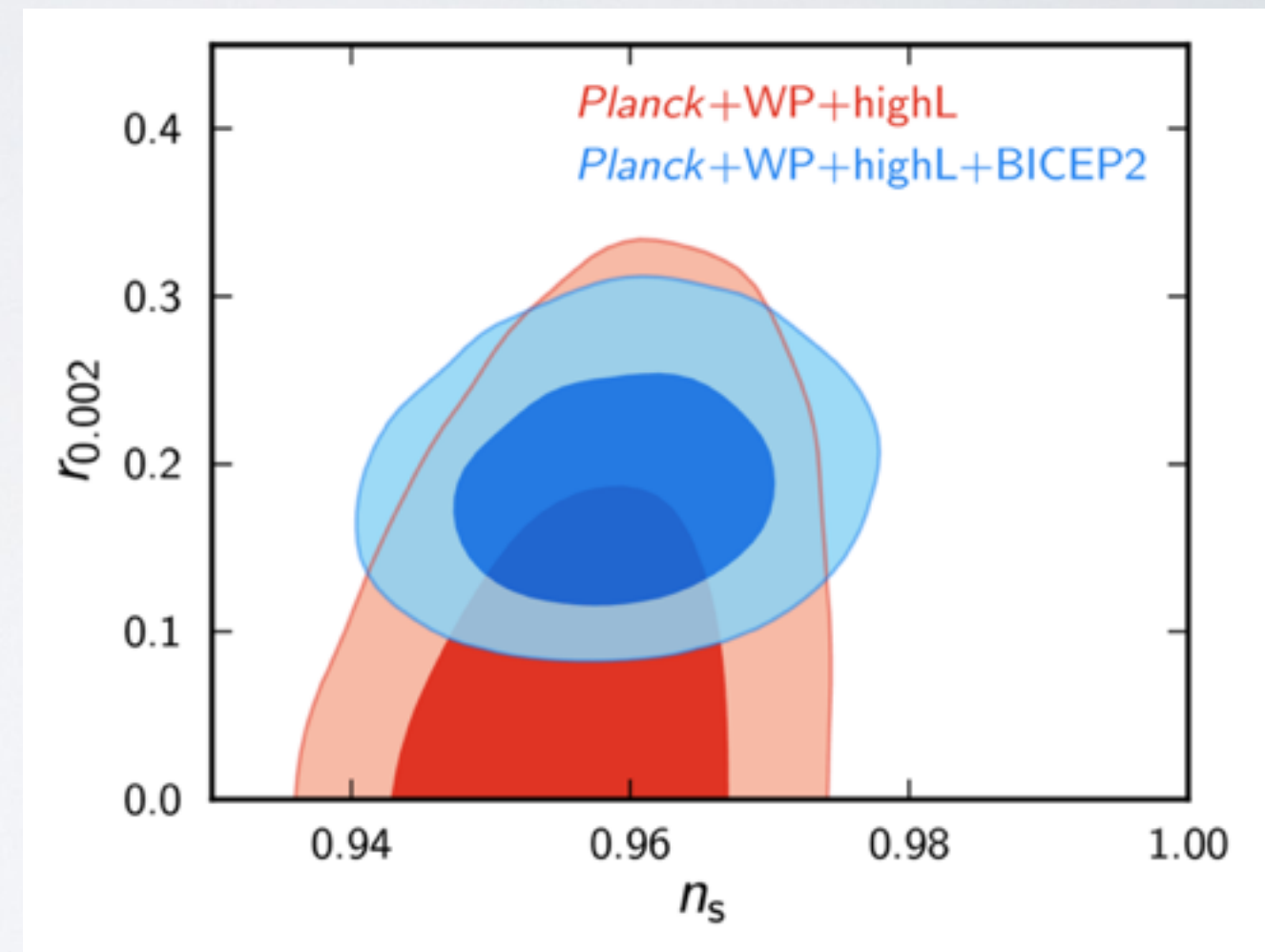
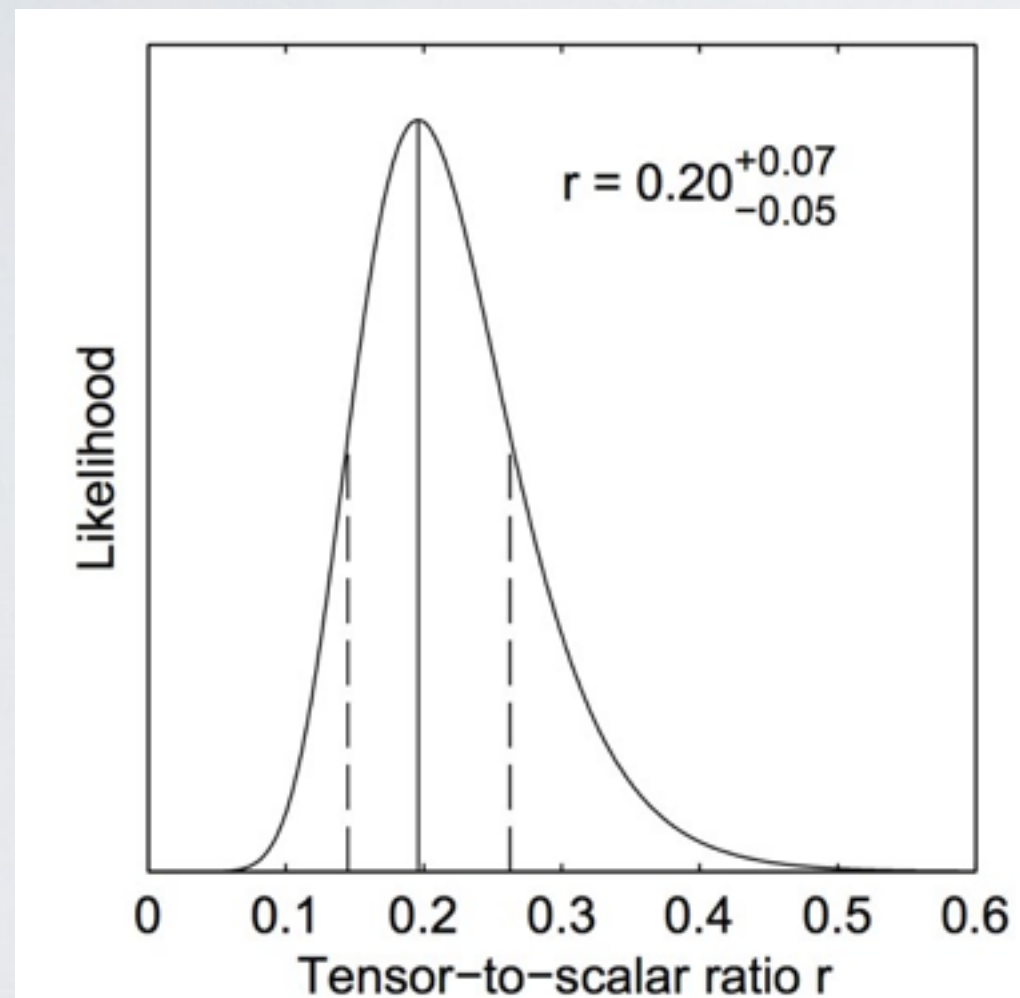
Planck 2013



# Inflation in 2014

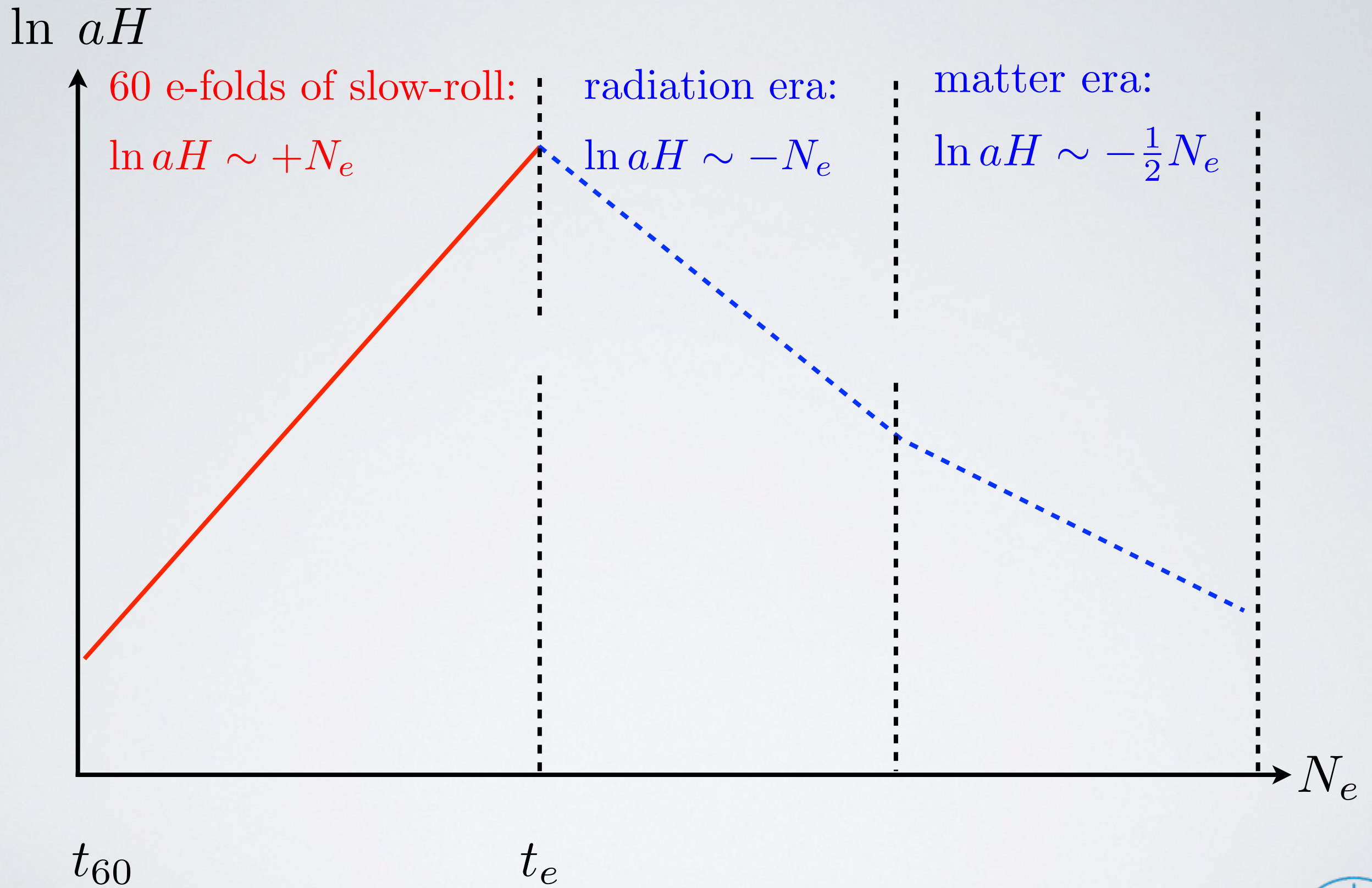
Claimed detection of primordial gravitational waves

BICEP II 2014

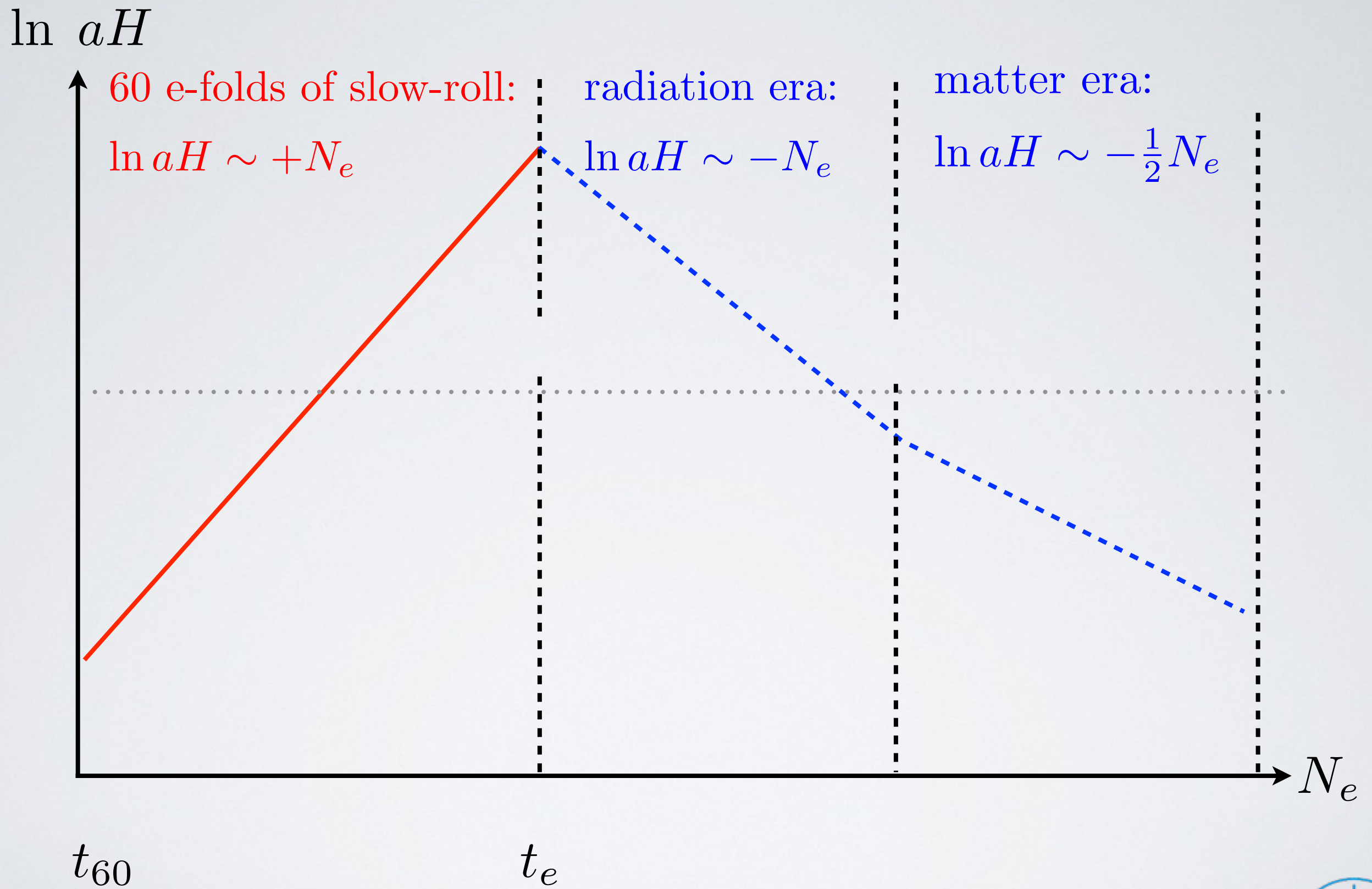


Awaiting confirmation by Planck's B-mode analysis

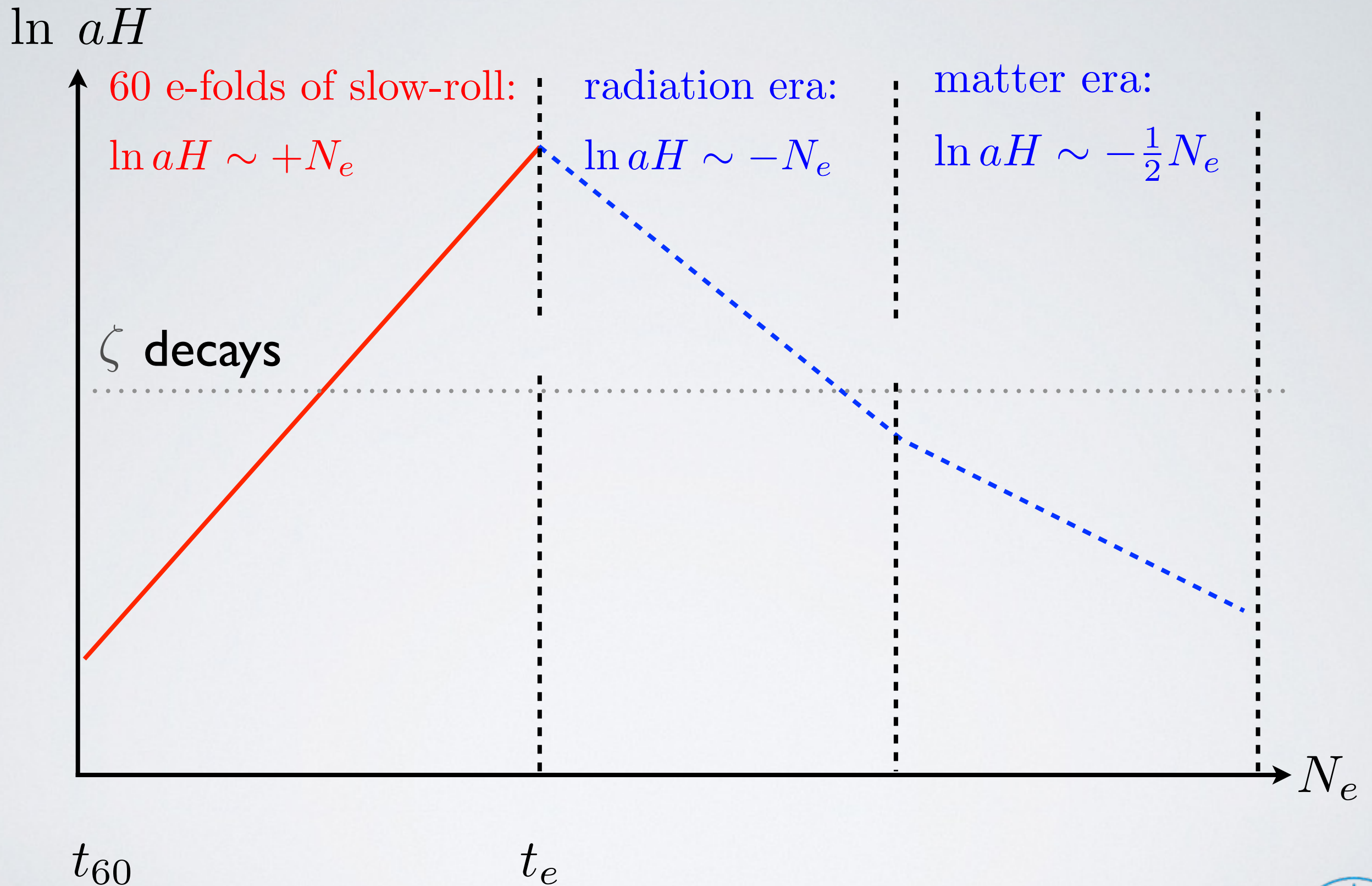
# The standard picture



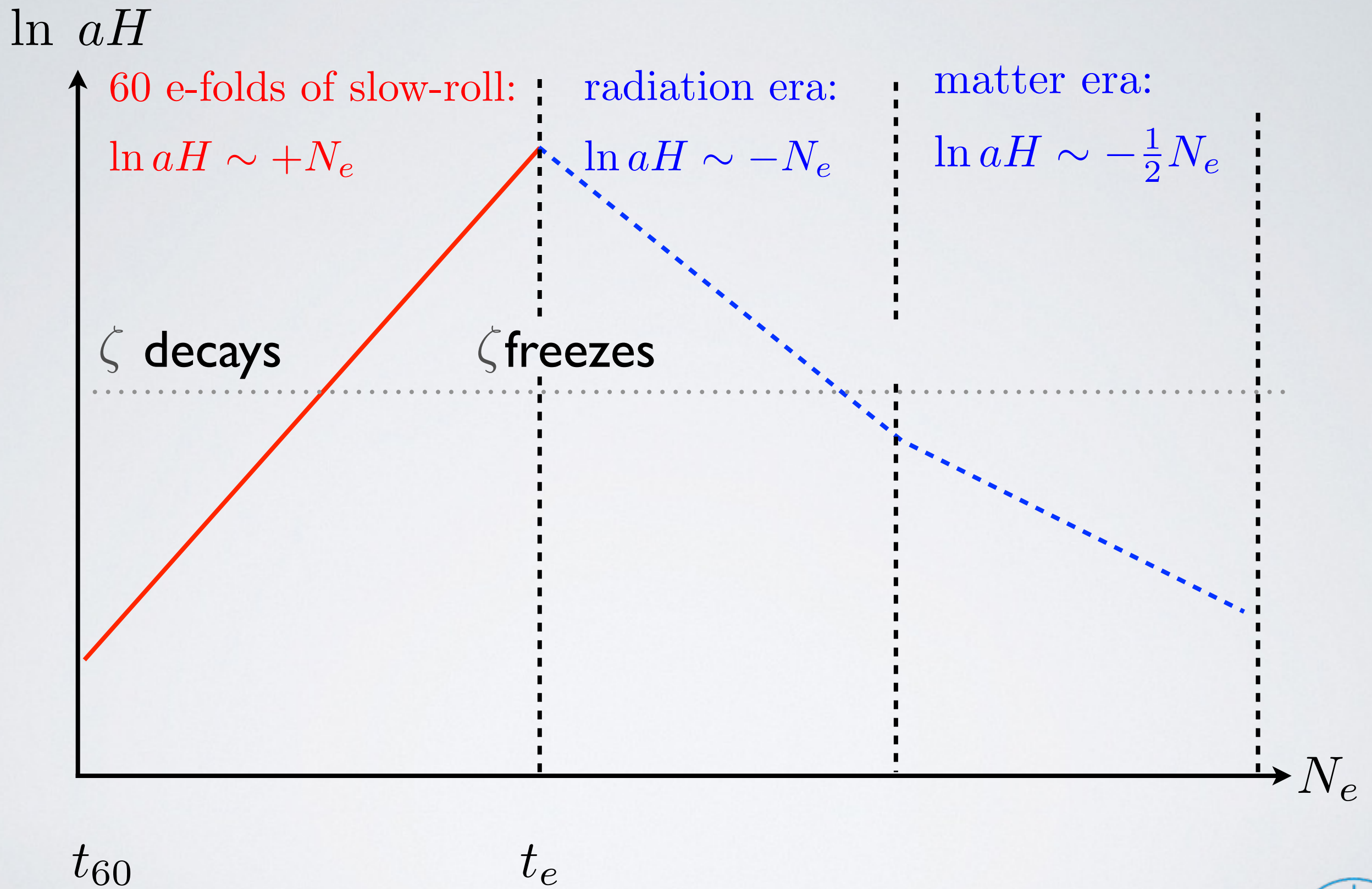
# The standard picture



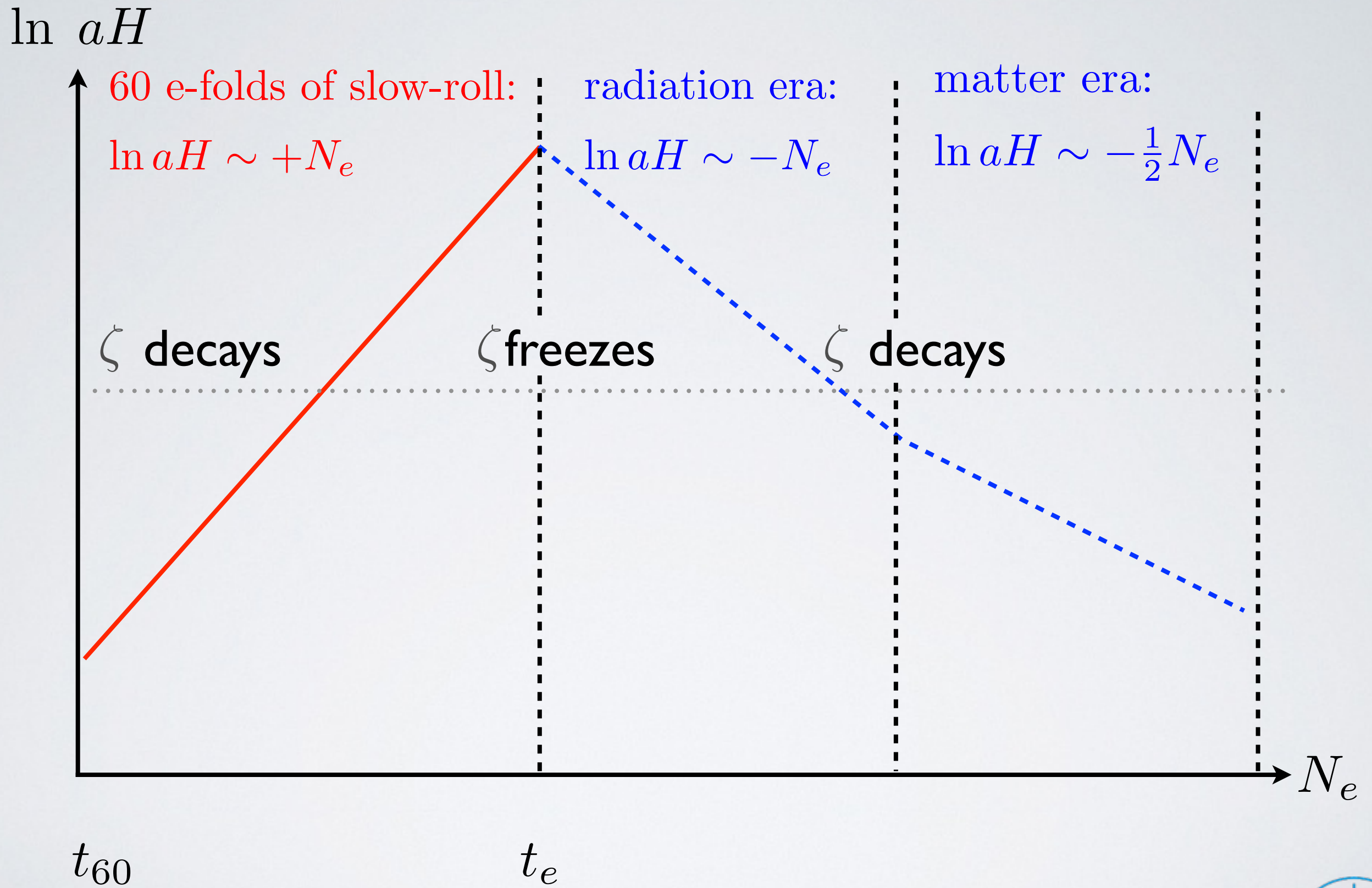
# The standard picture



# The standard picture



# The standard picture



# The Mukhanov-Sasaki Equation

curvature perturbation:  $\zeta$        $u \equiv \zeta z$       with     $z \equiv a\sqrt{2\epsilon_H}$

$$u'' + \left( k^2 - \frac{z''}{z} \right) u = 0$$

Useful to use efolds as ‘time’ coordinate

Assume background of the form:

$$aH \sim e^{\xi N}$$

inflation:

$$\xi = 1 + \mathcal{O}(\epsilon_H, \eta_H)$$

$$u_{\alpha\alpha} + \xi u_\alpha + \left\{ \left( \frac{k}{aH} \right)^2 - (1 + \xi) \right\} u = 0$$

# The Mukhanov-Sasaki Equation

Behaviour of curvature pert. depends on  $L_{hor} \equiv H^{-1}$

during inflation:

$k > aH \leftrightarrow \lambda_{phys} < H^{-1}$  **inside** horizon,  $\zeta$  **decays**

$k < aH \leftrightarrow \lambda_{phys} > H^{-1}$  **outside** horizon,  $\zeta$  **freezes**

$$u = C^{(1)} \frac{1}{\sqrt{\xi a H}} H_\nu^{(1)} \left( \frac{k}{\xi a H} \right) + C^{(2)} \frac{1}{\sqrt{\xi a H}} H_\nu^{(2)} \left( \frac{k}{\xi a H} \right)$$

$C^{(1)}, C^{(2)}$  set by ics/vacuum choice

$$\nu = \left| \frac{2 + \xi}{2\xi} \right|$$

# The spectrum of slow-roll inflation

deep inside horizon       $\lambda_{phys} \ll H^{-1}$  modes do not feel curvature

# The spectrum of slow-roll inflation

deep inside horizon       $\lambda_{phys} \ll H^{-1}$  modes do not feel curvature

flat space mode functions

**Bunch-Davis bcs:**

$$C^{(1)} = \sqrt{\pi/2}$$

$$C^{(2)} = 0$$

# The spectrum of slow-roll inflation

deep inside horizon       $\lambda_{phys} \ll H^{-1}$  modes do not feel curvature

flat space mode functions

**Bunch-Davis bcs:**

$$C^{(1)} = \sqrt{\pi/2}$$

$$C^{(2)} = 0$$



$$u = \frac{\sqrt{\pi/2}}{\sqrt{aH}} H_\nu^{(1)} \left( \frac{k}{aH} \right)$$

$$\nu = \frac{3}{2} + \epsilon_H + \frac{1}{2}\eta_H$$

$$\xi = 1 + \mathcal{O}(\epsilon_H, \eta_H)$$

# The spectrum of slow-roll inflation

deep inside horizon       $\lambda_{phys} \ll H^{-1}$  modes do not feel curvature

flat space mode functions

**Bunch-Davis bcs:**

$$C^{(1)} = \sqrt{\pi/2}$$

$$C^{(2)} = 0$$



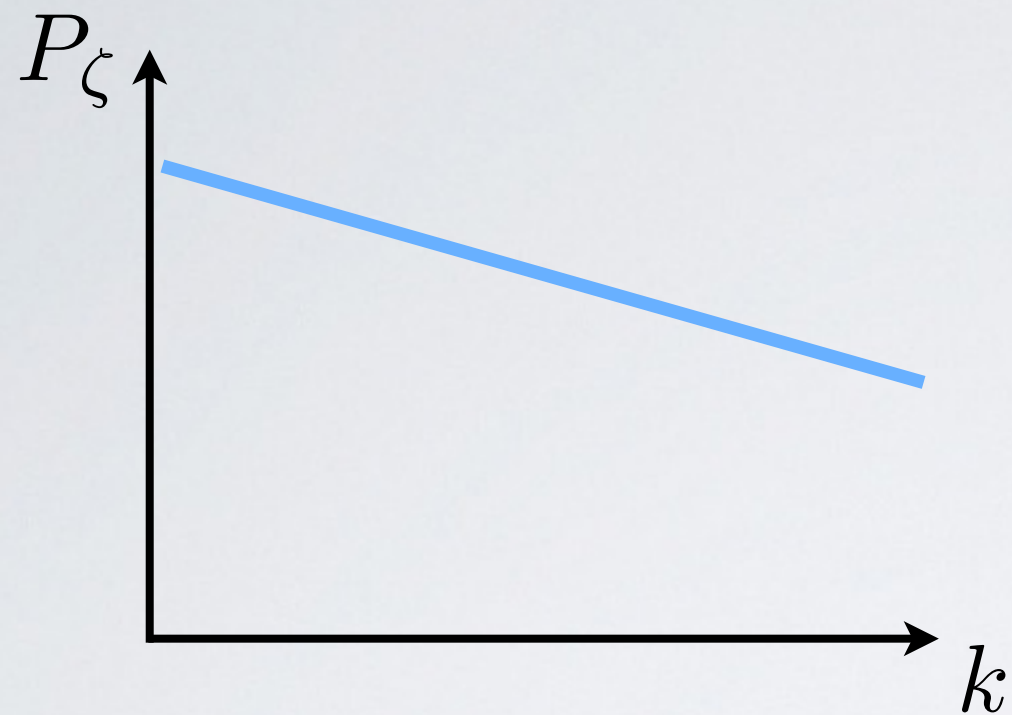
$$u = \frac{\sqrt{\pi/2}}{\sqrt{aH}} H_\nu^{(1)} \left( \frac{k}{aH} \right)$$

$$\nu = \frac{3}{2} + \epsilon_H + \frac{1}{2}\eta_H$$

$$\xi = 1 + \mathcal{O}(\epsilon_H, \eta_H)$$

$$P_k \equiv k^3 \left| \frac{u}{z} \right|^2 \sim \frac{H^2}{\epsilon_H} k^{3-2\nu}$$

# The spectrum of slow-roll inflation



Planck XXII:

$$n_s = 0.9603 \pm 0.0073$$

$$\ln(10^{10} A_s) = 3.089_{-0.027}^{+0.024}$$

$$P_k = A_s \left( \frac{k}{k_*} \right)^{n_s - 1}$$

$$k_* = 0.002 \text{ Mpc}^{-1}$$

Scale invariance is excluded by more than  $5\sigma$

# Observational hints for power-loss

Astronomy & Astrophysics manuscript no. 0\_Like\_top  
26th March 2013

© ESO 2013

## Planck 2013 results. XV. CMB power spectra and likelihood

Planck Collaboration: P. A. R. Ade<sup>39</sup>, N. Aghanim<sup>62</sup>, C. Armitage-Caplan<sup>94</sup>, M. Arnaud<sup>36</sup>, M. Ashdown<sup>73,6</sup>, F. Atrio-Barandela<sup>39</sup>, J. Aumont<sup>62</sup>, C. Baccigalupi<sup>38</sup>, A. J. Banday<sup>97,10</sup>, R. B. Barreiro<sup>70</sup>, J. G. Bartlett<sup>1,71</sup>, E. Battaner<sup>26</sup>, K. Benabed<sup>63,96</sup>, A. Benoit<sup>60</sup>, A. Benoit-Lévy<sup>26,63,96</sup>, J.-P. Bernard<sup>10</sup>, M. Bersanelli<sup>16,82</sup>, P. Bielewicz<sup>97,10,88</sup>, J. Bobin<sup>36</sup>, J. J. Bock<sup>71,11</sup>, A. Bonaldi<sup>72</sup>, L. Bonavera<sup>30</sup>, J. R. Bond<sup>9</sup>, J. Boerill<sup>14,91</sup>, F. R. Boucher<sup>63,94</sup>, F. Boulanger<sup>62</sup>, M. Bridges<sup>73,6,68</sup>, M. Bucher<sup>1</sup>, C. Burigana<sup>51,34</sup>, R. C. Butler<sup>51</sup>, E. Calabrese<sup>64</sup>, J.-P. Cardoso<sup>71,183</sup>, A. Catalano<sup>78,79</sup>, A. Challinor<sup>66,73,12</sup>, A. Chamballu<sup>26,16,62</sup>, L.-Y. Chiang<sup>63</sup>, H. C. Chiang<sup>28,7</sup>, P. R. Christensen<sup>84,40</sup>, S. Church<sup>93</sup>, D. L. Clements<sup>38</sup>, S. Colombo<sup>63,96</sup>, L. P. L. Colombo<sup>25,71</sup>, C. Combet<sup>79</sup>, F. Couchot<sup>79</sup>, A. Coulais<sup>73</sup>, B. P. Crill<sup>71,87</sup>, A. Curto<sup>5,70</sup>, F. Cuttaia<sup>51</sup>, L. Danese<sup>48</sup>, R. D. Davies<sup>72</sup>, R. J. Davis<sup>72</sup>, P. de Bernardis<sup>35</sup>, A. de Rosa<sup>51</sup>, G. de Zotti<sup>21,39</sup>, J. Delabrouille<sup>1</sup>, J.-M. Delouis<sup>63,96</sup>, F.-X. Désert<sup>15</sup>, C. Dickinson<sup>72</sup>, J. M. Diego<sup>70</sup>, H. Dole<sup>62,61</sup>, S. Donzelli<sup>52</sup>, O. Doré<sup>71,11</sup>, M. Douspis<sup>62</sup>, J. Dunkley<sup>61</sup>, X. Dupac<sup>43</sup>, G. Efstathiou<sup>66</sup>, P. Elsner<sup>63,96</sup>, T. A. Enßlin<sup>81</sup>, H. K. Eriksen<sup>68</sup>, F. Finelli<sup>51,53</sup>, O. Forni<sup>97,10</sup>, M. Frailis<sup>50</sup>, A. A. Fraisse<sup>28</sup>, E. Franceschi<sup>51</sup>, T. C. Gaier<sup>71</sup>, S. Galeotta<sup>50</sup>, S. Galli<sup>63</sup>, K. Gangar<sup>1</sup>, M. Giard<sup>37,10</sup>, G. Giardino<sup>64</sup>, Y. Giraud-Héraud<sup>1</sup>, E. Gjerløw<sup>68</sup>, J. González-Nuevo<sup>70,88</sup>, K. M. Góeski<sup>71,100</sup>, S. Gratton<sup>73,66</sup>, A. Gregorio<sup>37,50</sup>, A. Gruppuso<sup>51</sup>, J. E. Guðmundsson<sup>26</sup>, F. K. Hansen<sup>68</sup>, D. Hanson<sup>82,71,9</sup>, D. Harrison<sup>66,73</sup>, G. Helou<sup>11</sup>, S. Henrot-Versillé<sup>74</sup>, C. Hernández-Monteagudo<sup>13,81</sup>, D. Herranz<sup>20</sup>, S. R. Hildebrandt<sup>21</sup>, E. Hivon<sup>63,96</sup>, M. Hobson<sup>6</sup>, W. A. Holmes<sup>71</sup>, A. Hornstrup<sup>17</sup>, W. Hovest<sup>81</sup>, K. M. Huffenberger<sup>69</sup>, G. Hurier<sup>62,78</sup>, T. R. Jaffe<sup>97,10</sup>, A. H. Jaffe<sup>68</sup>, J. Jewell<sup>71</sup>, W. C. Jones<sup>28</sup>, M. Juvela<sup>27</sup>, E. Keihänen<sup>27</sup>, R. Keskitalo<sup>23,14</sup>, K. Kiiveri<sup>27,47</sup>, T. S. Kisner<sup>80</sup>, R. Kneissl<sup>42,8</sup>, J. Knoche<sup>81</sup>, L. Knox<sup>30</sup>, M. Kunz<sup>18,62,3</sup>, H. Kurki-Suonio<sup>27,47</sup>, G. Lagache<sup>62</sup>, A. Lähteenmäki<sup>2,47</sup>, J.-M. Lamarre<sup>79</sup>, A. Lasenby<sup>53</sup>, M. Lattanzi<sup>64</sup>, R. J. Laureijs<sup>64</sup>, C. R. Lawrence<sup>71</sup>, M. Le Jeune<sup>1</sup>, S. Leach<sup>48</sup>, J. P. Leahy<sup>72</sup>, R. Leonardi<sup>43</sup>, J. León-Tavares<sup>65,2</sup>, J. Lesgourgues<sup>95,87</sup>, M. Liguori<sup>73</sup>, P. B. Lilje<sup>68</sup>, V. Lindholm<sup>27,47</sup>, M. Linden-Vørnle<sup>17</sup>, M. López-Caniego<sup>70</sup>, P. M. Lubin<sup>31</sup>, J. F. Macías-Pérez<sup>79</sup>, B. Maffei<sup>72</sup>, D. Maino<sup>66,52</sup>, N. Mandelis<sup>51,5,34</sup>, D. Marinucci<sup>19</sup>, M. Maris<sup>50</sup>, D. J. Marshall<sup>76</sup>, P. G. Martin<sup>9</sup>, E. Martínez-González<sup>70</sup>, S. Masi<sup>35</sup>, S. Matamese<sup>31</sup>, F. Matthai<sup>81</sup>, P. Mazzotta<sup>28</sup>, P. R. Meinhold<sup>31</sup>, A. Melchiorri<sup>33,34</sup>, L. Mendes<sup>43</sup>, E. Menegoni<sup>35</sup>, A. Mennella<sup>36,52</sup>, M. Migliaccio<sup>66,73</sup>, M. Millea<sup>50</sup>, S. Mitra<sup>57,71</sup>, M.-A. Miville-Deschénes<sup>62,9</sup>, D. Molinari<sup>51</sup>, A. Moneti<sup>63</sup>, L. Montier<sup>67,10</sup>, G. Morgante<sup>21</sup>, D. Mortlock<sup>28</sup>, A. Moss<sup>60</sup>, D. Munshi<sup>39</sup>, P. Naselsky<sup>64,40</sup>, F. Natoli<sup>35</sup>, P. Natoli<sup>34,4,51</sup>, C. B. Netterfield<sup>21</sup>, H. U. Nørgaard-Nielsen<sup>17</sup>, F. Noviello<sup>72</sup>, D. Novikov<sup>58</sup>, I. Novikov<sup>54</sup>, L. J. O'Dwyer<sup>71</sup>, F. Orioux<sup>63</sup>, S. Osborne<sup>69</sup>, C. A. Oxborrow<sup>17</sup>, P. Paci<sup>69</sup>, L. Pagano<sup>35,54</sup>, F. Pajot<sup>62</sup>, R. Paladini<sup>29</sup>, D. Paoletti<sup>51,53</sup>, B. Partridge<sup>46</sup>, F. Pasian<sup>50</sup>, G. Patanchon<sup>1</sup>, P. Paykari<sup>76</sup>, O. Perdereau<sup>74</sup>, L. Perotto<sup>76</sup>, F. Perrotta<sup>68</sup>, F. Piacentini<sup>35</sup>, M. Piat<sup>1</sup>, E. Pierpaoli<sup>25</sup>, D. Pietrobon<sup>71</sup>, S. Ptaszczyński<sup>24</sup>, E. Pointecouteau<sup>97,10</sup>, G. Polenta<sup>6,69</sup>, N. Ponthieu<sup>62,35</sup>, L. Popa<sup>64</sup>, T. Poutanen<sup>61,27,2</sup>, G. W. Pratt<sup>76</sup>, G. Prézeau<sup>31,71</sup>, S. Prunet<sup>63,96</sup>, J.-L. Puget<sup>62</sup>, J. P. Rachén<sup>22,81</sup>, A. Rahlin<sup>78</sup>, R. Rebolo<sup>69,13,41</sup>, M. Reinecke<sup>81</sup>, M. Remazeilles<sup>62,1</sup>, C. Renault<sup>78</sup>, S. Ricciardi<sup>21</sup>, T. Riller<sup>81</sup>, C. Ringeval<sup>10,7,63,96</sup>, L. Ristorcelli<sup>97,70</sup>, G. Rocha<sup>21,11</sup>, C. Rosset<sup>1</sup>, G. Roudier<sup>3,73,71</sup>, M. Rowan-Robinson<sup>58</sup>, J. A. Rubiño-Martín<sup>60,41</sup>, B. Rusholme<sup>39</sup>, M. Sandri<sup>21</sup>, L. Sanselme<sup>78</sup>, D. Santos<sup>78</sup>, G. Savini<sup>16</sup>, D. Scott<sup>24</sup>, M. D. Seiffert<sup>71,11</sup>, E. P. S. Shellard<sup>12</sup>, L. D. Spencer<sup>39</sup>, J.-L. Starck<sup>26</sup>, V. Stolyarov<sup>6,73,92</sup>, R. Stompor<sup>1</sup>, R. Sudilovska<sup>79</sup>, F. Sureau<sup>26</sup>, D. Sutton<sup>66,73</sup>, A.-S. Suur-Uski<sup>27,47</sup>, J.-F. Sygnet<sup>63</sup>, J. A. Tauber<sup>44</sup>, D. Tavagnacco<sup>50,37</sup>, L. Terenzi<sup>21</sup>, L. Toffolatti<sup>20,70</sup>, M. Tomasi<sup>52</sup>, M. Tristram<sup>74</sup>, M. Tucci<sup>18,74</sup>, J. Tuovinen<sup>83</sup>, M. Türler<sup>56</sup>, L. Valenziano<sup>21</sup>, J. Valiviita<sup>27,27,68</sup>, B. Van Tent<sup>79</sup>, J. Varis<sup>83</sup>, P. Vielva<sup>70</sup>, F. Villa<sup>21</sup>, N. Vittorio<sup>38</sup>, L. A. Wade<sup>71</sup>, B. D. Wandelt<sup>63,96,32</sup>, I. K. Wehus<sup>71</sup>, M. White<sup>79</sup>, S. D. M. White<sup>81</sup>, D. Yvon<sup>16</sup>, A. Zacchei<sup>50</sup>, and A. Zonca<sup>21</sup>

(Affiliations can be found after the references)

Preprint online version: 26th March 2013

### Abstract

This paper presents the *Planck* likelihood, a complete statistical description of the two-point correlation function of the CMB temperature fluctuations that accounts for all known relevant uncertainties, both instrumental and astrophysical in nature. We use this likelihood to derive our best estimate of the CMB angular power spectrum from *Planck* over three decades in multipole moment,  $\ell$ , covering  $2 \leq \ell \leq 2500$ . The main source of error at  $\ell \leq 1500$  is cosmic variance. Uncertainties in small-scale foreground modelling and instrumental noise dominate the error budget at higher  $\ell$ s. For  $\ell < 50$ , our likelihood exploits all *Planck* frequency channels from 30 to 353 GHz, separating the cosmological CMB signal from diffuse Galactic foregrounds through a physically motivated Bayesian component separation technique. At  $\ell \geq 50$ , we employ a correlated Gaussian likelihood approximation based on a fine-grained set of angular cross-spectra derived from multiple detector combinations between the 100, 143, and 217 GHz frequency channels, marginalizing over power spectrum foreground templates. We validate our likelihood through an extensive suite of consistency tests, and assess the impact of residual foreground and instrumental uncertainties on the final cosmological parameters. We find good internal agreement among the high- $\ell$  cross-spectra with residuals below a few  $\mu\text{K}^2$  at  $\ell \leq 1000$ , in agreement with estimated calibration uncertainties. We compare our results with foreground-cleaned CMB maps derived from all *Planck* frequencies, as well as with cross-spectra derived from the 70 GHz *Planck* map, and find broad agreement in terms of spectrum residuals and cosmological parameters. We further show that the best-fit  $\Lambda\text{CDM}$  cosmology is in excellent agreement with preliminary *Planck* *EE* and *TE* polarisation spectra. We find that the standard  $\Lambda\text{CDM}$  cosmology is well constrained by *Planck* from the measurements at  $\ell \leq 1500$ . One specific example is the spectral index of scalar perturbations, for which we report a  $5.4\sigma$  deviation from scale invariance,  $n_s \neq 1$ . Increasing the multipole range beyond  $\ell \approx 1500$  does not increase our accuracy for the  $\Lambda\text{CDM}$  parameters, but instead allows us to study extensions beyond the standard model. We find no indication of significant departures from the  $\Lambda\text{CDM}$  framework. Finally, we report a tension between the *Planck* best-fit  $\Lambda\text{CDM}$  model and the low- $\ell$  spectrum in the form of a power deficit of 5–10% at  $\ell \leq 40$ , with a statistical significance of  $2.5$ – $3\sigma$ . Without a theoretically motivated model for this power deficit, we do not elaborate further on its cosmological implications, but note that this is our most puzzling finding in an otherwise remarkably consistent dataset.

**Key words.** Cosmology: cosmic background radiation – Surveys – Methods: data analysis

arXiv:1303.5075v2 [astro-ph.CO] 25 Mar 2013



# Observational hints for power-loss

Astronomy & Astrophysics manuscript no. 0\_Like\_top  
26th March 2013

© ESO 2013

## Planck 2013 results. XV. CMB power spectra and likelihood

Planck Collaboration: P. A. R. Ade<sup>49</sup>, N. Aghanim<sup>62</sup>, C. Armitage-Caplan<sup>94</sup>, M. Arnaud<sup>56</sup>, M. Ashdown<sup>73,6</sup>, F. Atrio-Barandela<sup>39</sup>, J. Aumont<sup>62</sup>, C. Baccigalupi<sup>88</sup>, A. J. Banday<sup>97,10</sup>, R. B. Barreiro<sup>70</sup>, J. G. Bartlett<sup>1,71</sup>, E. Battaner<sup>96</sup>, K. Benabed<sup>63,96</sup>, A. Benoît<sup>60</sup>, A. Benoit-Lévy<sup>26,63,96</sup>,

J.-P. Bernard<sup>1</sup>, F. R. Boudet<sup>1</sup>, A. Catalano<sup>78</sup>, S. Colombi<sup>1</sup>, R. D. Davies<sup>1</sup>, J. M. Diego<sup>47</sup>, H. K. Eriksen<sup>1</sup>, M. Giard<sup>1,10</sup>, A. González<sup>1</sup>, C. Hernández<sup>78</sup>, K. M. Huffen<sup>1</sup>, K. Kiiveri<sup>47,47</sup>, J.-M. Lamarre<sup>1</sup>, J. León-Tavares<sup>1</sup>, F. Ma<sup>1</sup>, E. Martínez-Gómez<sup>1</sup>, A. Mennella<sup>1</sup>, G. Mivianus<sup>51</sup>, F. Montiel<sup>77</sup>, R. Padin<sup>29</sup>, I. M. Plat<sup>1</sup>, E. Piat<sup>1</sup>, G. W. Pratt<sup>76</sup>, C. Renault<sup>78</sup>, S. J. S. Rubiño-Montero<sup>1</sup>, D. Spencer<sup>1</sup>, J. A. Taube<sup>1</sup>, L. Valenziano<sup>1</sup>

### Abstract

This paper presents the *Planck* likelihood, a complete statistical description of the two-point correlation function of the CMB temperature fluctuations that accounts for all known relevant uncertainties, both instrumental and astrophysical in nature. We use this likelihood to derive our best estimate of the CMB angular power spectrum from *Planck* over three decades in multipole moment,  $\ell$ , covering  $2 \leq \ell \leq 2500$ . The main source of error at  $\ell \lesssim 1500$  is cosmic variance. Uncertainties in small-scale foreground modelling and instrumental noise dominate the error budget at higher  $\ell$ s. For  $\ell < 50$ , our likelihood exploits all *Planck* frequency channels from 30 to 353 GHz, separating the cosmological CMB signal from diffuse Galactic foregrounds through a physically motivated Bayesian component separation technique. At  $\ell \geq 50$ , we employ a correlated Gaussian likelihood approximation based on a fine-grained set of angular cross-spectra derived from multiple detector combinations between the 100, 143, and 217 GHz frequency channels, marginalizing over power spectrum foreground templates. We validate our likelihood through an extensive suite of consistency tests, and assess the impact of residual foreground and instrumental uncertainties on the final cosmological parameters. We find good internal agreement among the high- $\ell$  cross-spectra with residuals below a few  $\mu\text{K}^2$  at  $\ell \lesssim 1000$ , in agreement with estimated calibration uncertainties. We compare our results with foreground-cleaned CMB maps derived from all *Planck* frequencies, as well as with cross-spectra derived from the 70 GHz *Planck* map, and find broad agreement in terms of spectrum residuals and cosmological parameters. We further show that the best-fit  $\Lambda\text{CDM}$  cosmology is in excellent agreement with preliminary *Planck* *EE* and *TE* polarisation spectra. We find that the standard  $\Lambda\text{CDM}$  cosmology is well constrained by *Planck* from the measurements at  $\ell \lesssim 1500$ . One specific example is the spectral index of scalar perturbations, for which we report a  $5.4\sigma$  deviation from scale invariance,  $n_s \neq 1$ . Increasing the multipole range beyond  $\ell \approx 1500$  does not increase our accuracy for the  $\Lambda\text{CDM}$  parameters, but instead allows us to study extensions beyond the standard model. We find no indication of significant departures from the  $\Lambda\text{CDM}$  framework. Finally, we report a tension between the *Planck* best-fit  $\Lambda\text{CDM}$  model and the low- $\ell$  spectrum in the form of a power deficit of 5–10% at  $\ell \lesssim 40$ , with a statistical significance of  $2.5\text{--}3\sigma$ . Without a theoretically motivated model for this power deficit, we do not elaborate further on its cosmological implications, but note that this is our most puzzling finding in an otherwise remarkably consistent dataset.

### Abstract

This paper presents the *Planck* likelihood, a complete statistical description of the two-point correlation function of the CMB temperature fluctuations that accounts for all known relevant uncertainties, both instrumental and astrophysical in nature. We use this likelihood to derive our best estimate of the CMB angular power spectrum from *Planck* over three decades in multipole moment,  $\ell$ , covering  $2 \leq \ell \leq 2500$ . The main source of error at  $\ell \lesssim 1500$  is cosmic variance. Uncertainties in small-scale foreground modelling and instrumental noise dominate the error budget at higher  $\ell$ s. For  $\ell < 50$ , our likelihood exploits all *Planck* frequency channels from 30 to 353 GHz, separating the cosmological CMB signal from diffuse Galactic foregrounds through a physically motivated Bayesian component separation technique. At  $\ell \geq 50$ , we employ a correlated Gaussian likelihood approximation based on a fine-grained set of angular cross-spectra derived from multiple detector combinations between the 100, 143, and 217 GHz frequency channels, marginalizing over power spectrum foreground templates. We validate our likelihood through an extensive suite of consistency tests, and assess the impact of residual foreground and instrumental uncertainties on the final cosmological parameters. We find good internal agreement among the high- $\ell$  cross-spectra with residuals below a few  $\mu\text{K}^2$  at  $\ell \lesssim 1000$ , in agreement with estimated calibration uncertainties. We compare our results with foreground-cleaned CMB maps derived from all *Planck* frequencies, as well as with cross-spectra derived from the 70 GHz *Planck* map, and find broad agreement in terms of spectrum residuals and cosmological parameters. We further show that the best-fit  $\Lambda\text{CDM}$  cosmology is in excellent agreement with preliminary *Planck* *EE* and *TE* polarisation spectra. We find that the standard  $\Lambda\text{CDM}$  cosmology is well constrained by *Planck* from the measurements at  $\ell \lesssim 1500$ . One specific example is the spectral index of scalar perturbations, for which we report a  $5.4\sigma$  deviation from scale invariance,  $n_s \neq 1$ . Increasing the multipole range beyond  $\ell \approx 1500$  does not increase our accuracy for the  $\Lambda\text{CDM}$  parameters, but instead allows us to study extensions beyond the standard model. We find no indication of significant departures from the  $\Lambda\text{CDM}$  framework. Finally, we report a tension between the *Planck* best-fit  $\Lambda\text{CDM}$  model and the low- $\ell$  spectrum in the form of a power deficit of 5–10% at  $\ell \lesssim 40$ , with a statistical significance of  $2.5\text{--}3\sigma$ . Without a theoretically motivated model for this power deficit, we do not elaborate further on its cosmological implications, but note that this is our most puzzling finding in an otherwise remarkably consistent dataset.

Key words: Cosmology: cosmic background radiation – Surveys – Methods: data analysis

arXiv:1202.5075v2 [astro-ph.CO] 25 Mar 2013



# Observational hints for power-loss

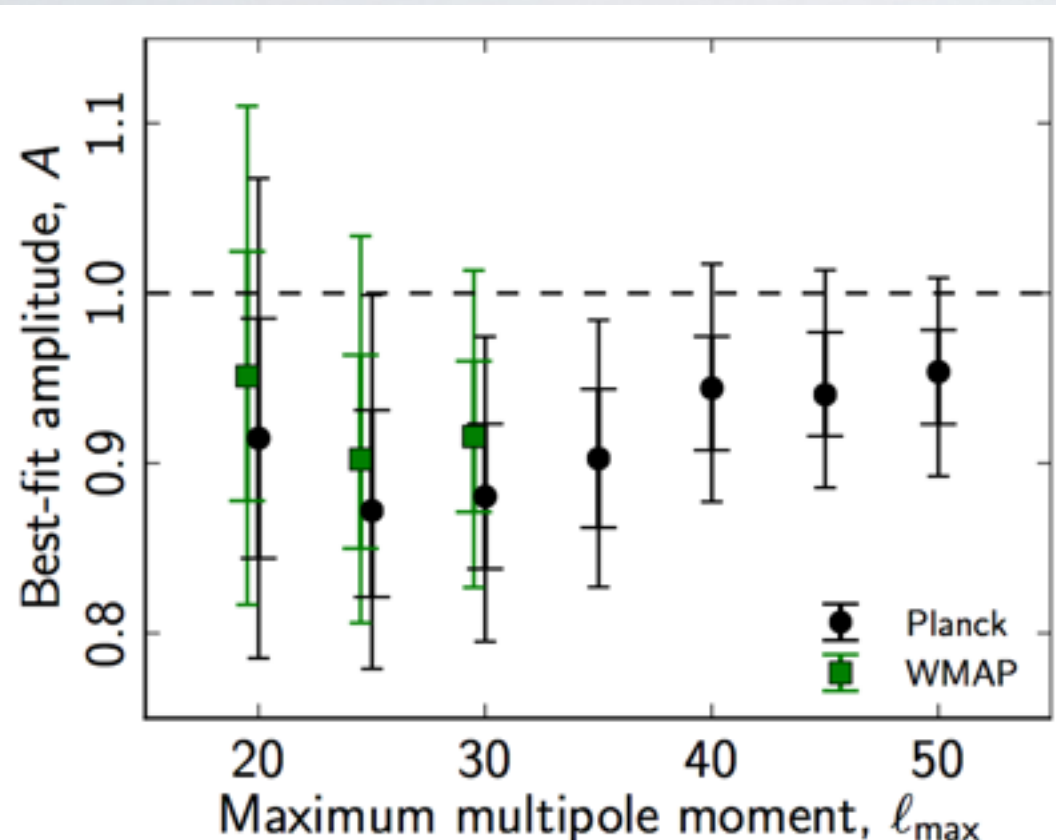


**Figure 39.** Power spectrum amplitude,  $q$ , relative to the best-fit *Planck* model as a function of  $\ell_{\text{max}}$ , as measured by the low- $\ell$  *Planck* and *WMAP* temperature likelihoods, respectively. Error bars indicate 68 and 95% confidence regions.

$$\mathcal{P}_{\mathcal{R}}(k) = \mathcal{P}_0(k) \left\{ 1 - \exp \left[ - \left( \frac{k}{k_c} \right)^{\lambda_c} \right] \right\}.$$

Model	$-2\Delta \ln \mathcal{L}_{\text{max}}$	$\ln B_{0X}$	Parameter	Best fit value
Wiggles	-9.0	1.5	$\alpha_w$	0.0294
			$\omega$	28.90
			$\varphi$	$0.075 \pi$
Step-inflation	-11.7	0.3	$\mathcal{A}_f$	0.102
			$\ln(\eta_f/\text{Mpc})$	8.214
			$\ln x_d$	4.47
Cutoff	-2.9	0.3	$\ln(k_c/\text{Mpc}^{-1})$	-8.493
			$\lambda_c$	0.474

**Table 11.** Improvement in fit and logarithm of the Bayes factor with respect to power law  $\Lambda\text{CDM}$  and best fit parameter values for the wiggles, step-inflation, and cutoff models. The larger  $\ln B_{0X}$ , the greater the preference for a featureless power law spectrum.

# Cosmic variance

We only have one sky

Measurements on largest scales are statistically limited

[Planck XV]

Cosmic variance

CV is the simplest explanation for low- $\ell$  anomaly

CV can be decreased using LSS data

[1309.4060]

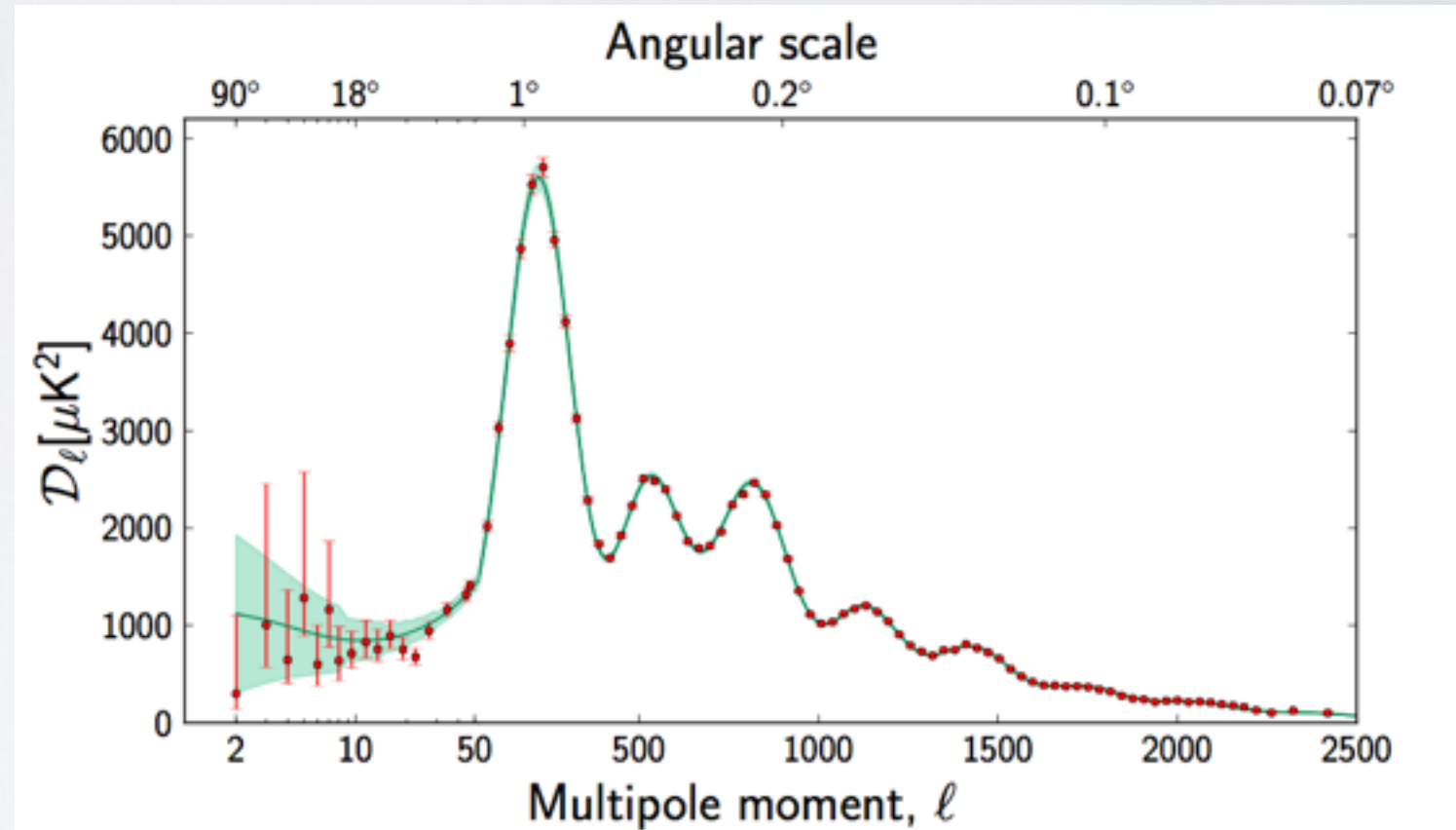


**Figure 37.** The 2013 *Planck* CMB temperature angular power spectrum. The error bars include cosmic variance, whose magnitude is indicated by the green shaded area around the best fit model. The low- $\ell$  values are plotted at 2, 3, 4, 5, 6, 7, 8, 9.5, 11.5, 13.5, 16, 19, 22.5, 27, 34.5, and 44.5.

# Pre-inflation and the power spectrum

?? What if inflation was short ??

# Pre-inflation and the power spectrum

?? What if inflation was short ??

Freivogel et al. 2007  
McAllister et al. 2013

theoretically well motivated:

$$P(N_e) \sim \left( \frac{1}{N_e} \right)^\alpha \quad \alpha > 0$$

# Pre-inflation and the power spectrum

?? What if inflation was short ??

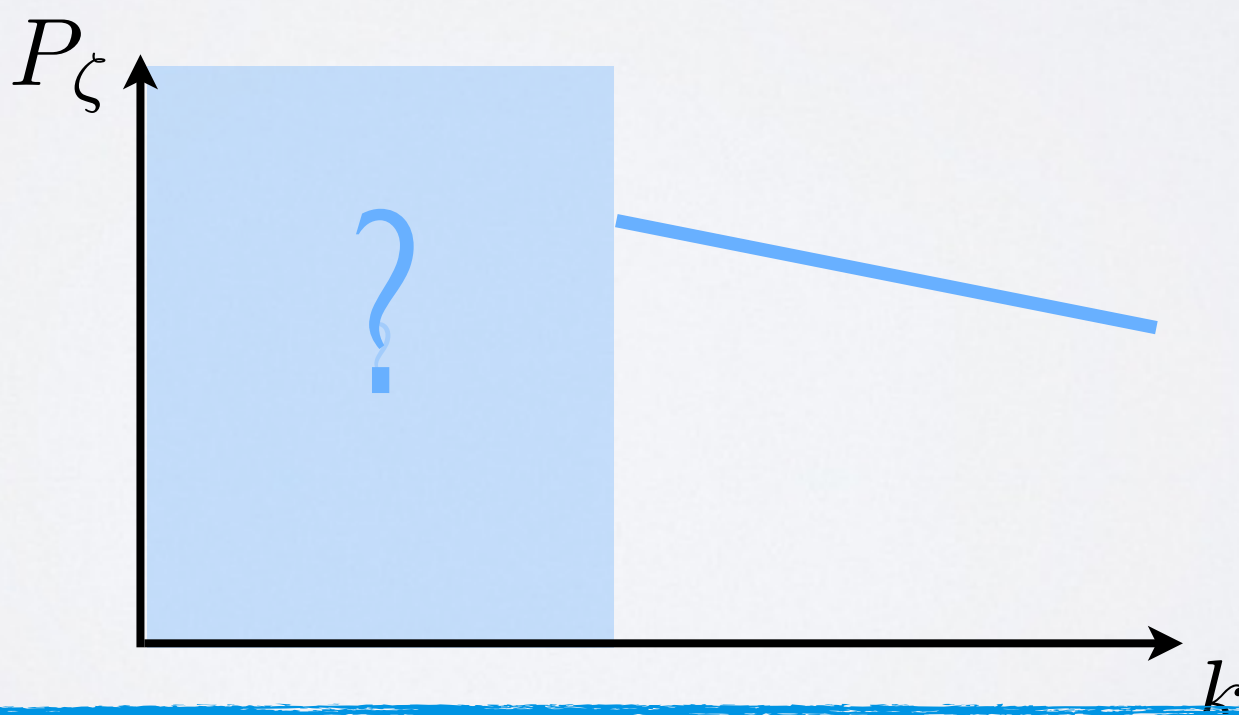
Freivogel et al. 2007  
McAllister et al. 2013

theoretically well motivated:

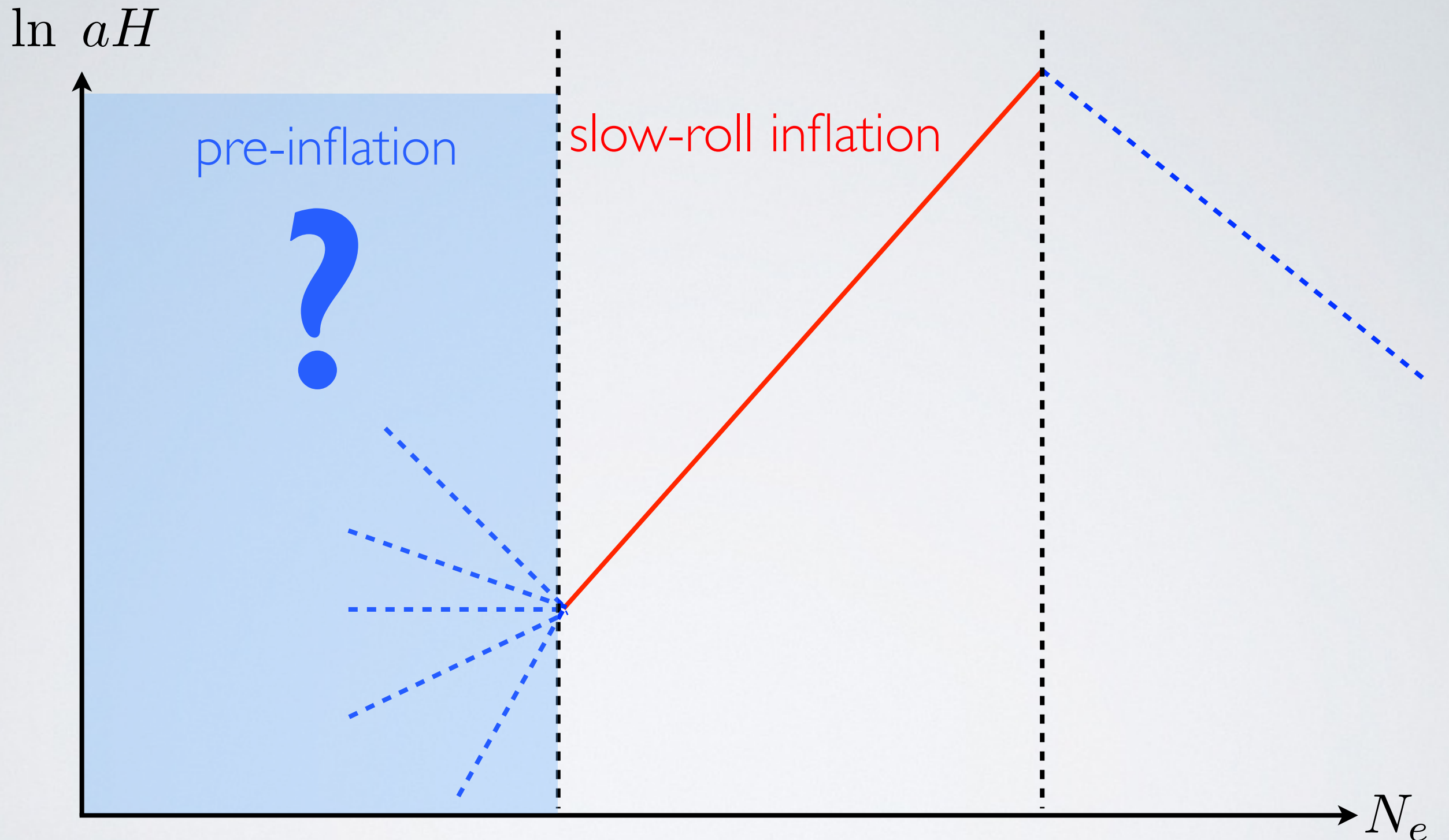
$$P(N_e) \sim \left(\frac{1}{N_e}\right)^\alpha \quad \alpha > 0$$

Can this leave an imprint on the power spectrum?

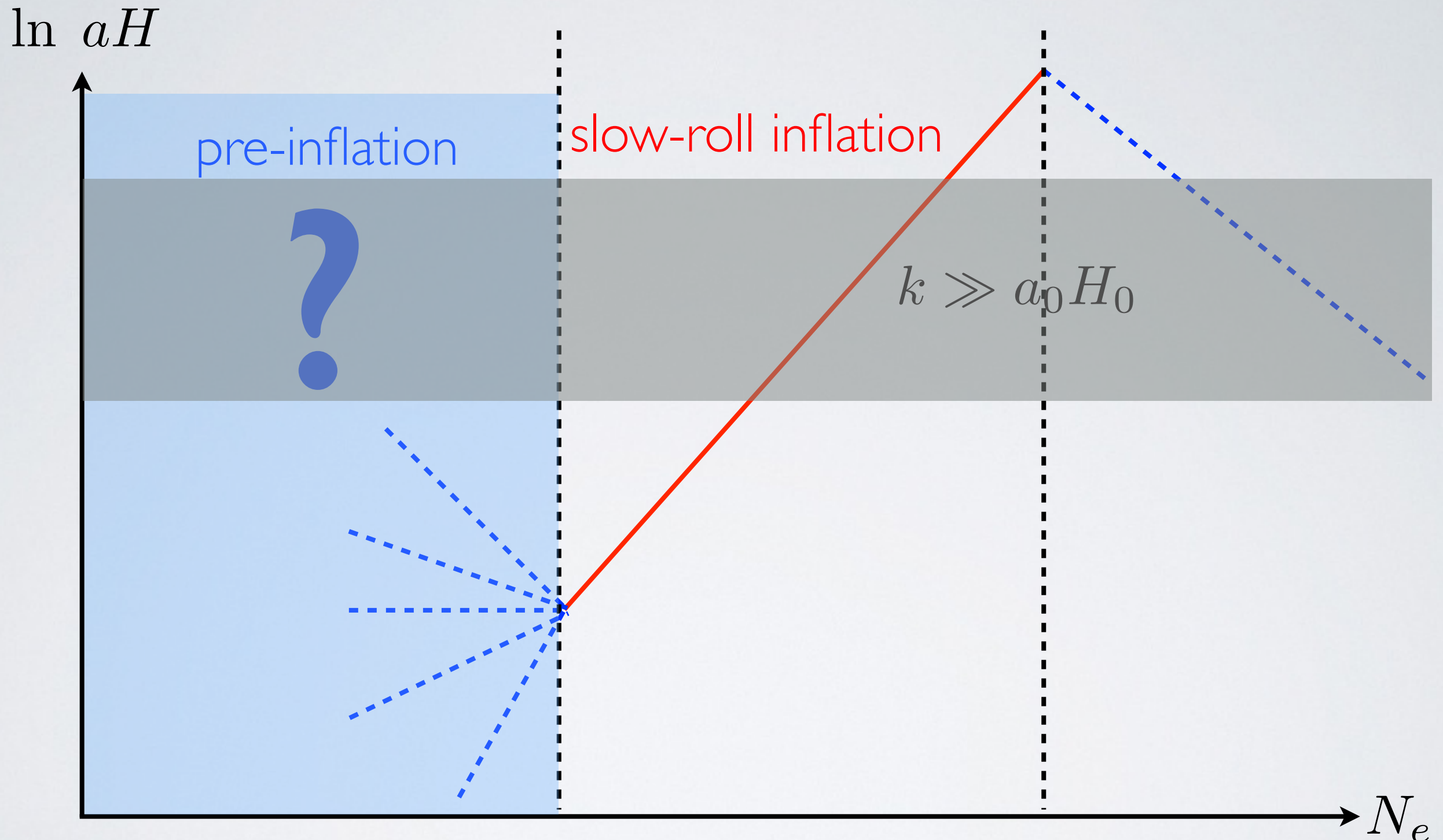
Modifies large scale part of spectrum



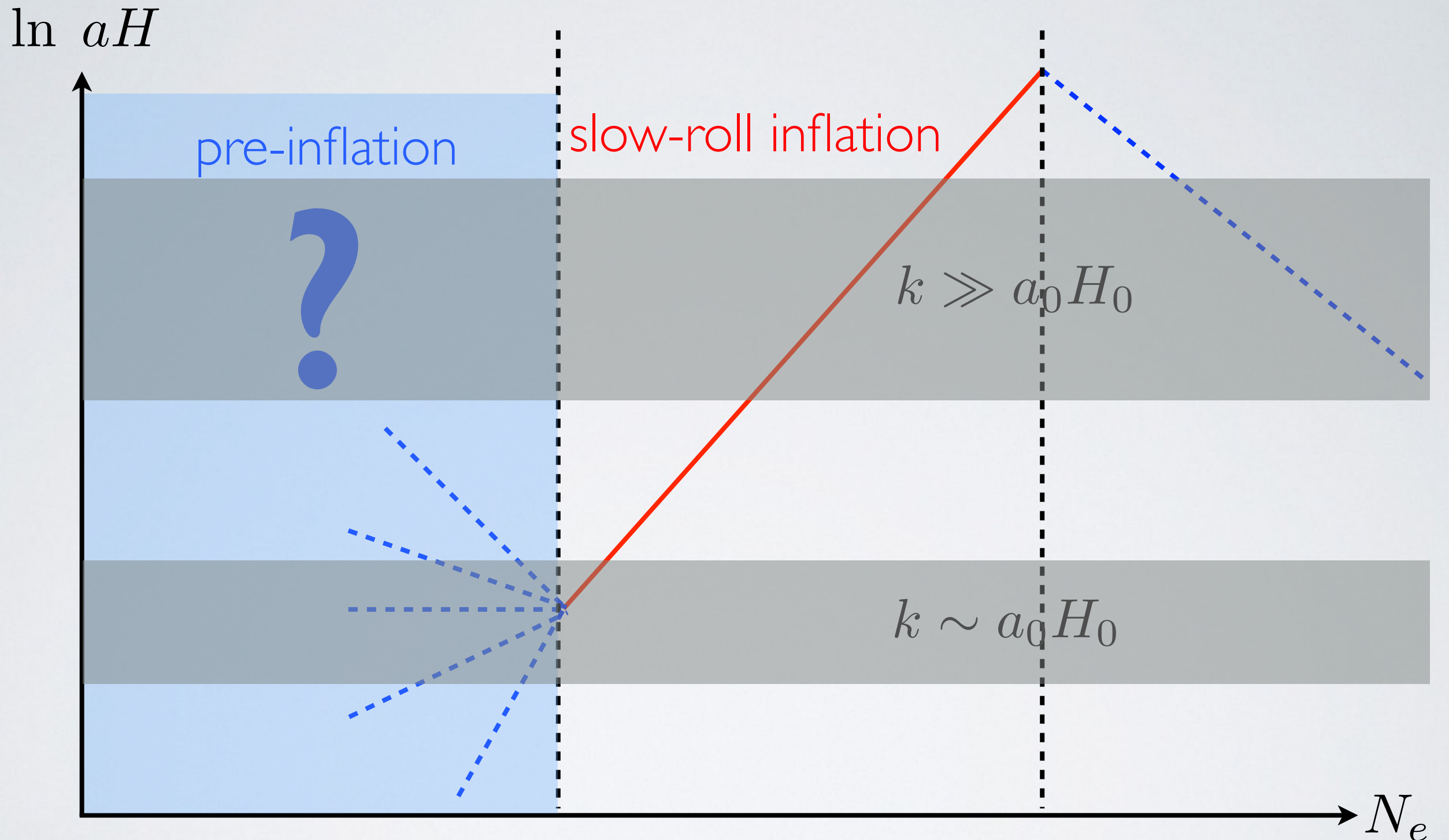
# Pre-inflation and the power spectrum



# Pre-inflation and the power spectrum



# Pre-inflation and the power spectrum



# The conservative approach

Power loss at 5-10% level  $\rightarrow$  attainable within slow roll

At the pivot scale  $n_s - 1 \sim -0.04 \rightarrow \epsilon \sim \eta \sim 0.01$

$$P_k \propto \frac{H^2}{\epsilon_H}$$

on larger scales:  $H_{\ell < 40} \sim H_{pivot}$  and  $\epsilon_{\ell < 40} \sim 1.1 \epsilon_{pivot}$

steepening within slow-roll

[FGP&Westphal 2013]

[Buosso et al. 2013]

[Cicoli et al. 2013]

asymmetric inflection point models

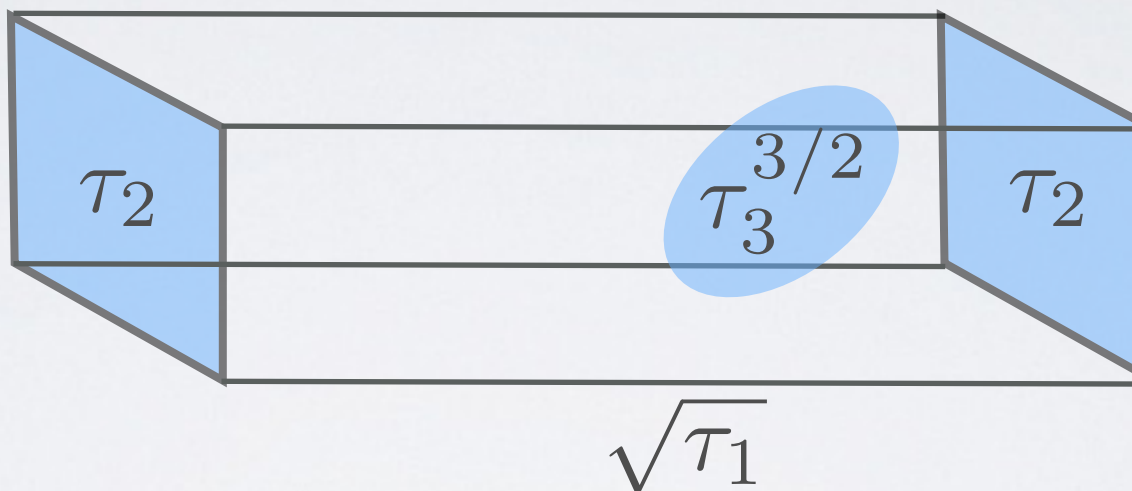
# Steepening in fibre inflation

[Cicoli et al., 2008]

Inflation in Type IIB string compactifications

Inflaton is a Kahler modulus

$$\mathcal{V} = \sqrt{\tau_1} \tau_2 - \tau_3^{3/2}$$

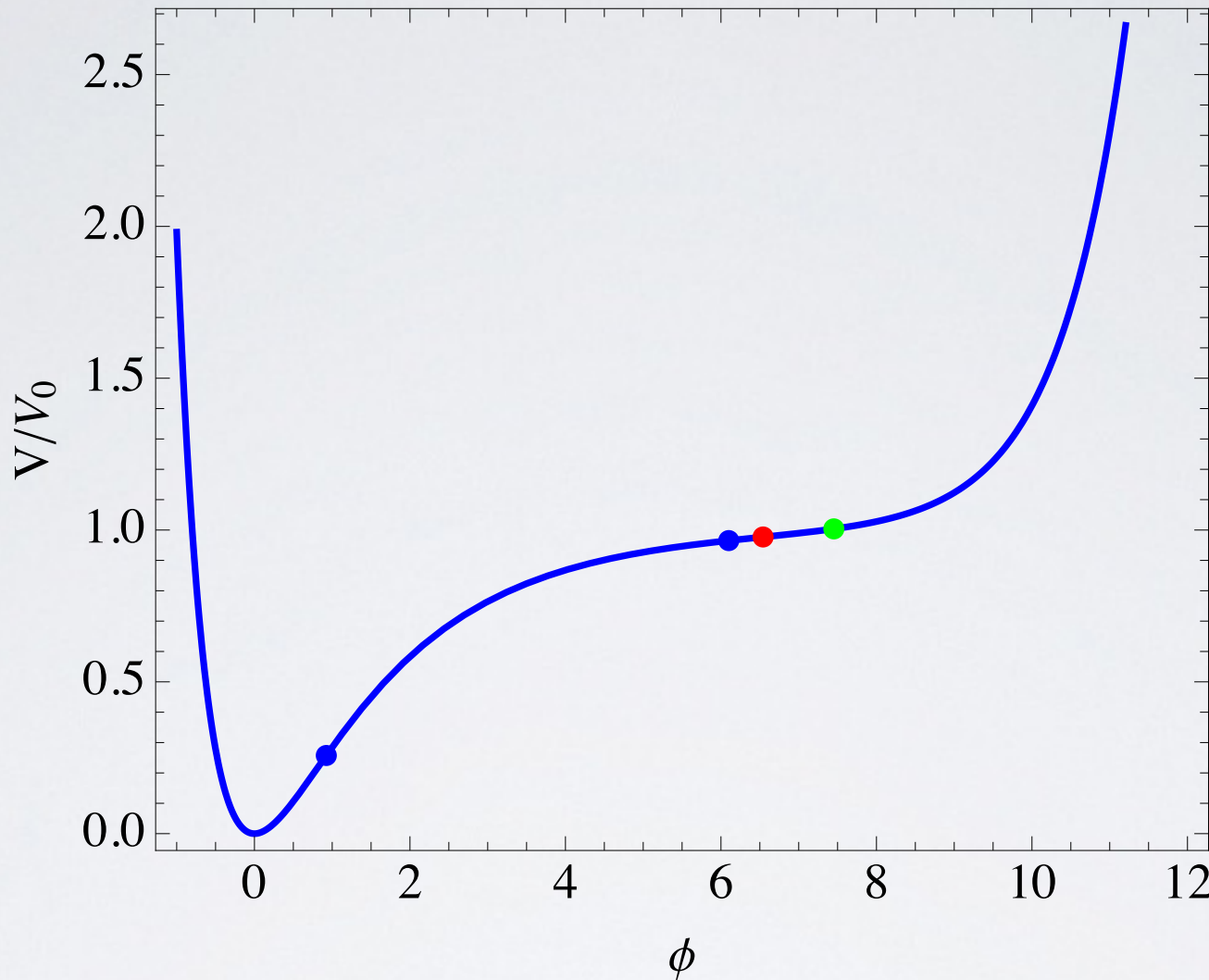


Fibre modulus' potential generated by perturbative corrections

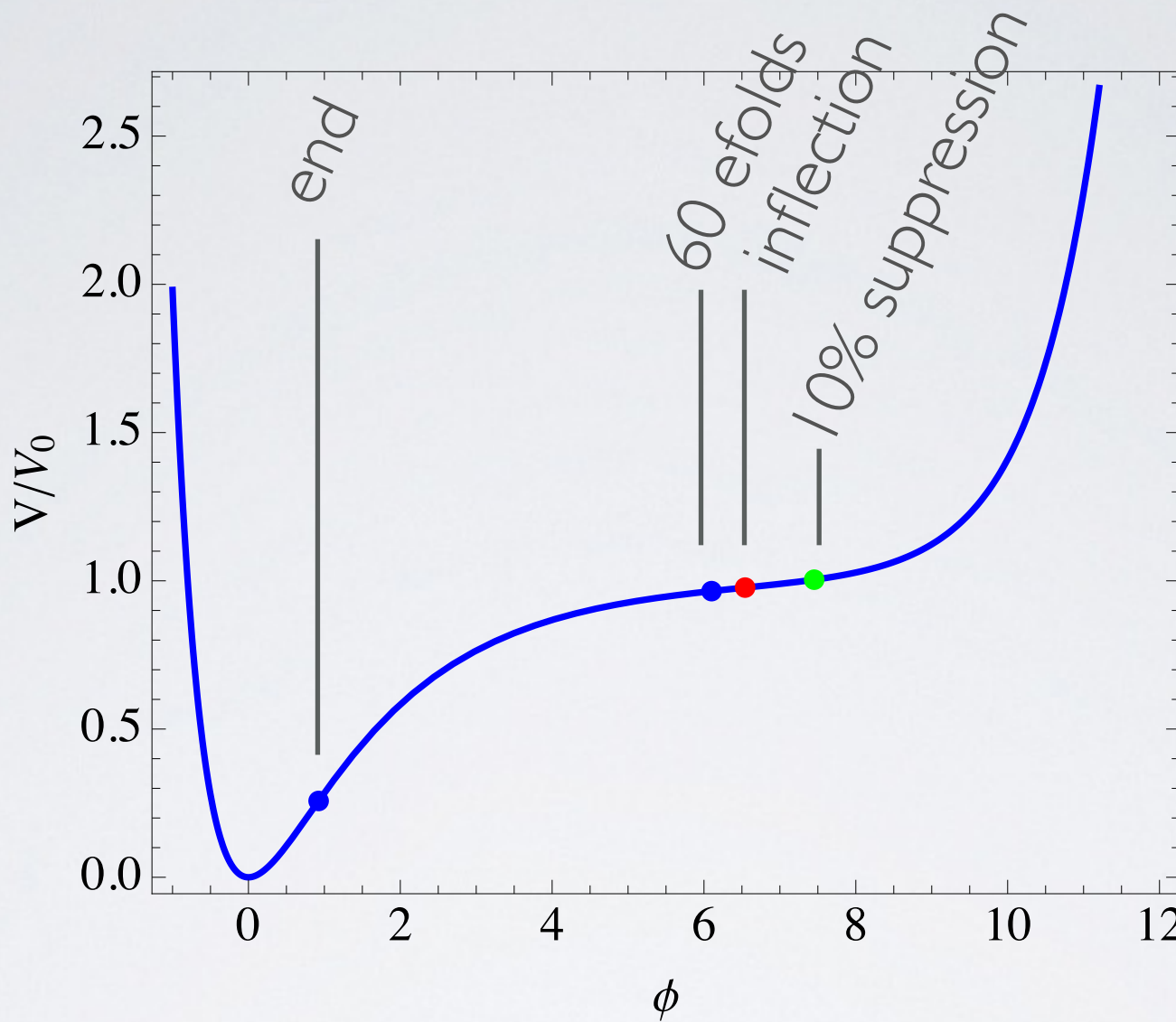
$$\tau_1 \equiv e^{\kappa\phi} \quad \kappa = 2/\sqrt{3}$$

$$V = V_0 \left( 1 - C_{1/2} e^{-\kappa\phi/2} + C_2 e^{-2\kappa\phi} + C_1 e^{\kappa\phi} \right)$$

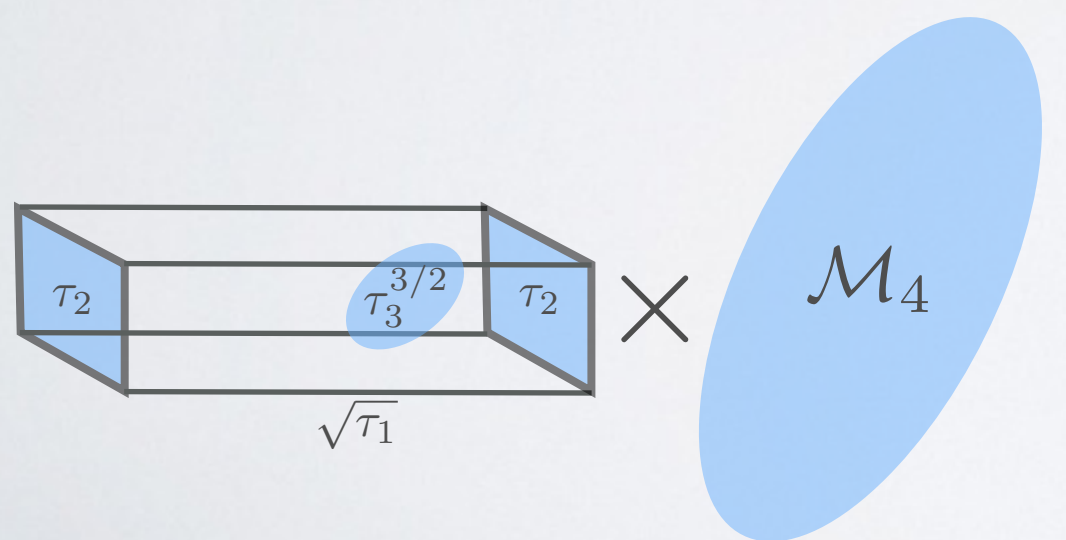
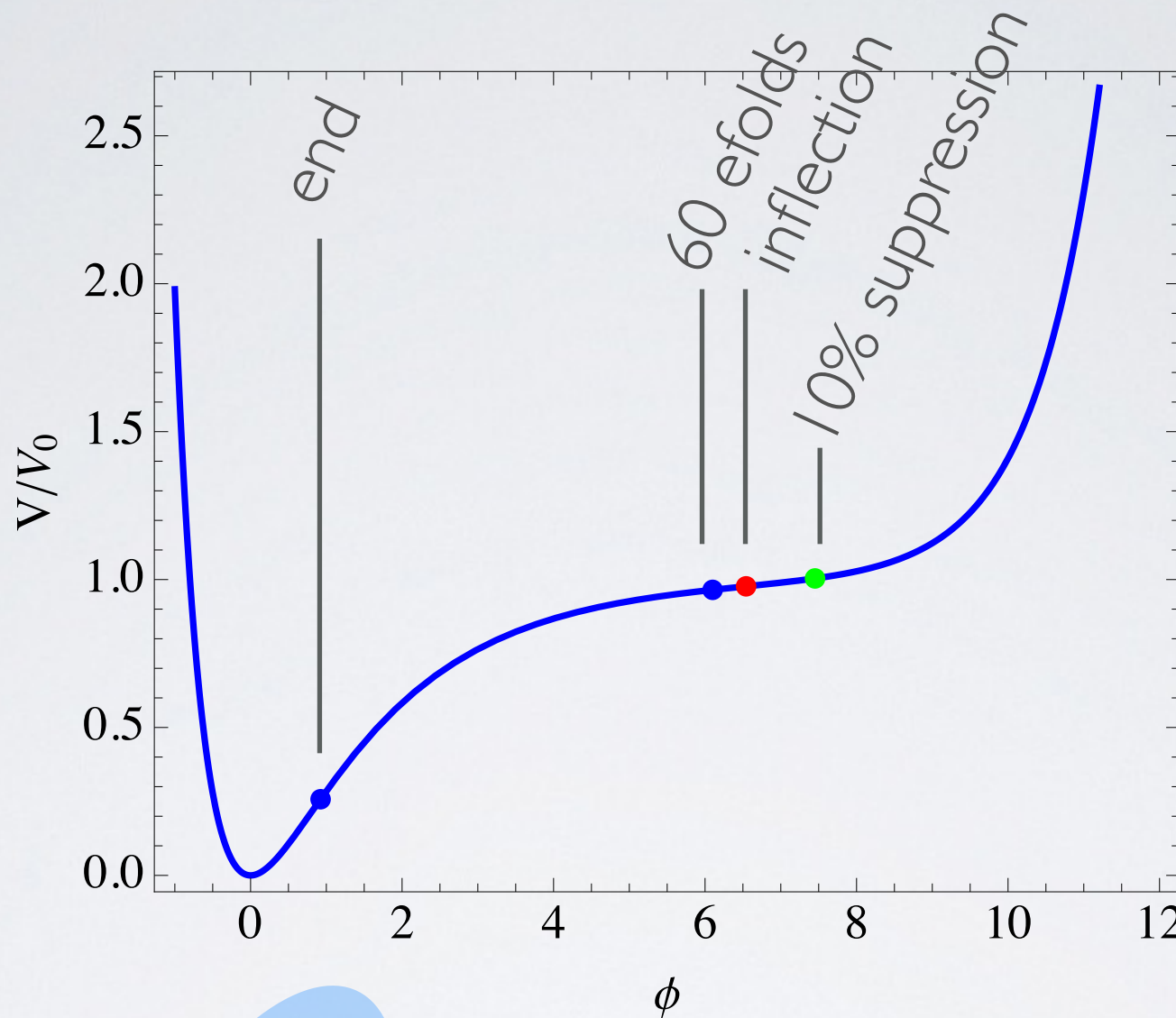
# Steepening in fibre inflation



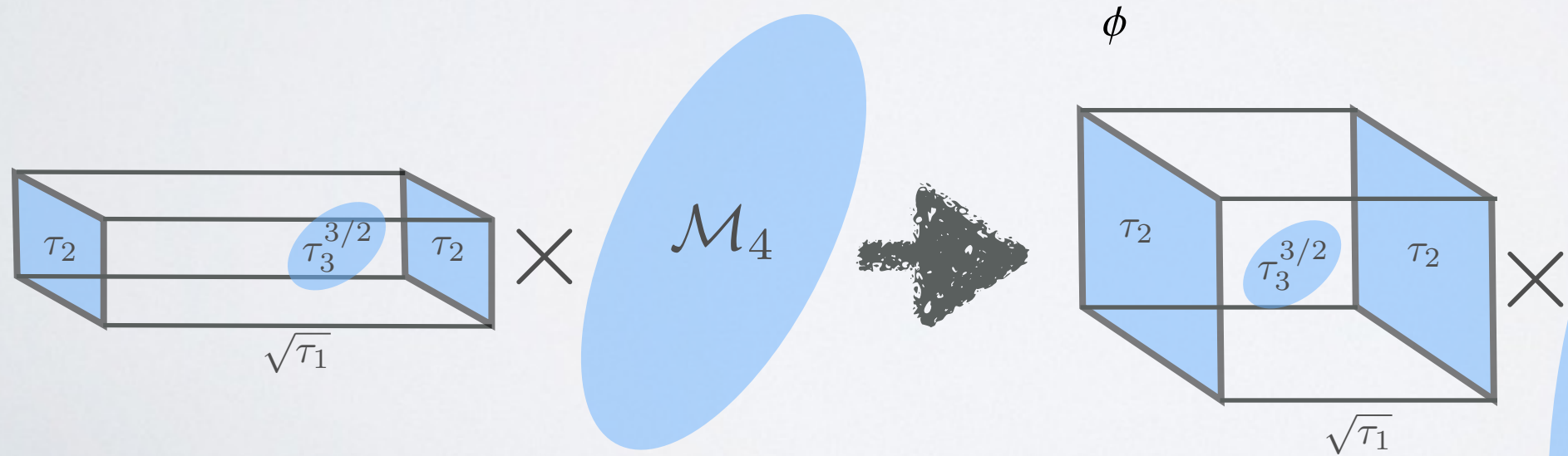
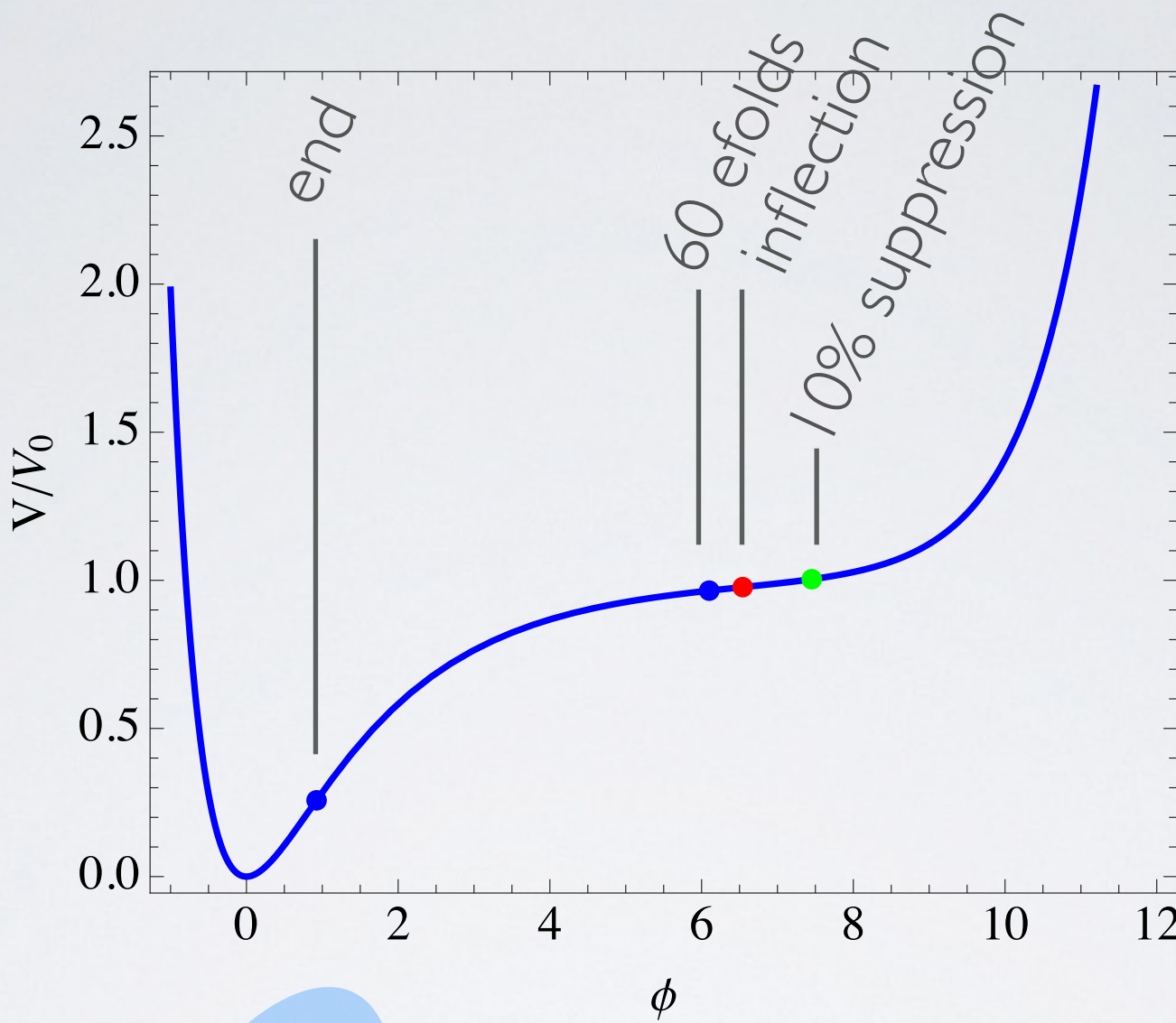
# Steepening in fibre inflation



# Steepening in fibre inflation



# Steepening in fibre inflation

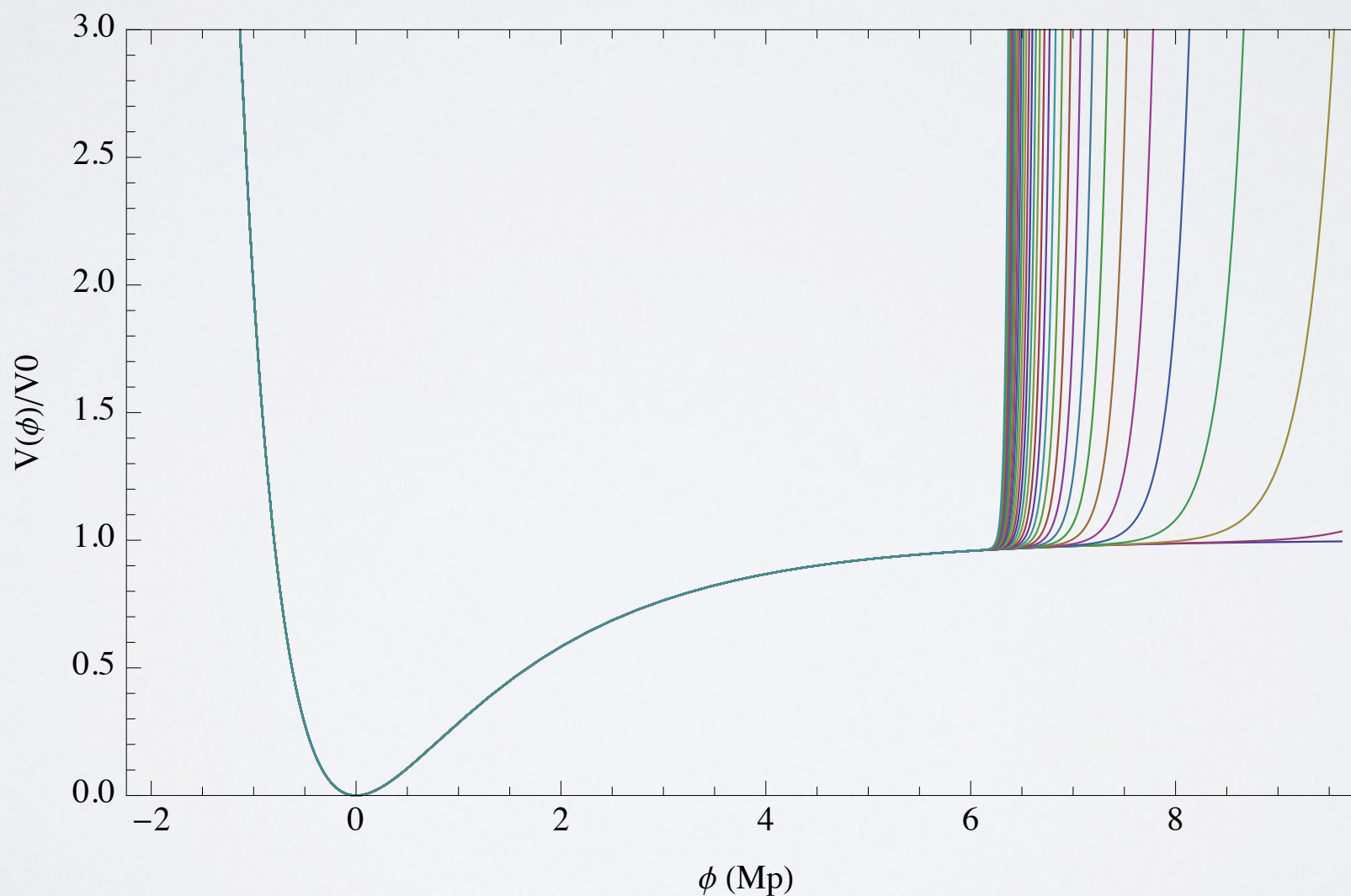


# Steepening in fibre inflation

Too much expansion  $\rightarrow$  power loss unobservable

Need steeper potential after inflection point

$$V \supset C_1 e^{\kappa\phi} \rightarrow C_1 e^{\tilde{\kappa}\phi} \quad \tilde{\kappa} > \kappa$$



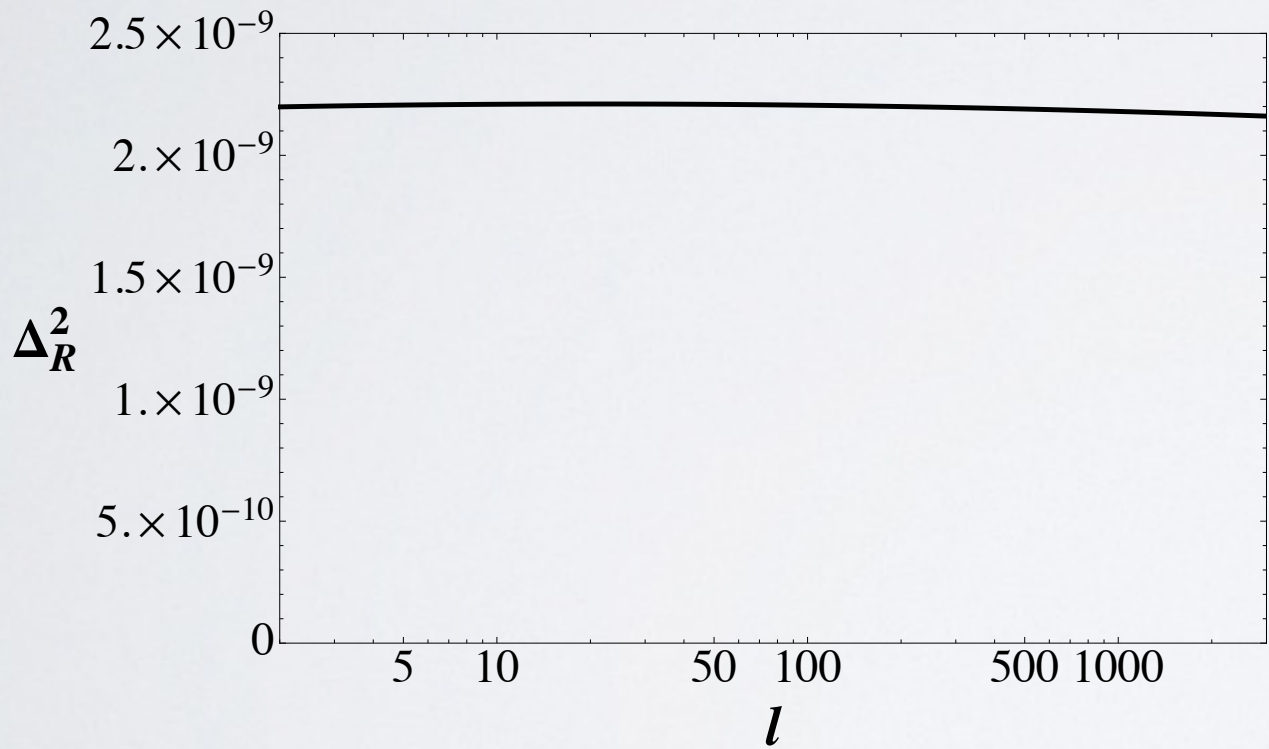
# Steepening in fibre inflation

Decreases  $\Delta N_e$  between suppression region and pivot scale

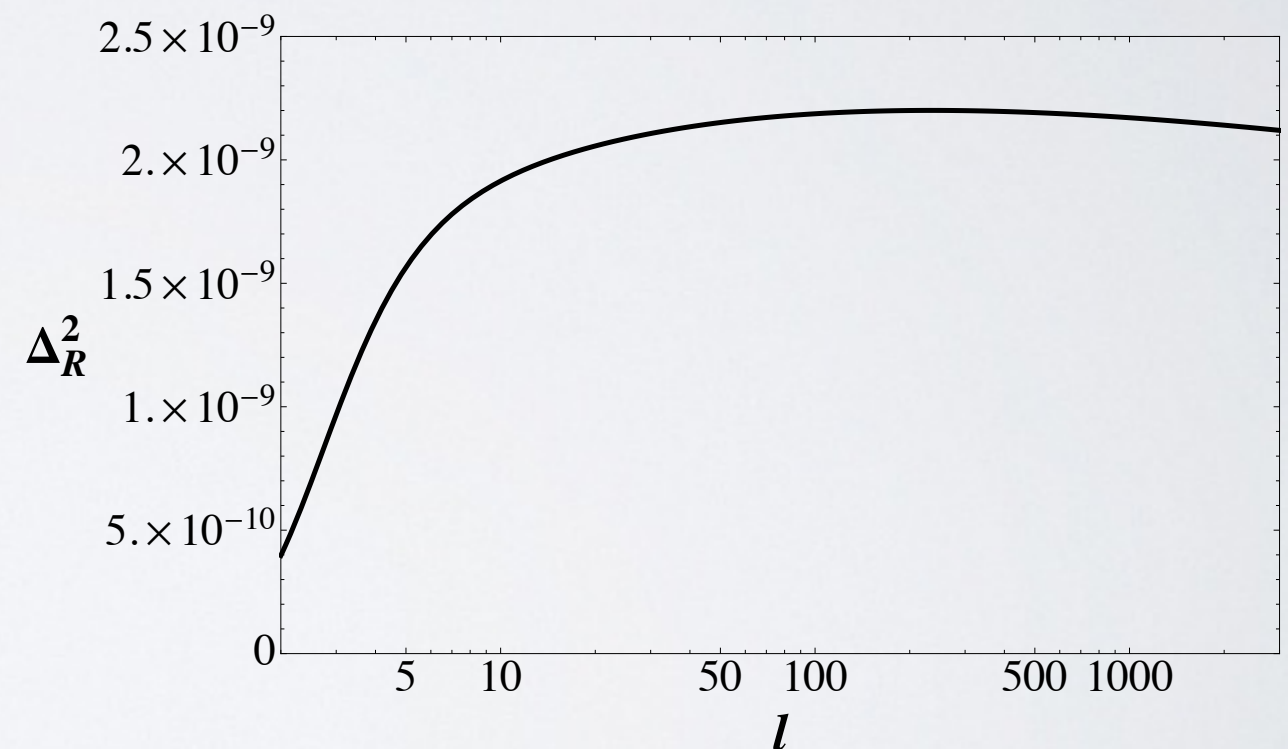
Renders suppression observable

Example:

original model



$\tilde{\kappa} \sim 10\kappa$



Modification of the string-loop effects generating  $\nabla$

# What pre-inflation?

Move **beyond slow-roll** and consider different dynamics:

- Fast-roll

$$\xi = -2$$

*Contaldi et al. 2003*

- Climbing scalars

*Sagnotti et al. 2012/14*

- Radiation domination

$$\xi = -1$$

*Nicholson&Contaldi 2007*

*Kinney&Powell 2008*

- Matter domination

$$\xi = -1/2$$

*Cline et al. 2003*

- Curvature domination

$$\xi = 0$$

*Linde et al. 1998,...,2011*

- Super inflation

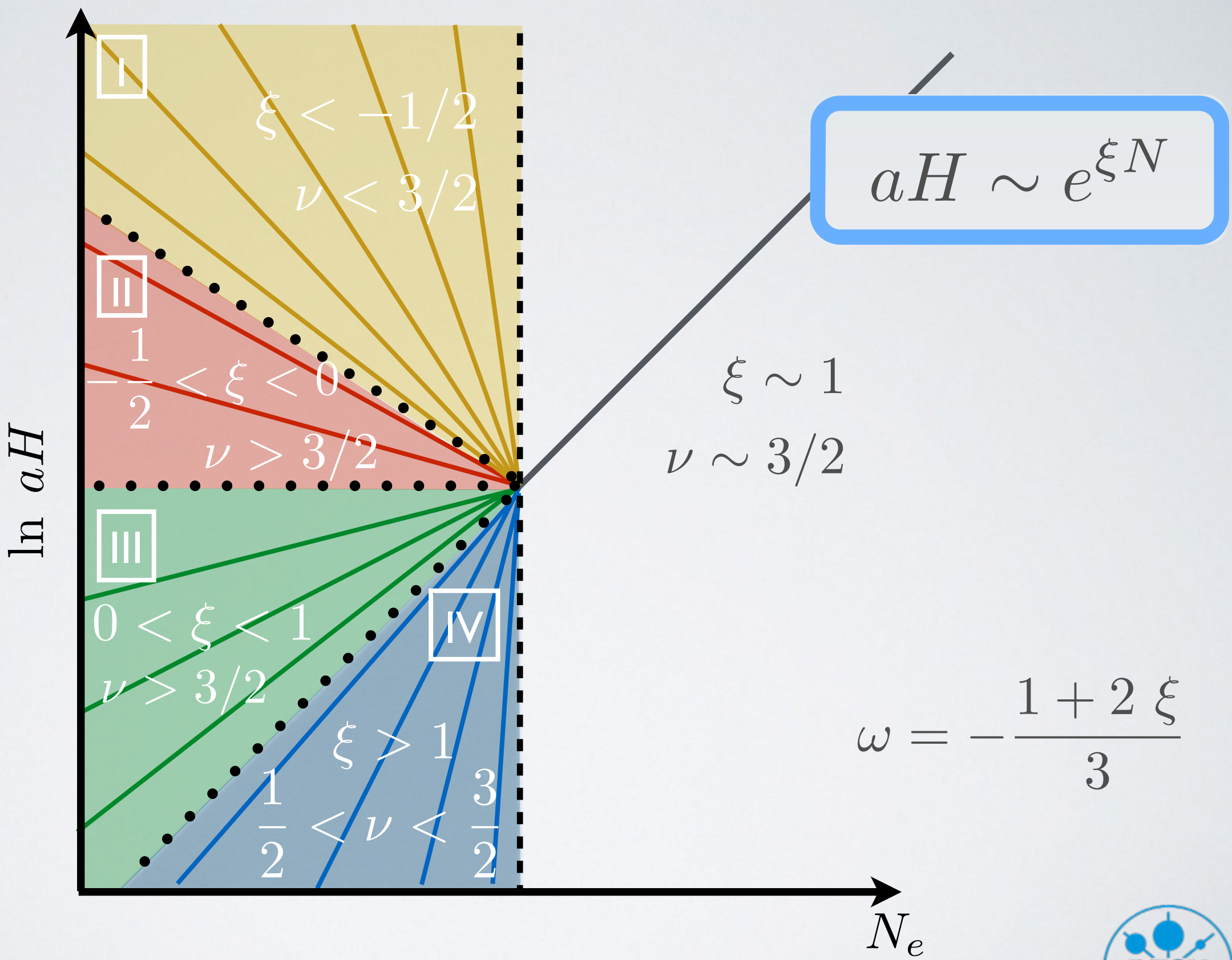
$$\xi = 2$$

*Liu et al. 2013*

- Emergent Universe

*Labrana 2013*

# What pre-inflation?



# Pre-inflation and power spectrum

Want to compute  $P_k \equiv k^3 \left| \frac{u}{z} \right|^2$  after the end of inflation

Analytical computation, assuming instantaneous transition

Similar to QM: require continuity&diff. of  $u$  across transitions

$$\begin{pmatrix} C_{i_{Max}}^{(1)} \\ C_{i_{Max}}^{(2)} \end{pmatrix} = \mathcal{A}^{i_{Max} \rightarrow i_{Max}-1} \times \dots \times \mathcal{A}^{3 \rightarrow 2} \times \mathcal{A}^{2 \rightarrow 1} \times \begin{pmatrix} C_1^{(1)} \\ C_1^{(2)} \end{pmatrix}$$

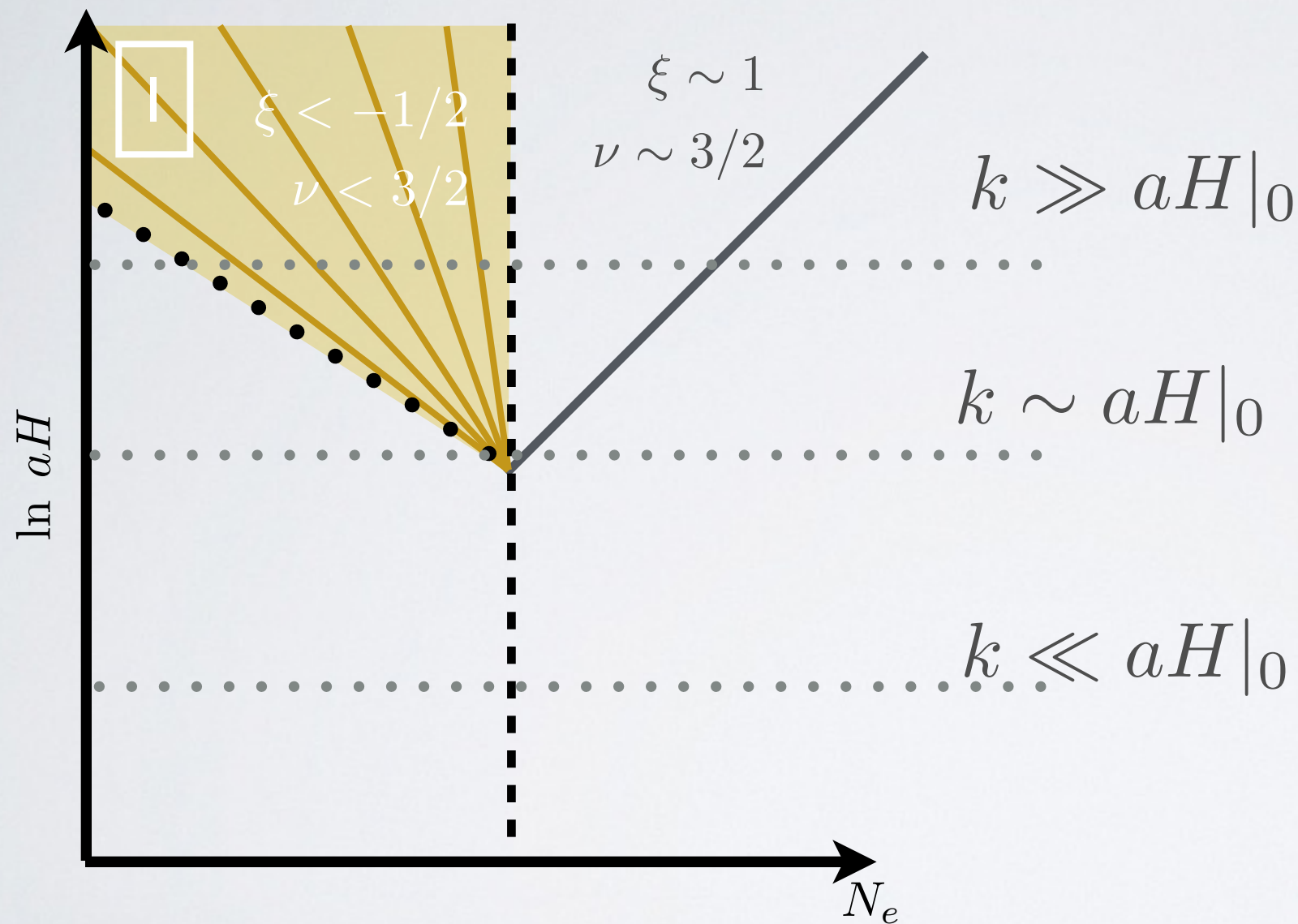
$$P_k \sim k^{n_s-1} \times \frac{H^2}{\epsilon_H} \times \boxed{\left| C^{(1)} - C^{(2)} \right|^2}$$

encodes pre-inflationary physics

# Type I backgrounds

Decelerated expansion:  $H$  decreases

Large scale spectrum from superhorizon modes

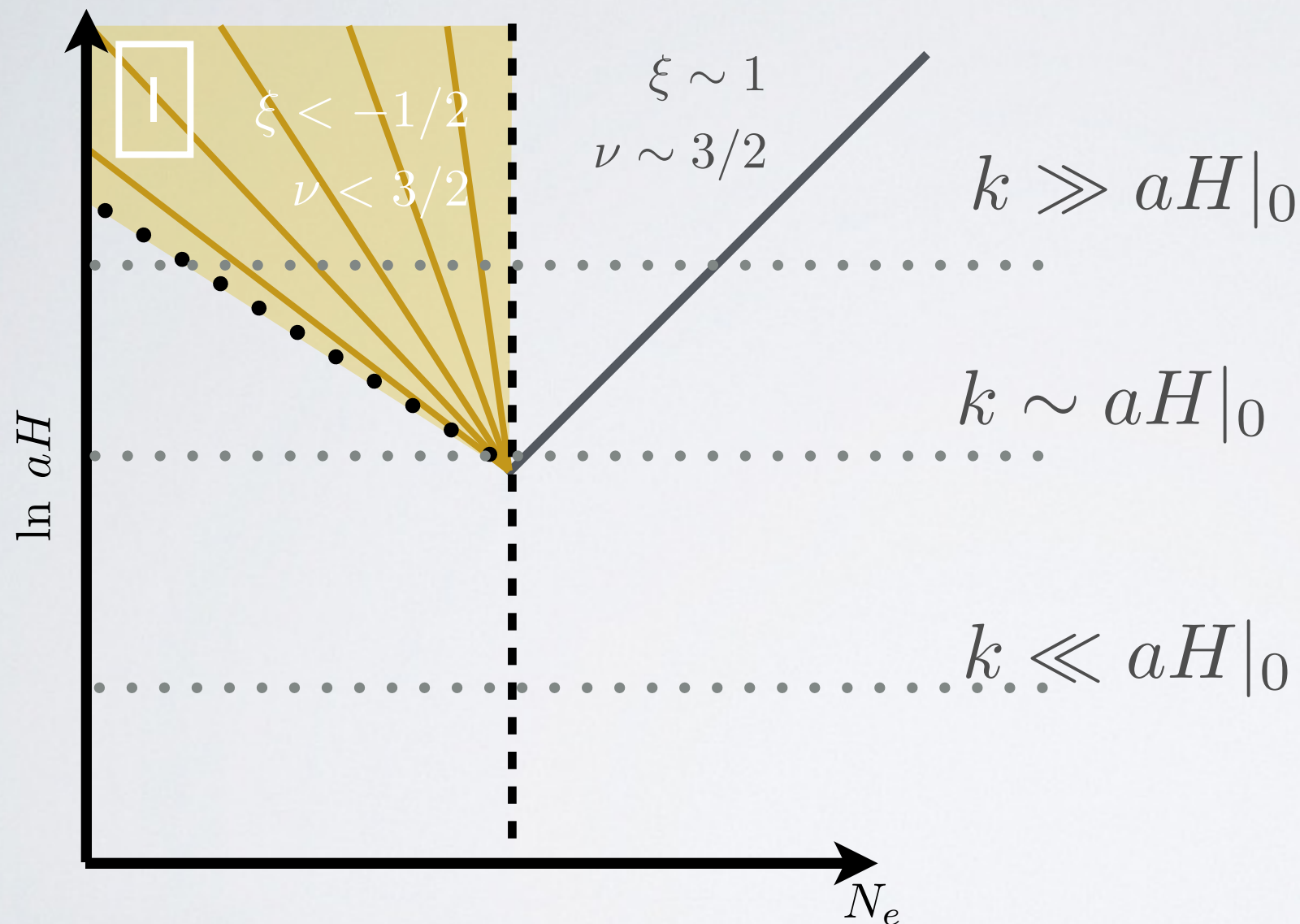


# Type I backgrounds

Decelerated expansion:  $H$  decreases

Large scale spectrum from superhorizon modes

large scale  
spectrum feels  
pre-inflationary  
vacuum

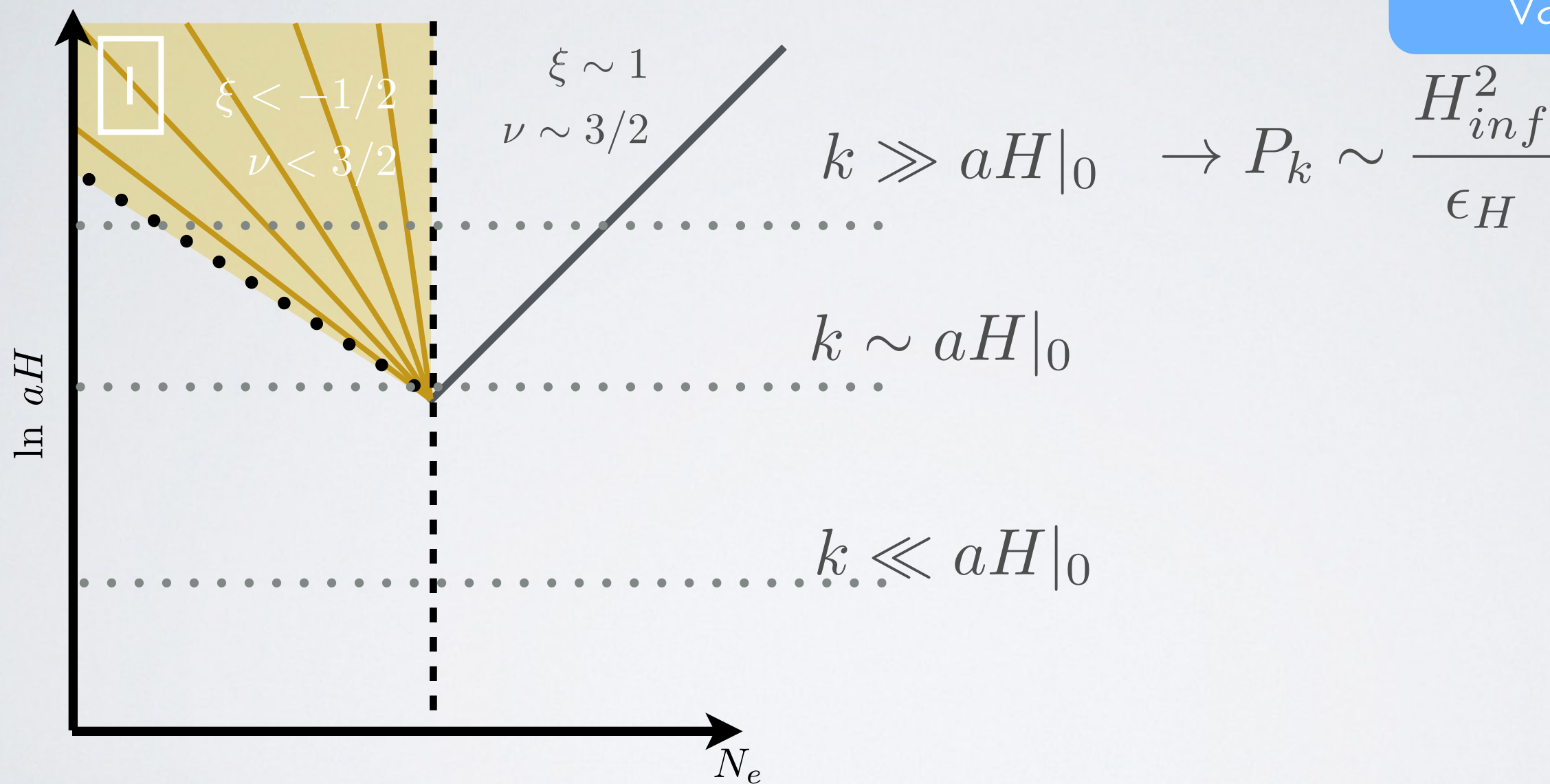


# Type I backgrounds

Decelerated expansion:  $H$  decreases

Large scale spectrum from superhorizon modes

large scale  
spectrum feels  
pre-inflationary  
vacuum

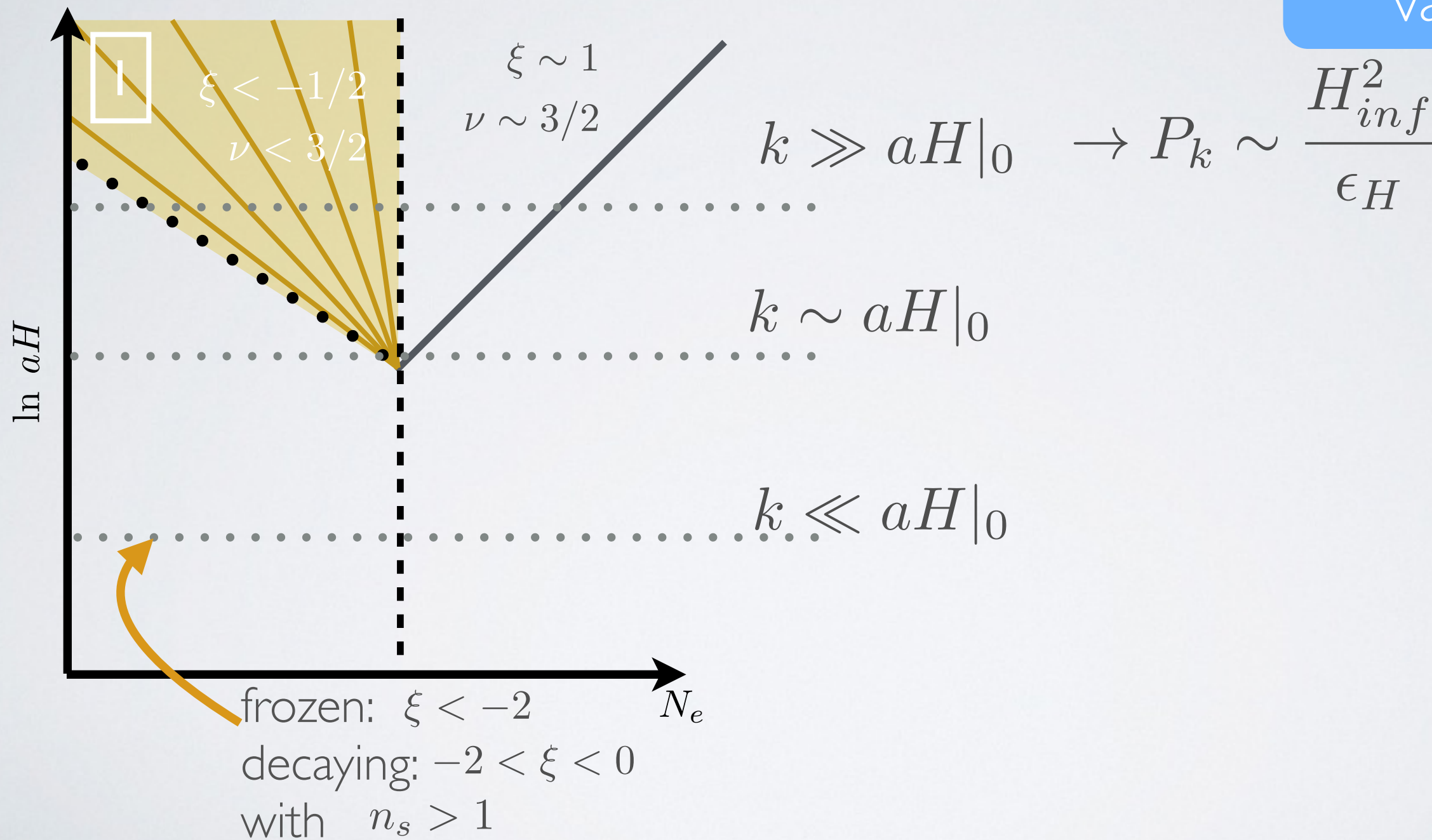


# Type I backgrounds

Decelerated expansion:  $H$  decreases

Large scale spectrum from superhorizon modes

large scale  
spectrum feels  
pre-inflationary  
vacuum

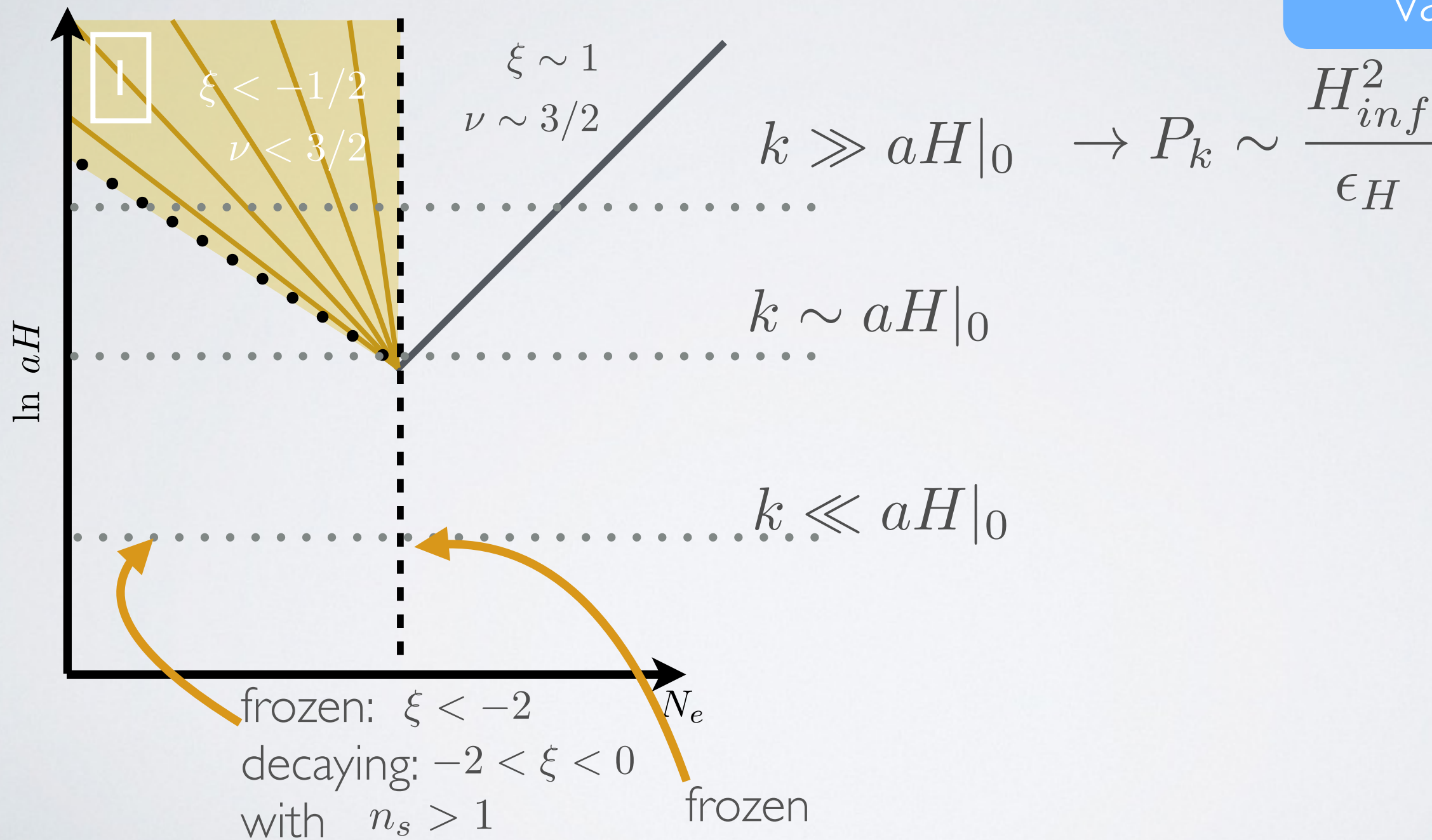


# Type I backgrounds

Decelerated expansion:  $H$  decreases

Large scale spectrum from superhorizon modes

large scale  
spectrum feels  
pre-inflationary  
vacuum

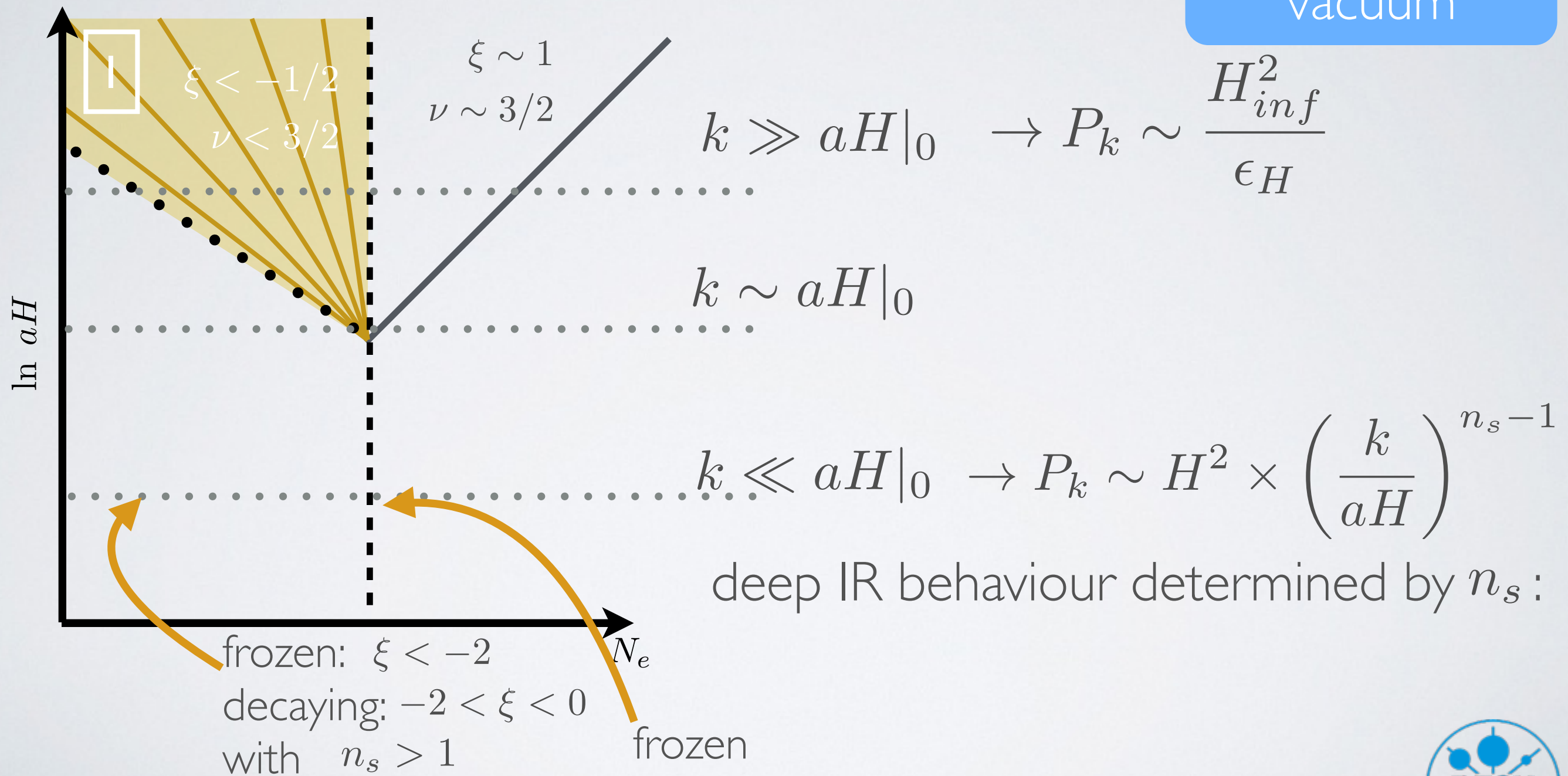


# Type I backgrounds

# Decelerated expansion: $H$ decreases

# Large scale spectrum from superhorizon modes

large scale  
spectrum feels  
pre-inflationary  
vacuum

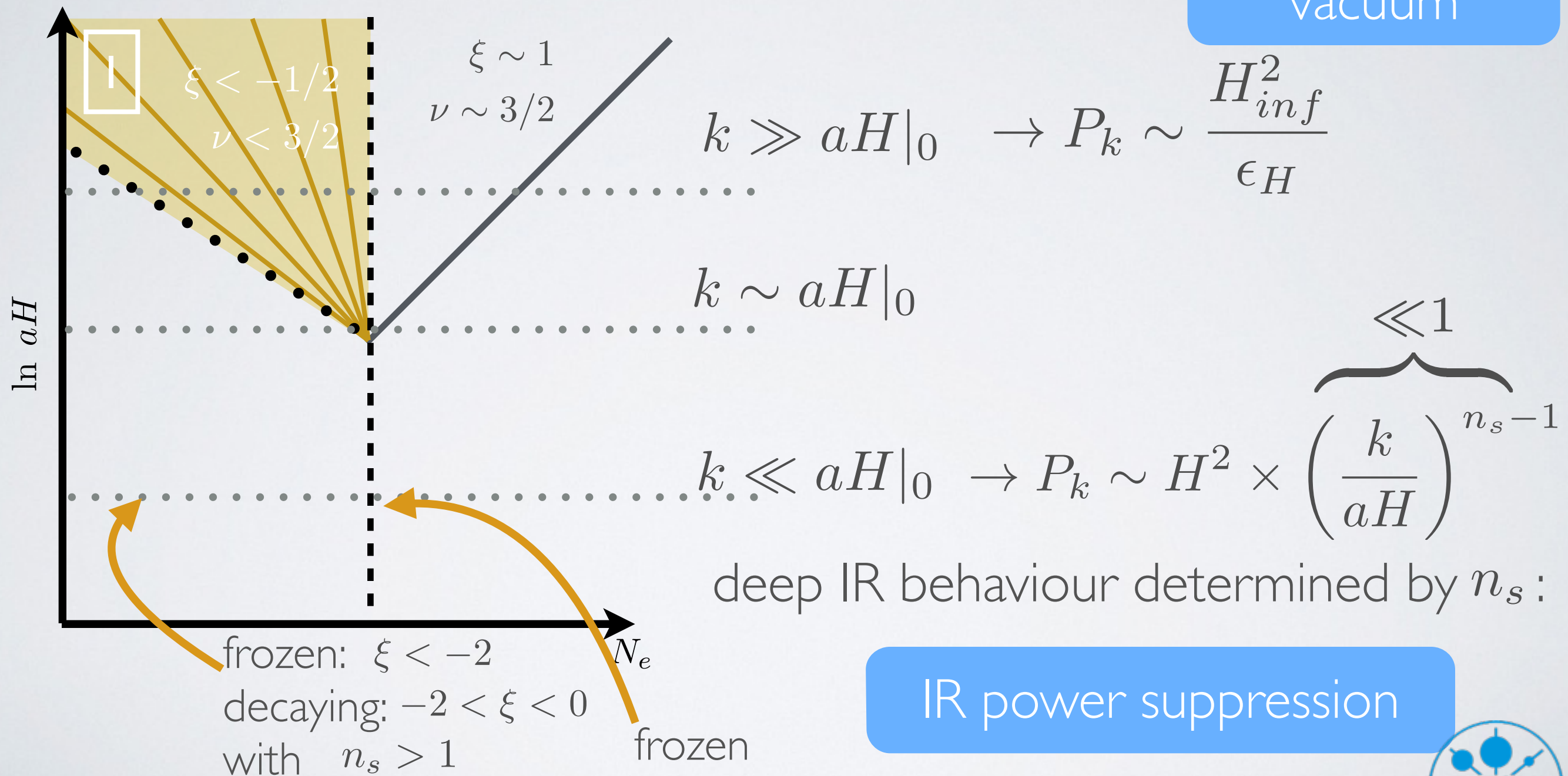


# Type I backgrounds

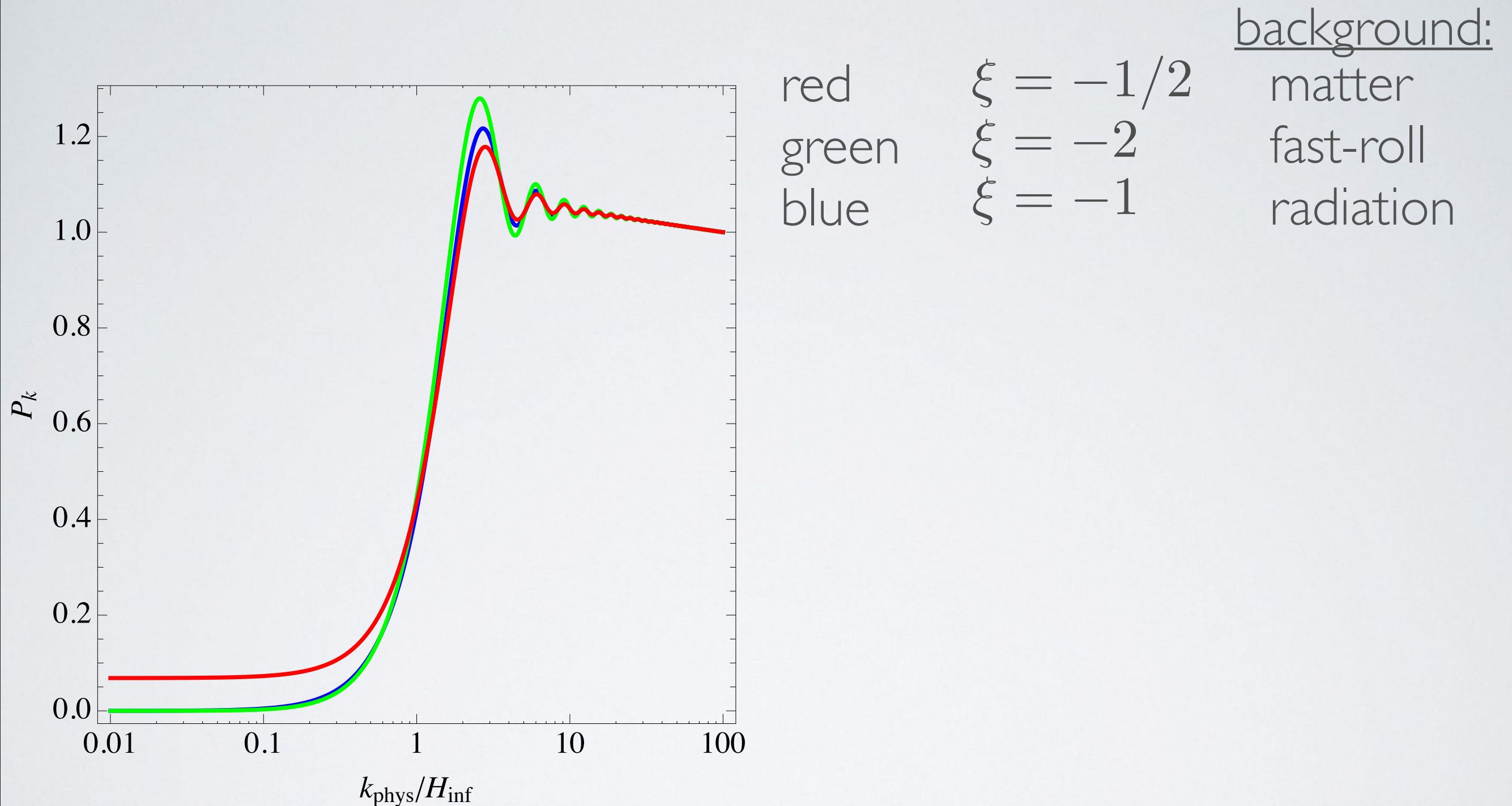
Decelerated expansion:  $H$  decreases

Large scale spectrum from superhorizon modes

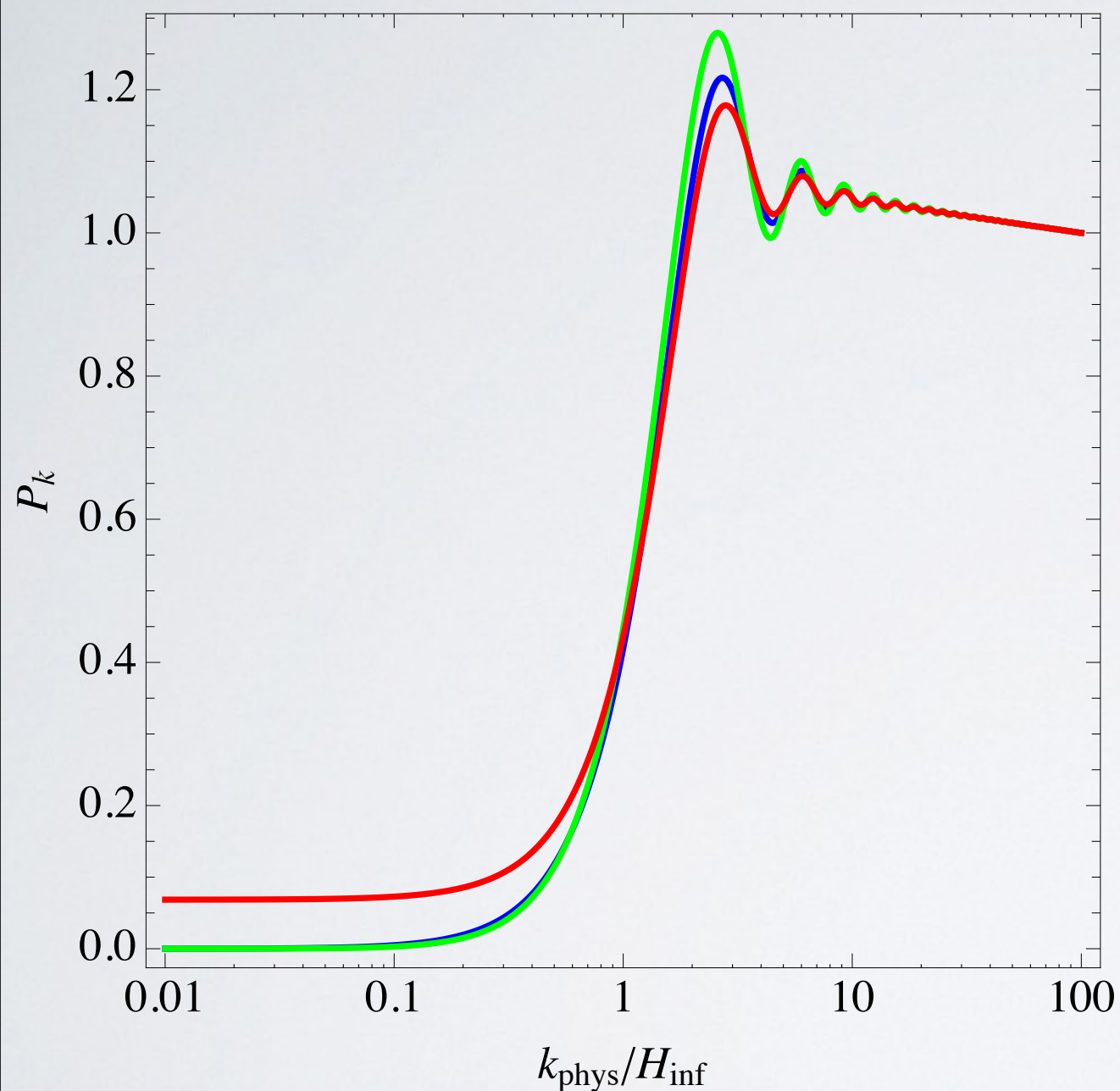
large scale  
spectrum feels  
pre-inflationary  
vacuum



# Type I backgrounds



# Type I backgrounds



red  
green  
blue

$\xi = -1/2$   
 $\xi = -2$   
 $\xi = -1$

background:  
matter  
fast-roll  
radiation

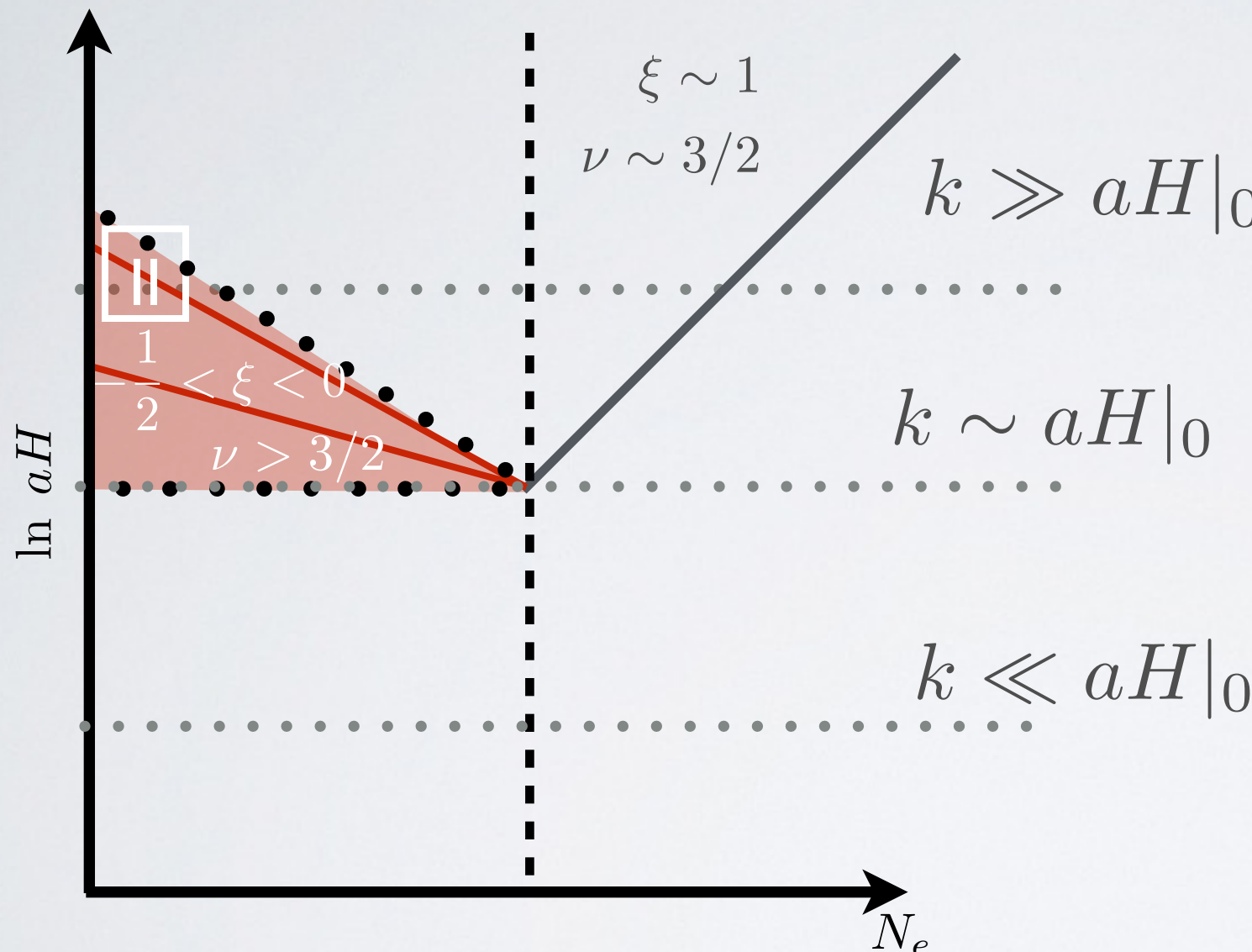
Same broad features

Different peak amplitude  
Different low-k fall-off

# Type II backgrounds

Decelerated expansion:  $H$  decreases

Large scale spectrum from superhorizon modes

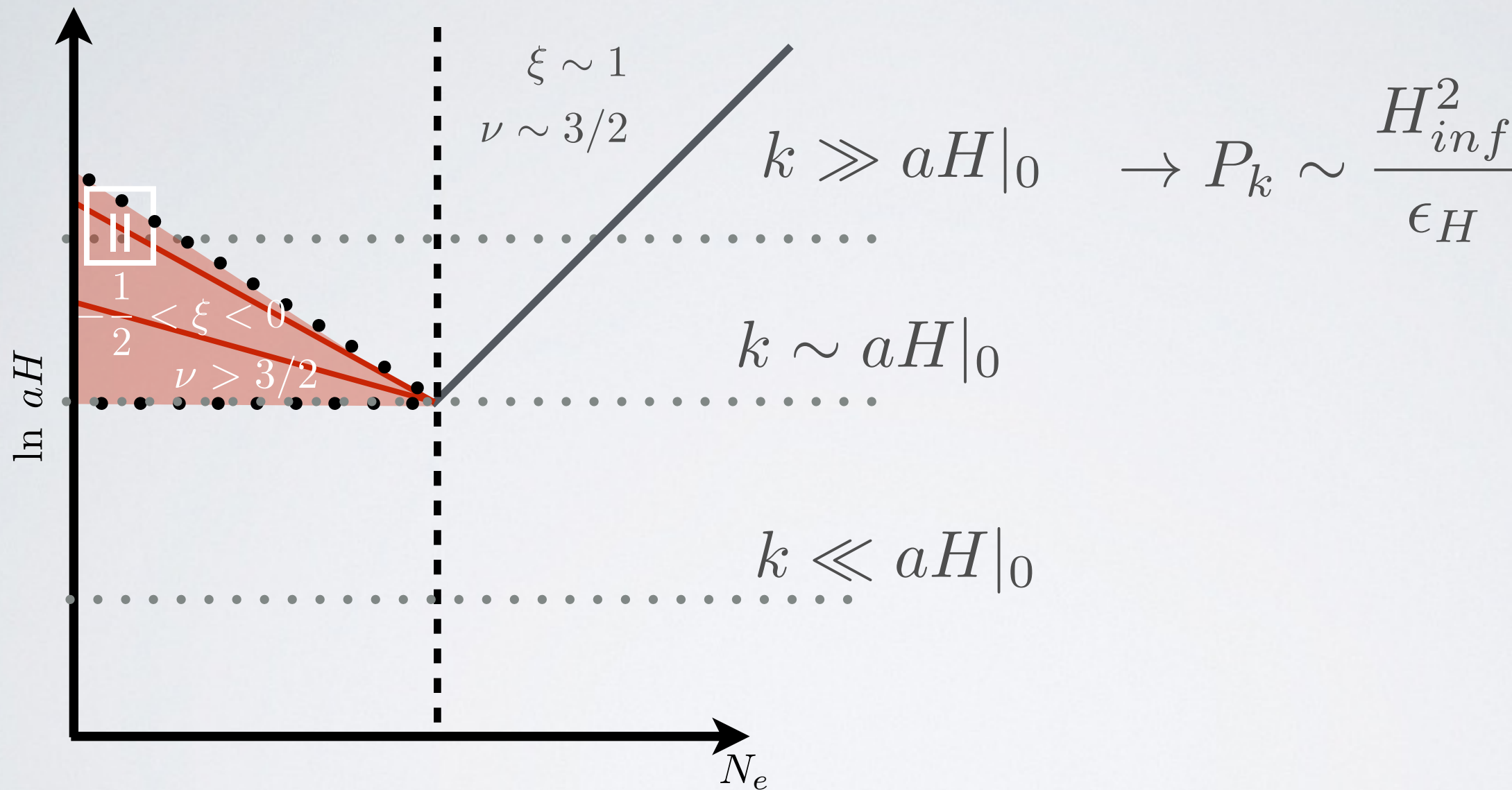


$$n_s < 1$$

# Type II backgrounds

Decelerated expansion:  $H$  decreases

Large scale spectrum from superhorizon modes

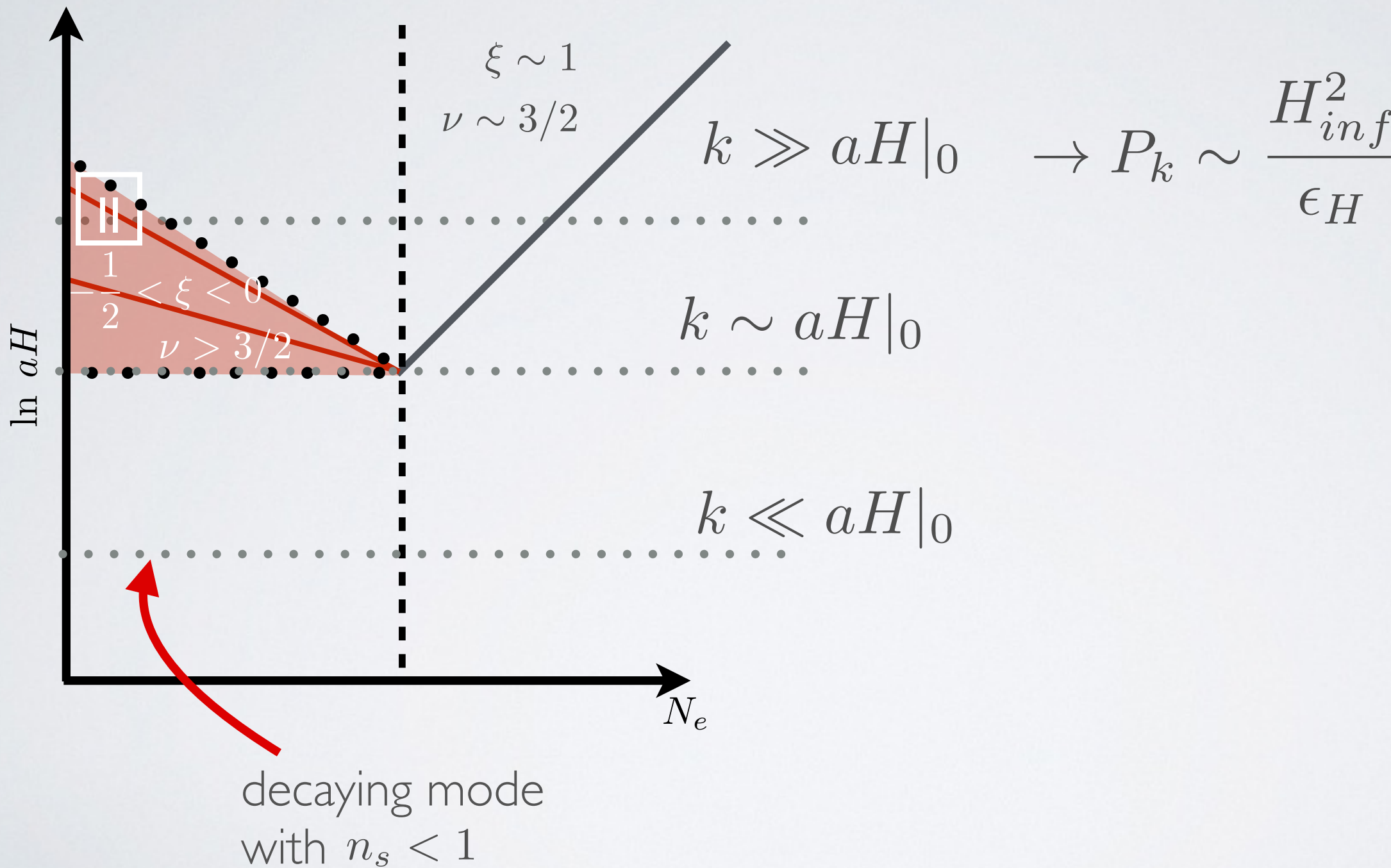


$$n_s < 1$$

# Type II backgrounds

Decelerated expansion:  $H$  decreases

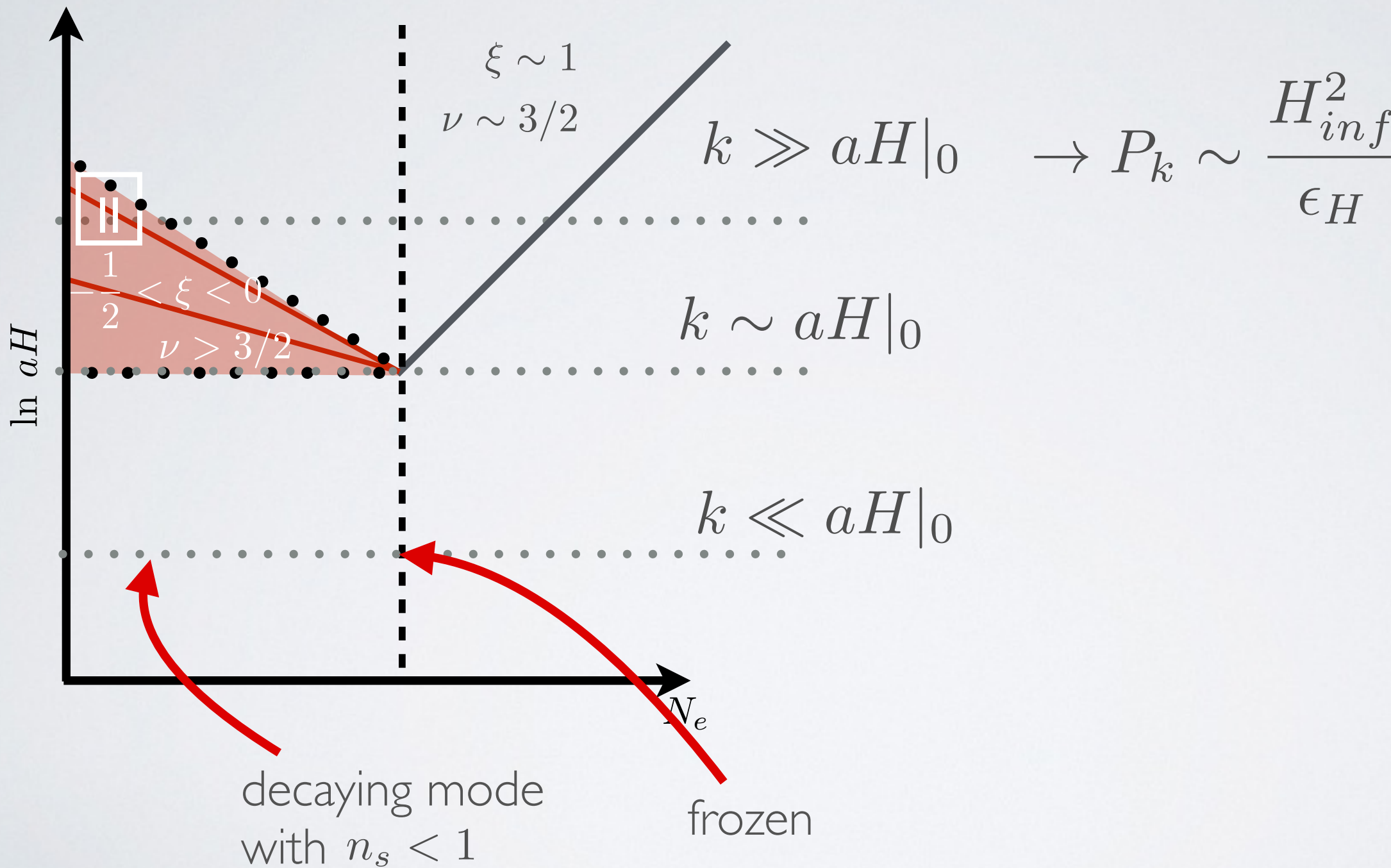
Large scale spectrum from superhorizon modes



# Type II backgrounds

Decelerated expansion:  $H$  decreases

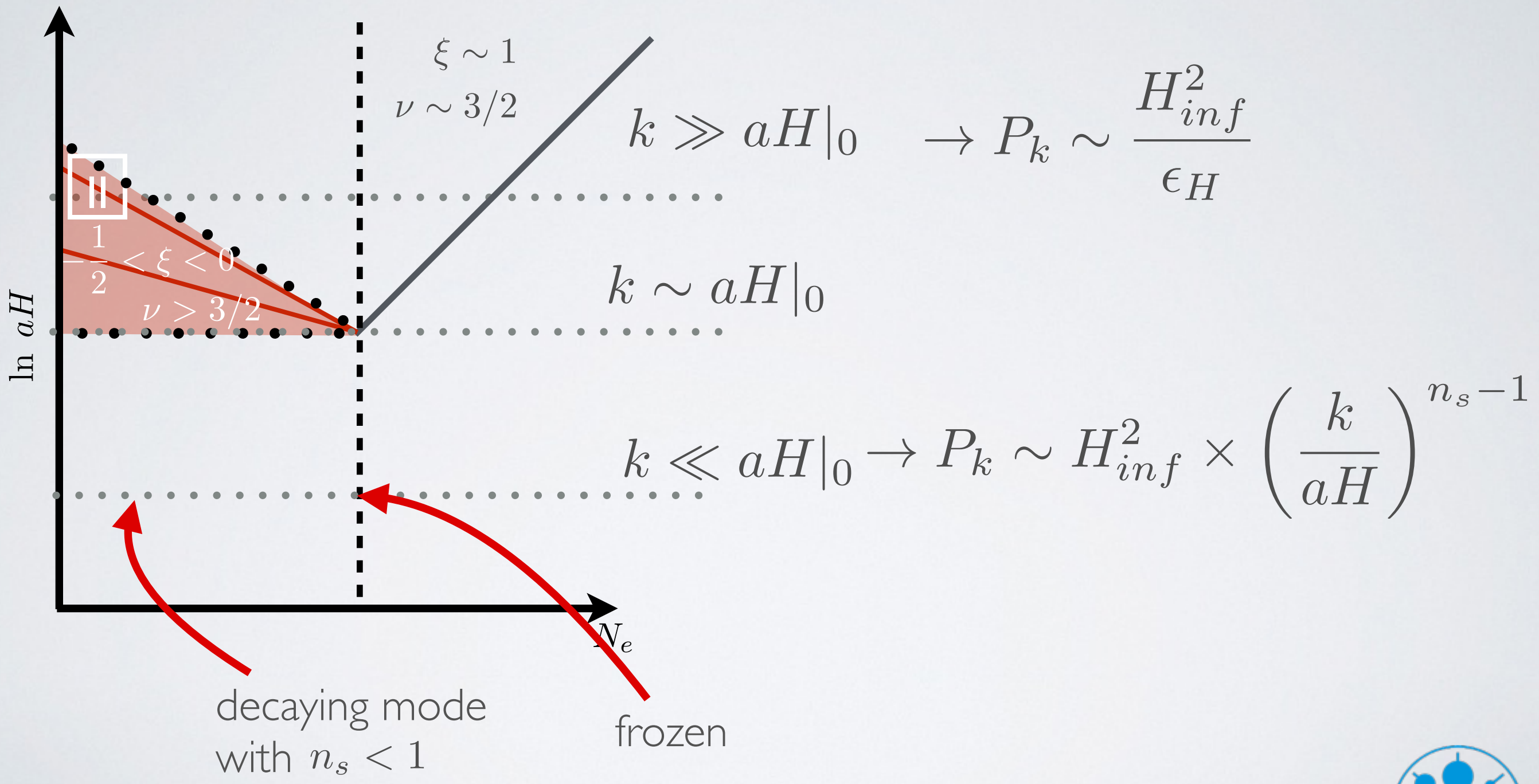
Large scale spectrum from superhorizon modes



# Type II backgrounds

Decelerated expansion:  $H$  decreases

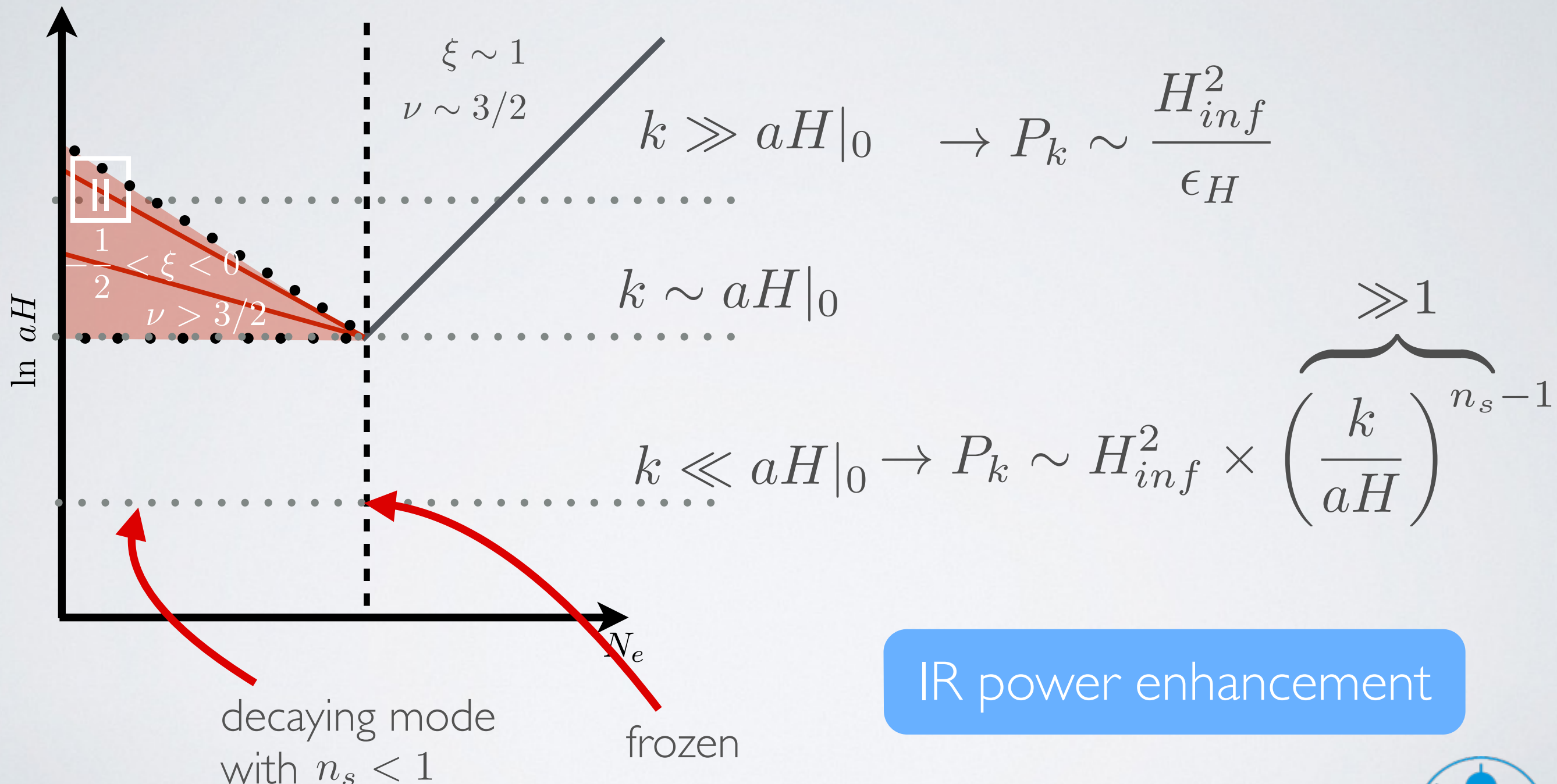
Large scale spectrum from superhorizon modes



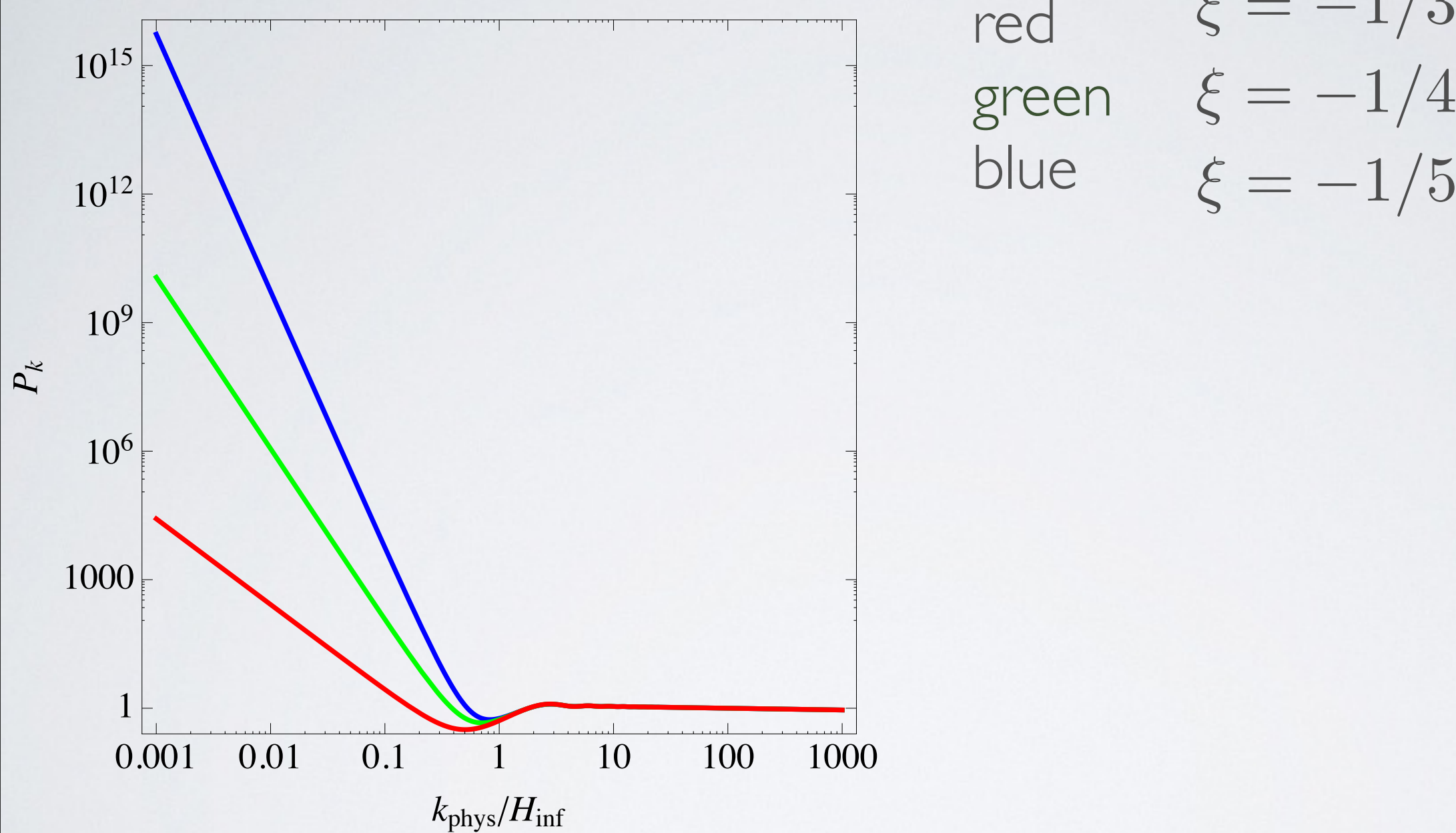
# Type II backgrounds

Decelerated expansion:  $H$  decreases

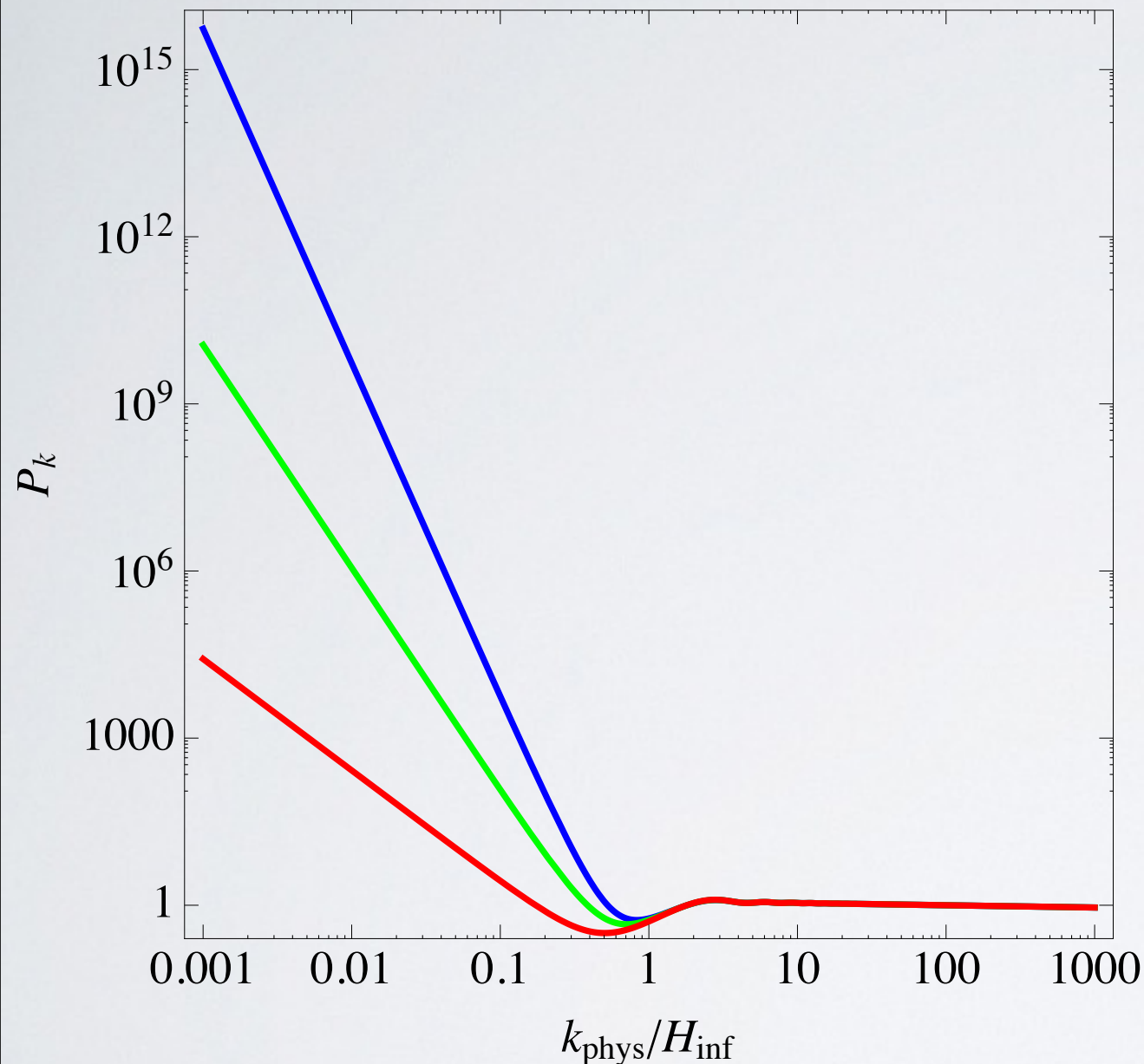
Large scale spectrum from superhorizon modes



# Type II backgrounds



# Type II backgrounds

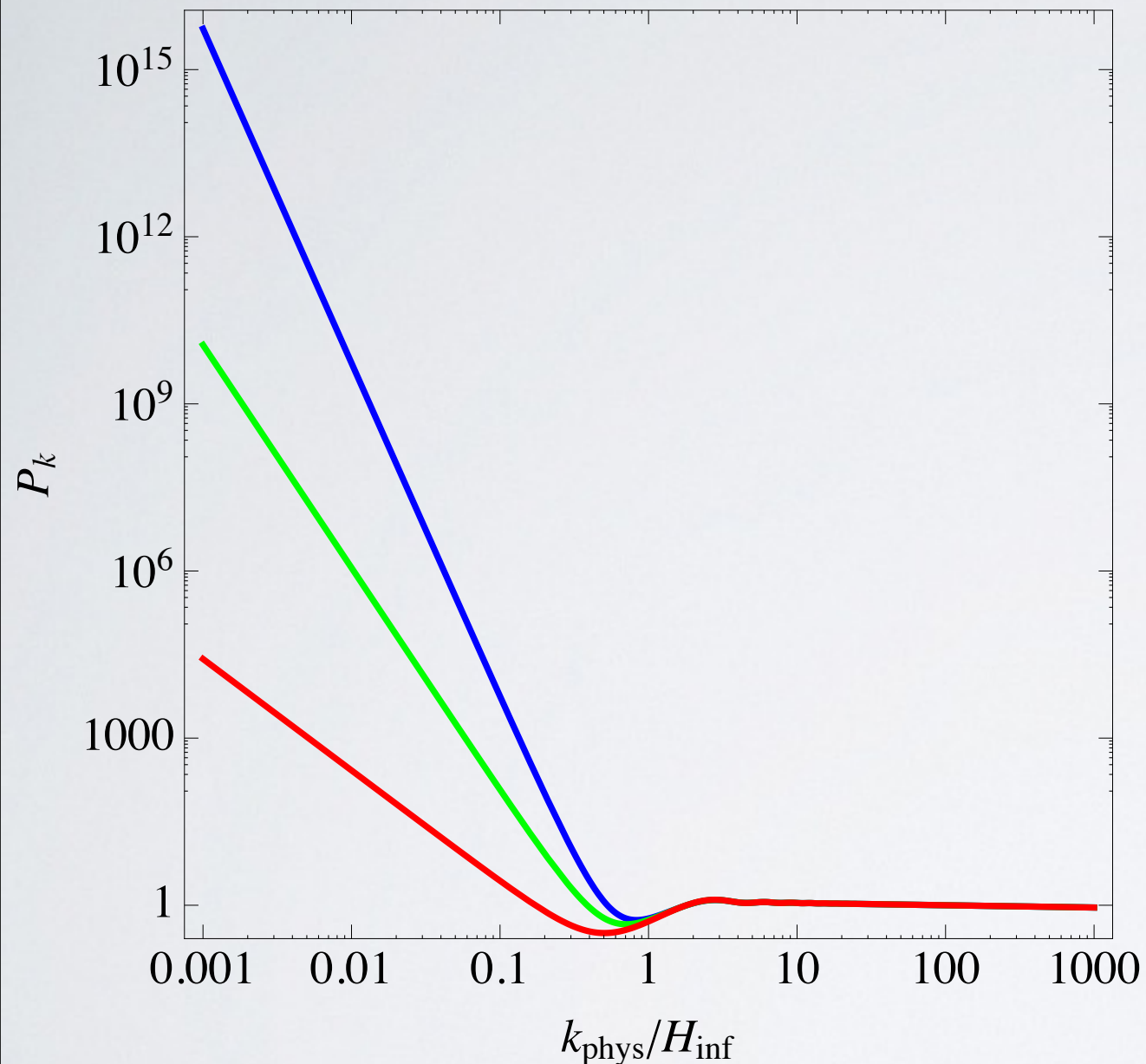


red       $\xi = -1/3$   
green     $\xi = -1/4$   
blue      $\xi = -1/5$

Same qualitative behaviour

Enhancement of power in  
the deep IR

# Type II backgrounds



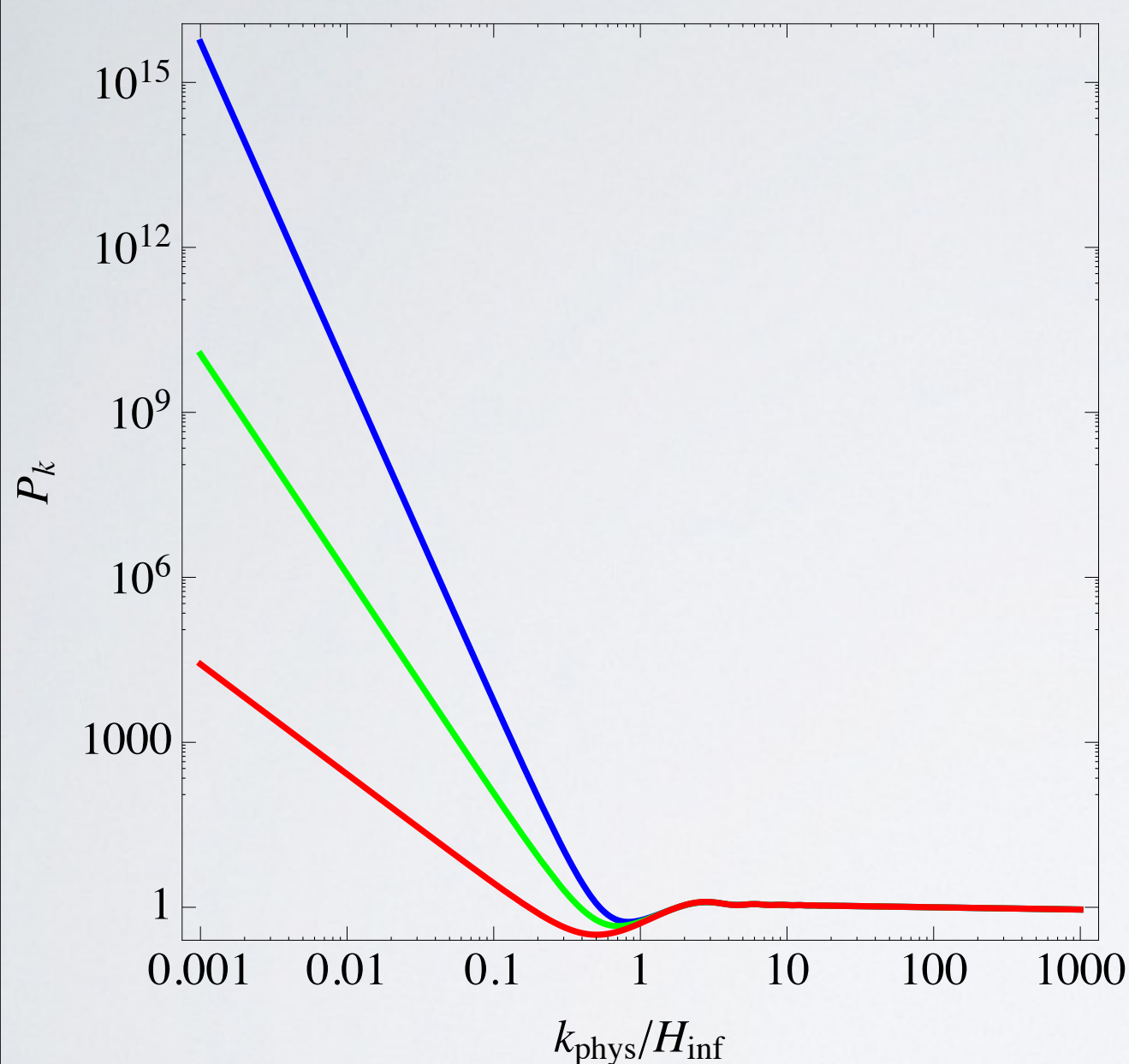
red	$\xi = -1/3$
green	$\xi = -1/4$
blue	$\xi = -1/5$

Same qualitative behaviour

Enhancement of power in  
the deep IR

Data hints at 5-10% suppression

# Type II backgrounds



red	$\xi = -1/3$
green	$\xi = -1/4$
blue	$\xi = -1/5$

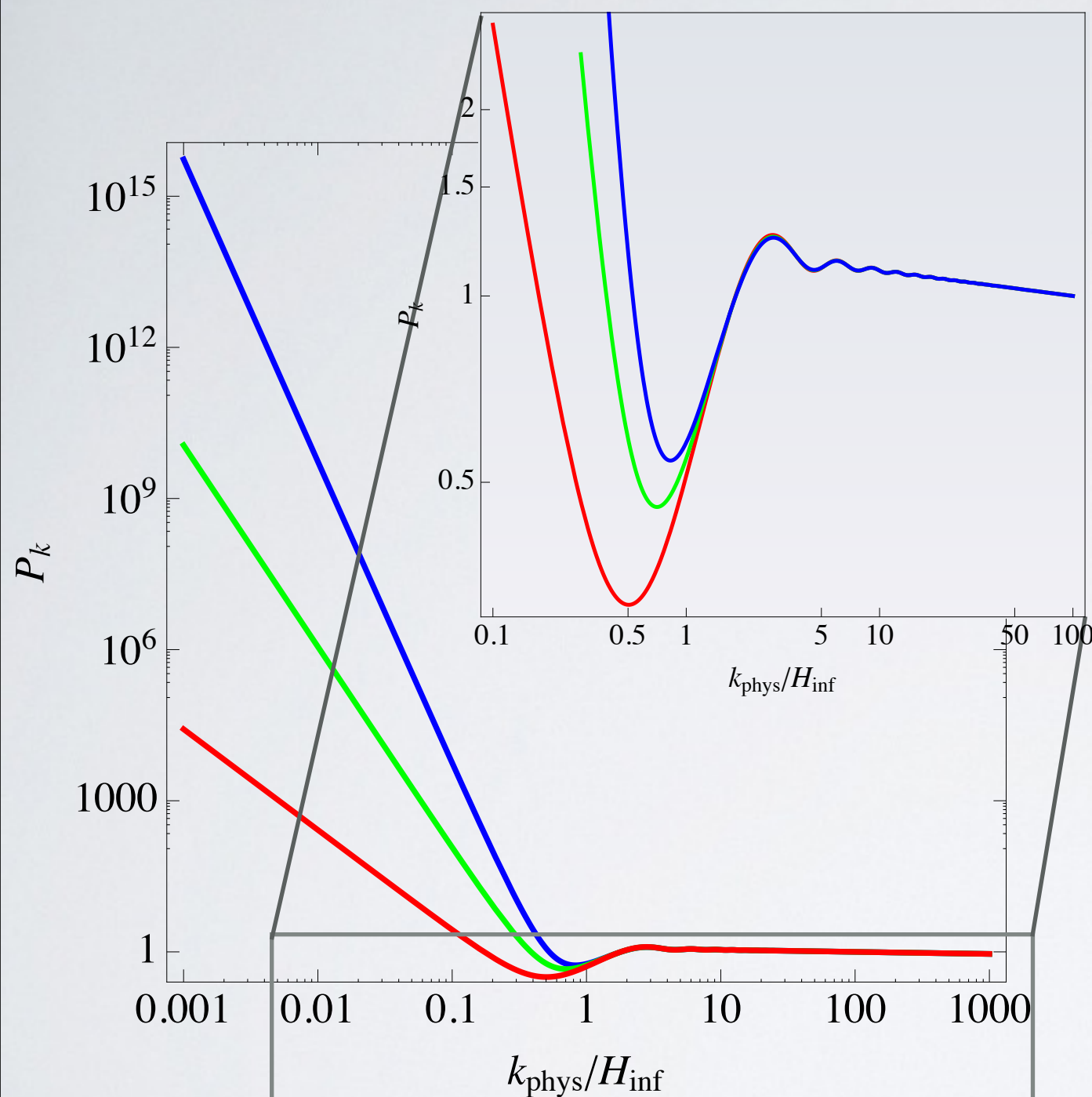
Same qualitative behaviour

Enhancement of power in  
the deep IR

Data hints at 5-10% suppression

?suppression in intermediate  
k range?

# Type II backgrounds



red       $\xi = -1/3$   
green     $\xi = -1/4$   
blue      $\xi = -1/5$

Same qualitative behaviour

Enhancement of power in  
the deep IR

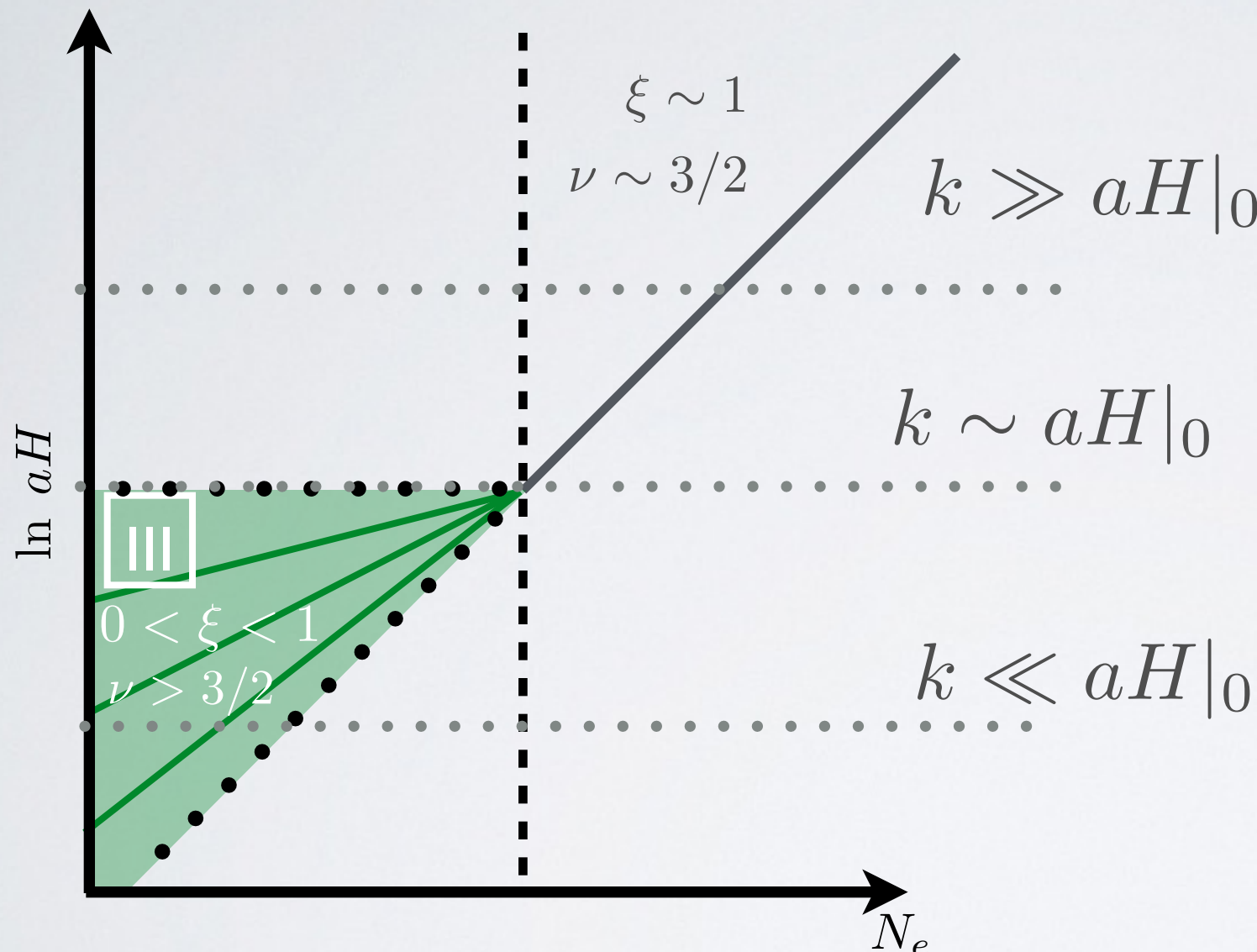
Data hints at 5-10% suppression

?suppression in intermediate  
k range?

# Type III backgrounds

Decelerated expansion:  $H$  decreases

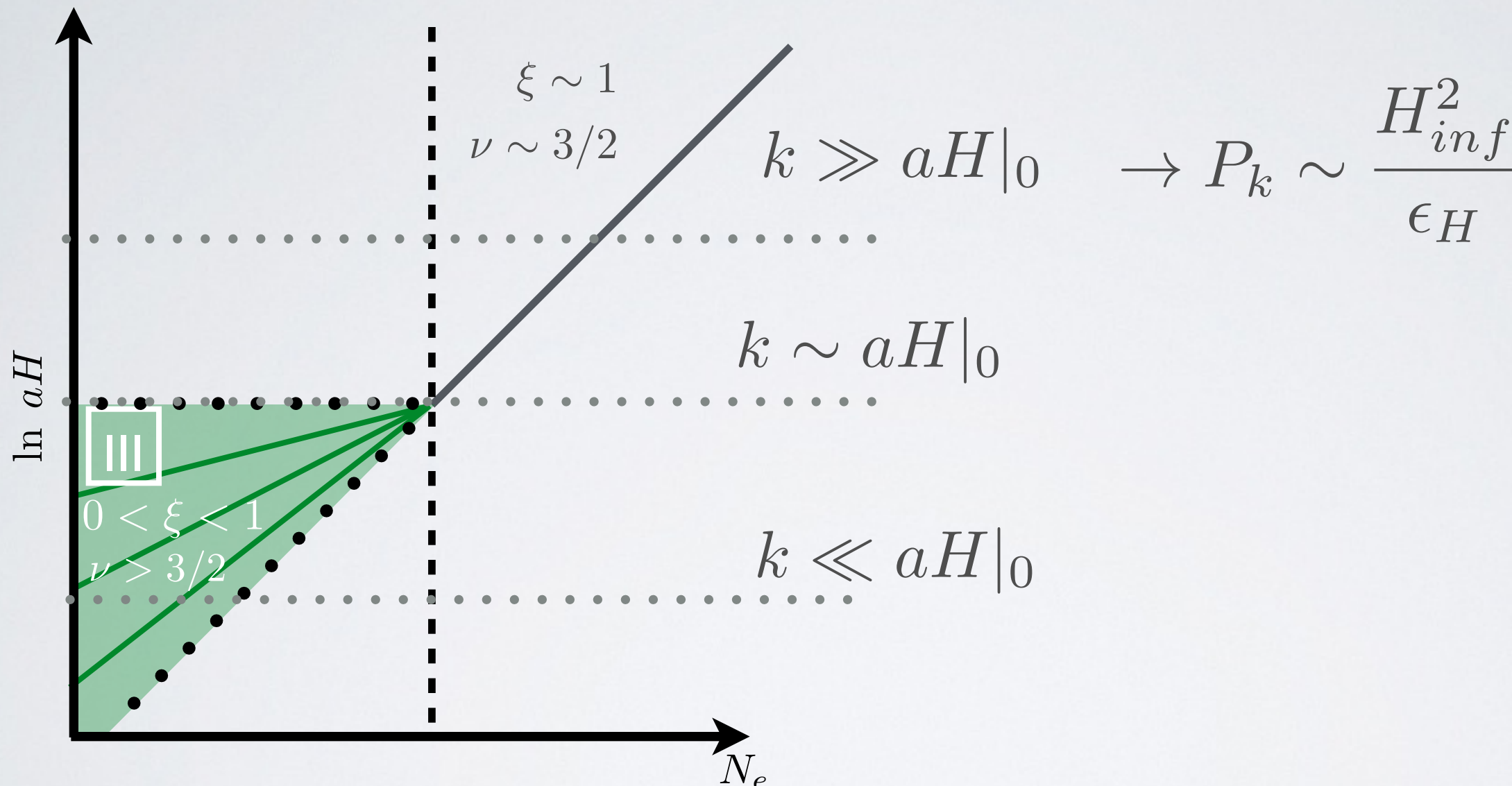
Large scale spectrum from modes that left horizon in pre-inflation



# Type III backgrounds

Decelerated expansion:  $H$  decreases

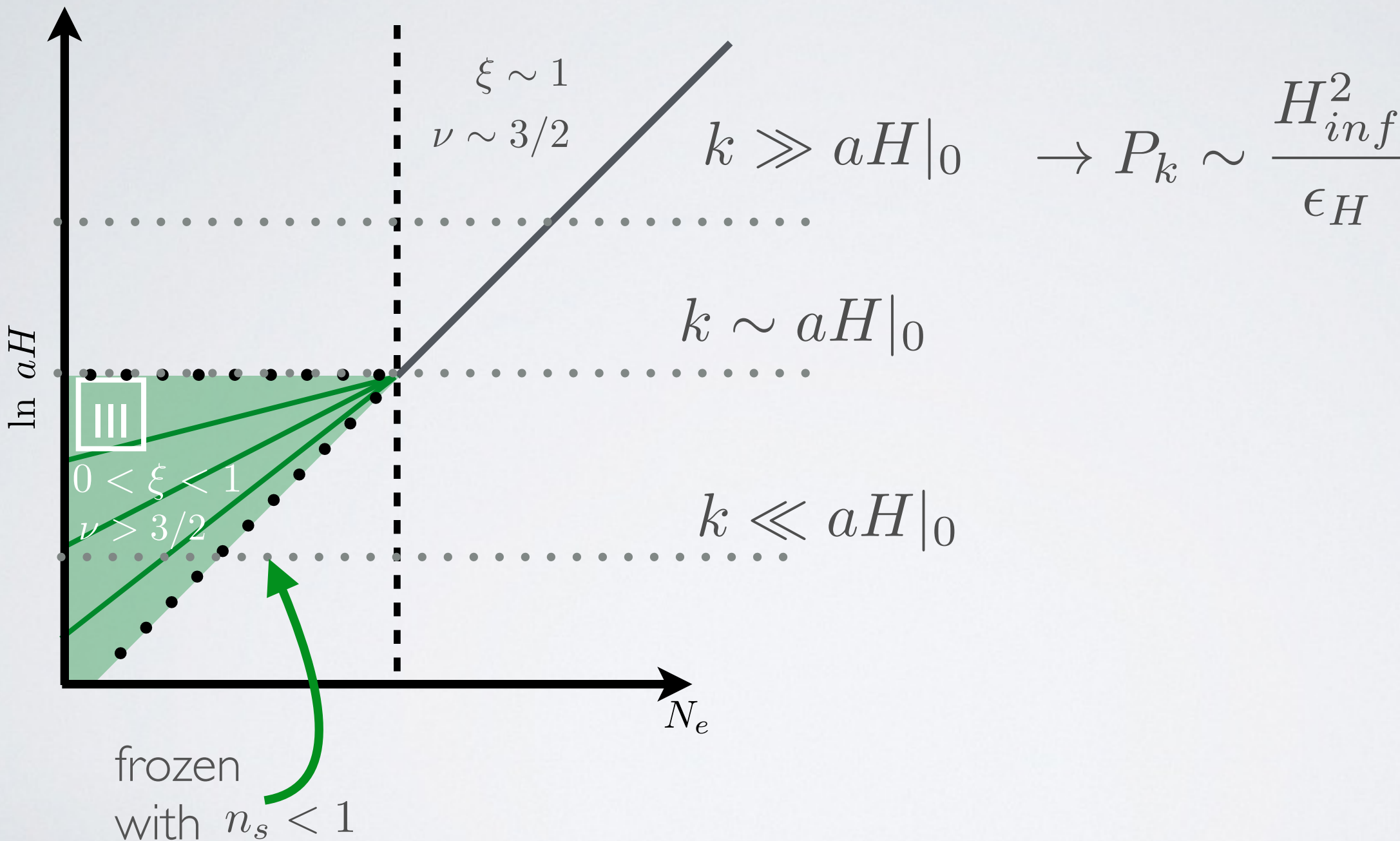
Large scale spectrum from modes that left horizon in pre-inflation



# Type III backgrounds

Decelerated expansion:  $H$  decreases

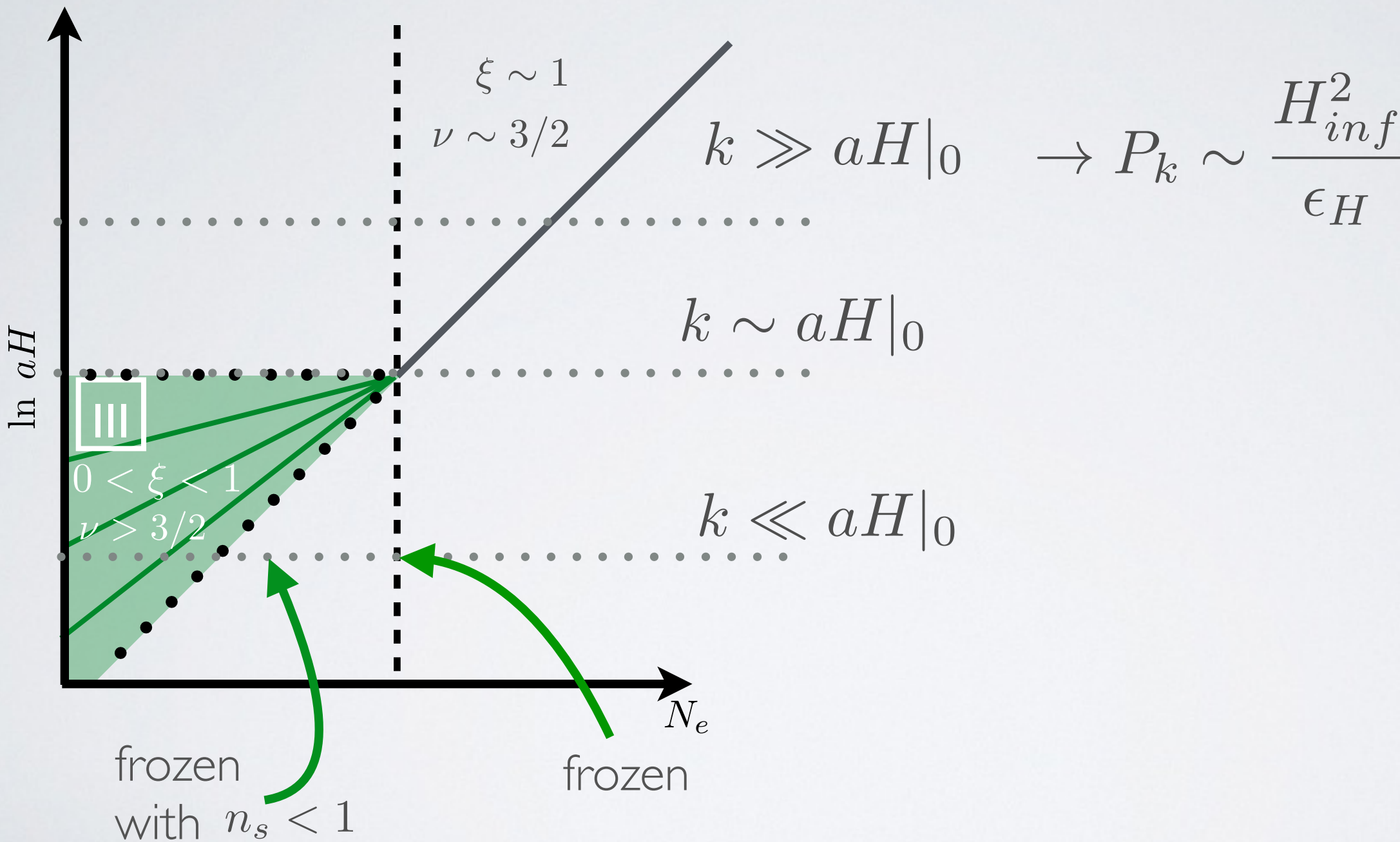
Large scale spectrum from modes that left horizon in pre-inflation



# Type III backgrounds

Decelerated expansion:  $H$  decreases

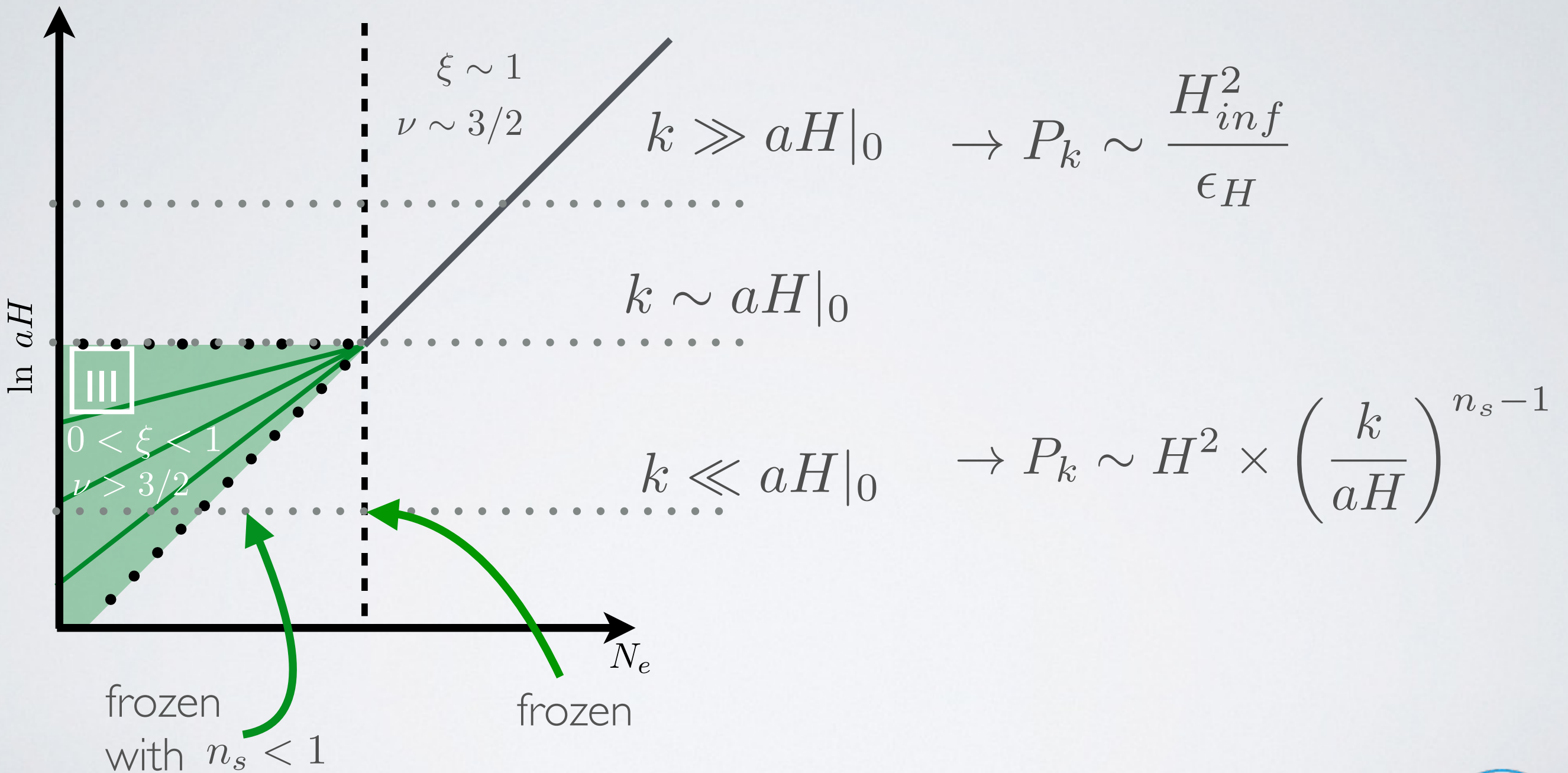
Large scale spectrum from modes that left horizon in pre-inflation



# Type III backgrounds

Decelerated expansion:  $H$  decreases

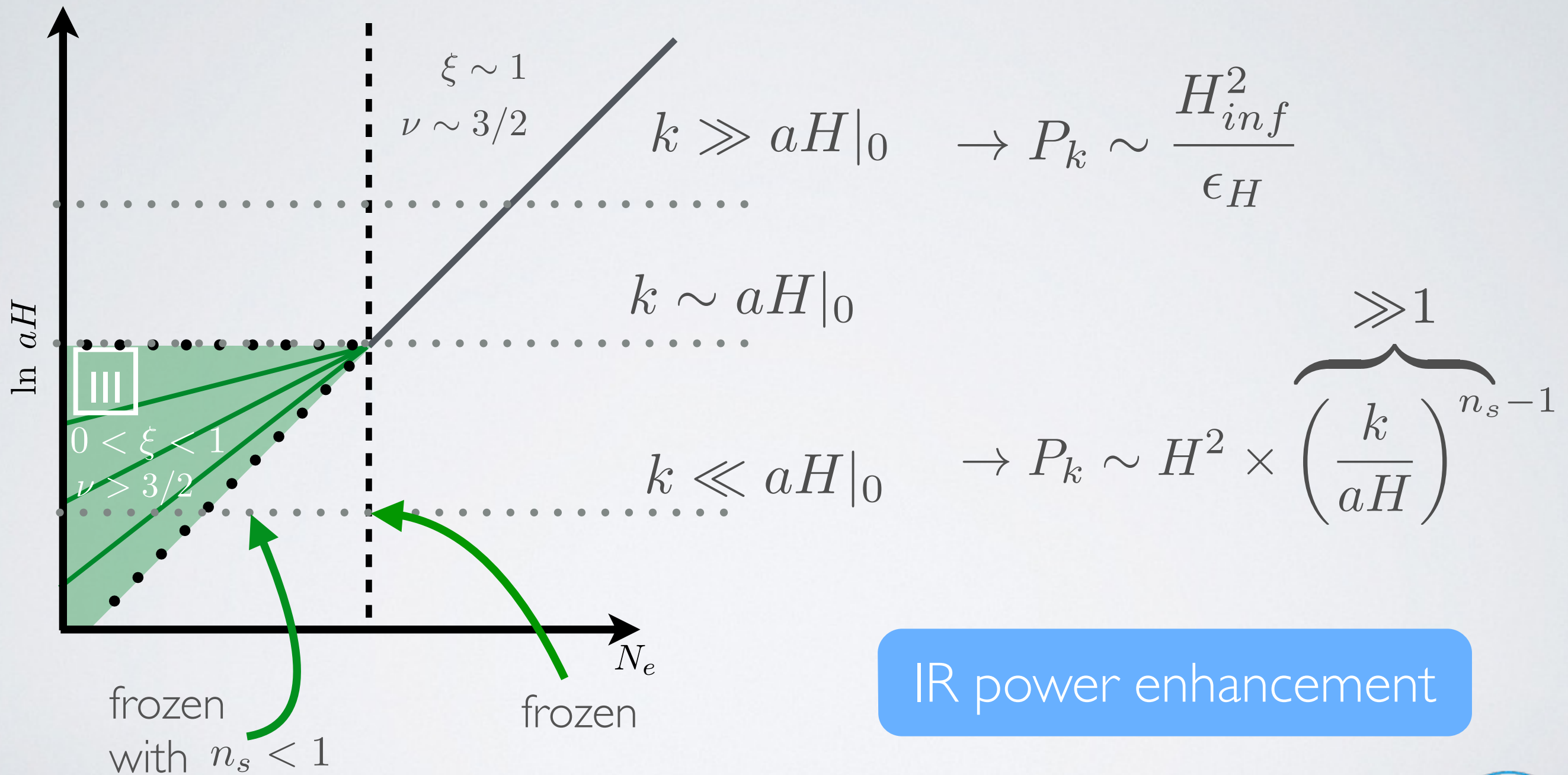
Large scale spectrum from modes that left horizon in pre-inflation



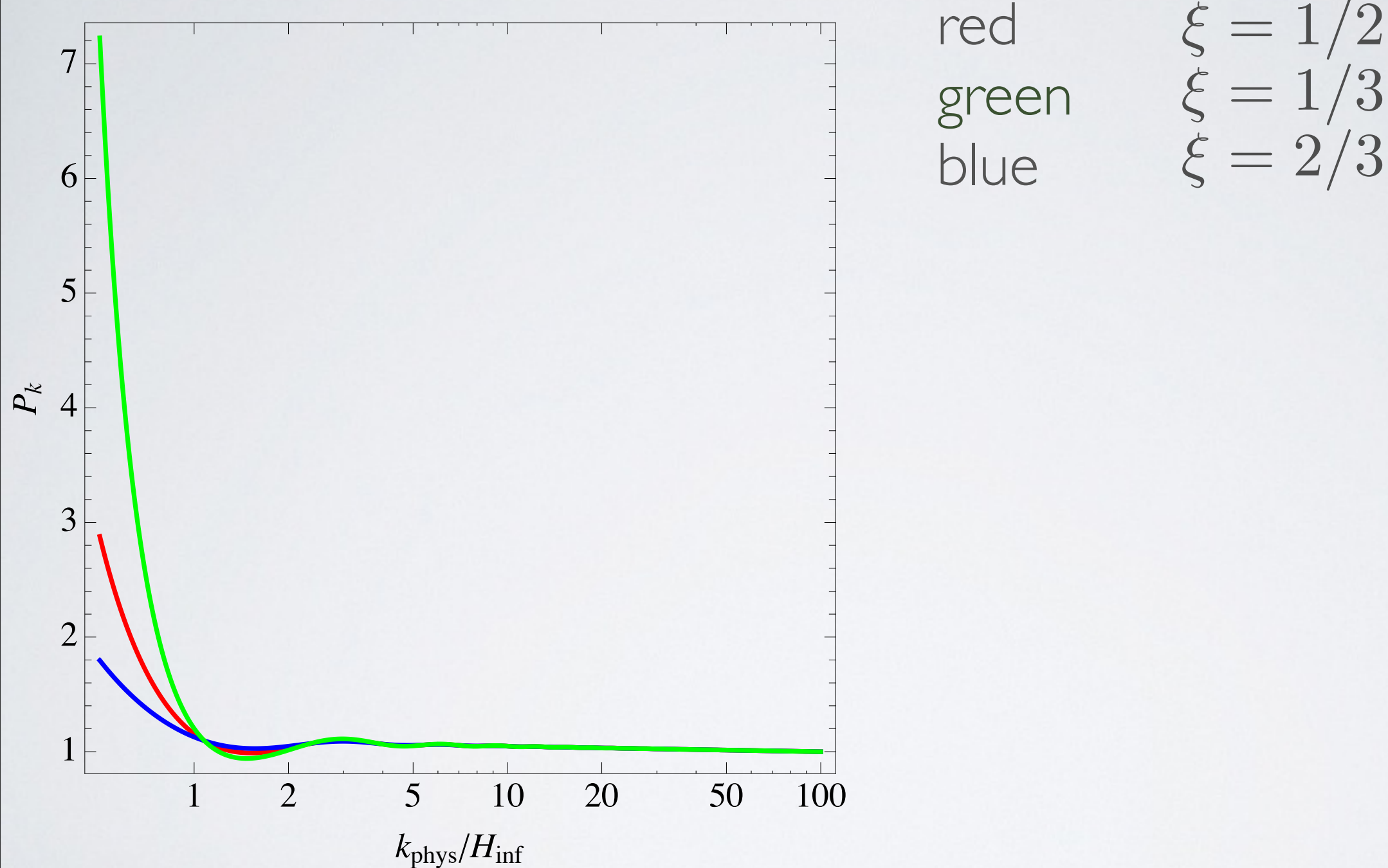
# Type III backgrounds

Decelerated expansion:  $H$  decreases

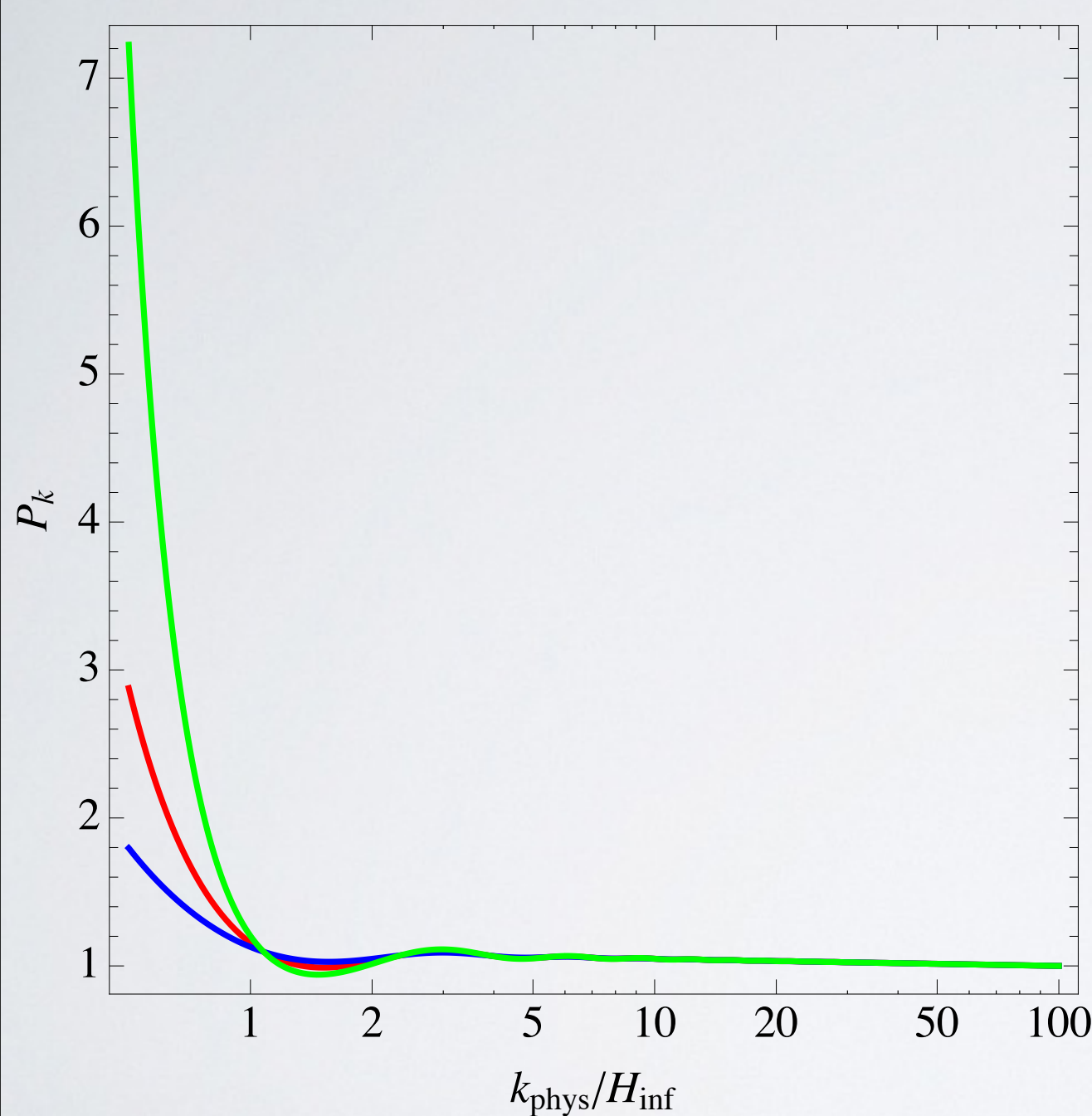
Large scale spectrum from modes that left horizon in pre-inflation



# Type III backgrounds



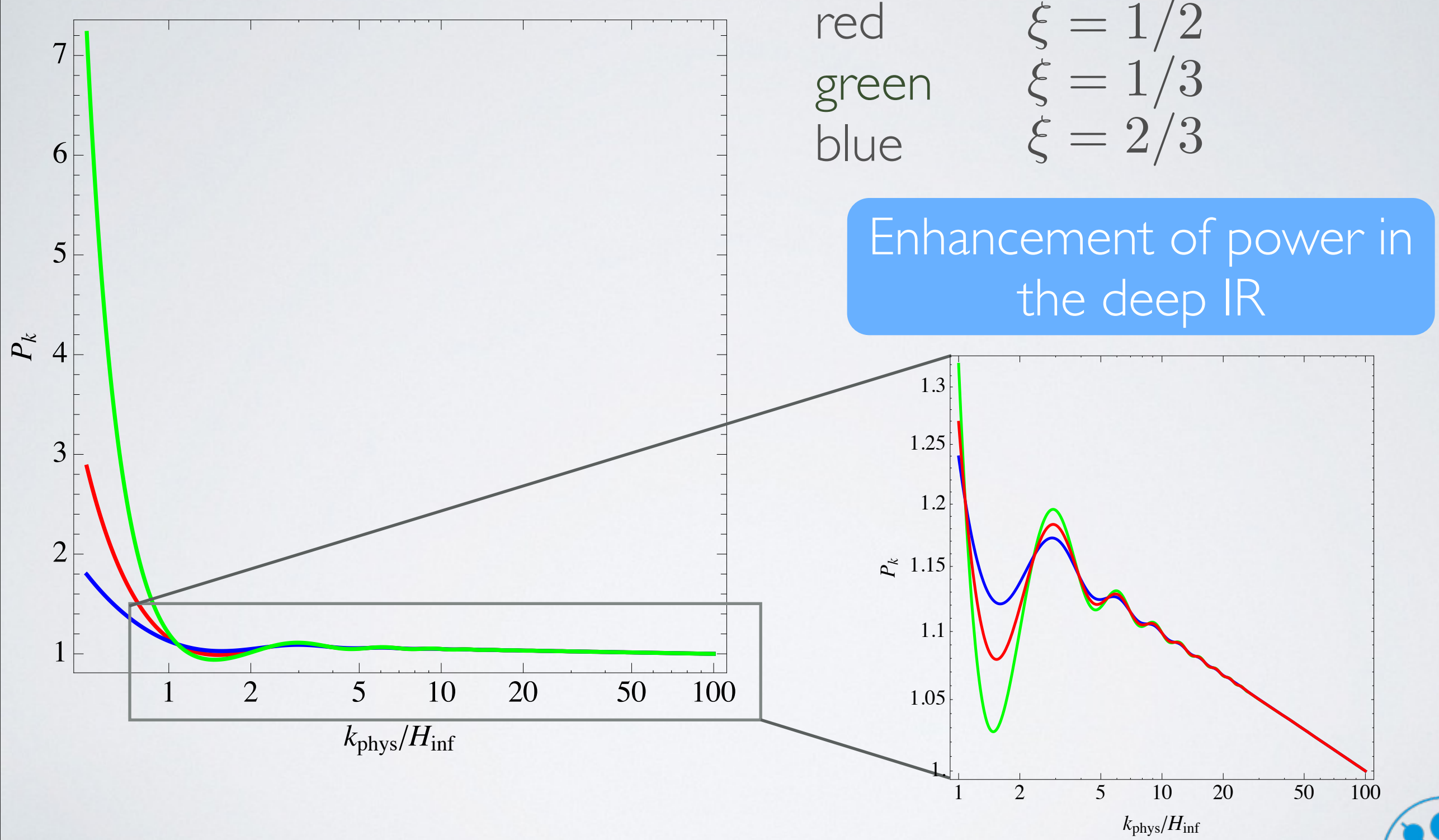
# Type III backgrounds



red       $\xi = 1/2$   
green     $\xi = 1/3$   
blue      $\xi = 2/3$

Enhancement of power in  
the deep IR

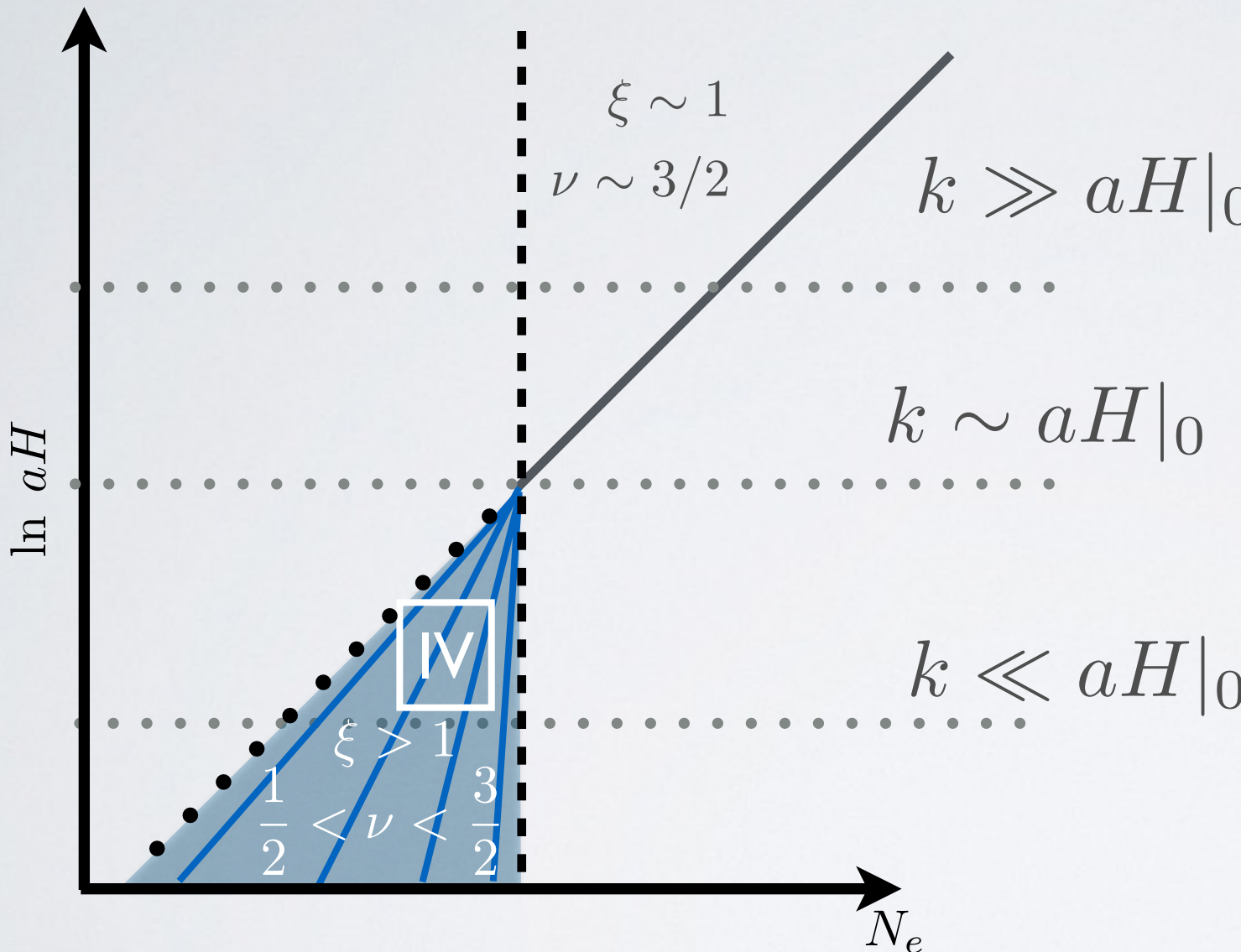
# Type III backgrounds



# Type IV backgrounds

Accelerated expansion:  $H$  is growing     $H \propto e^{(\xi-1)N_e}$

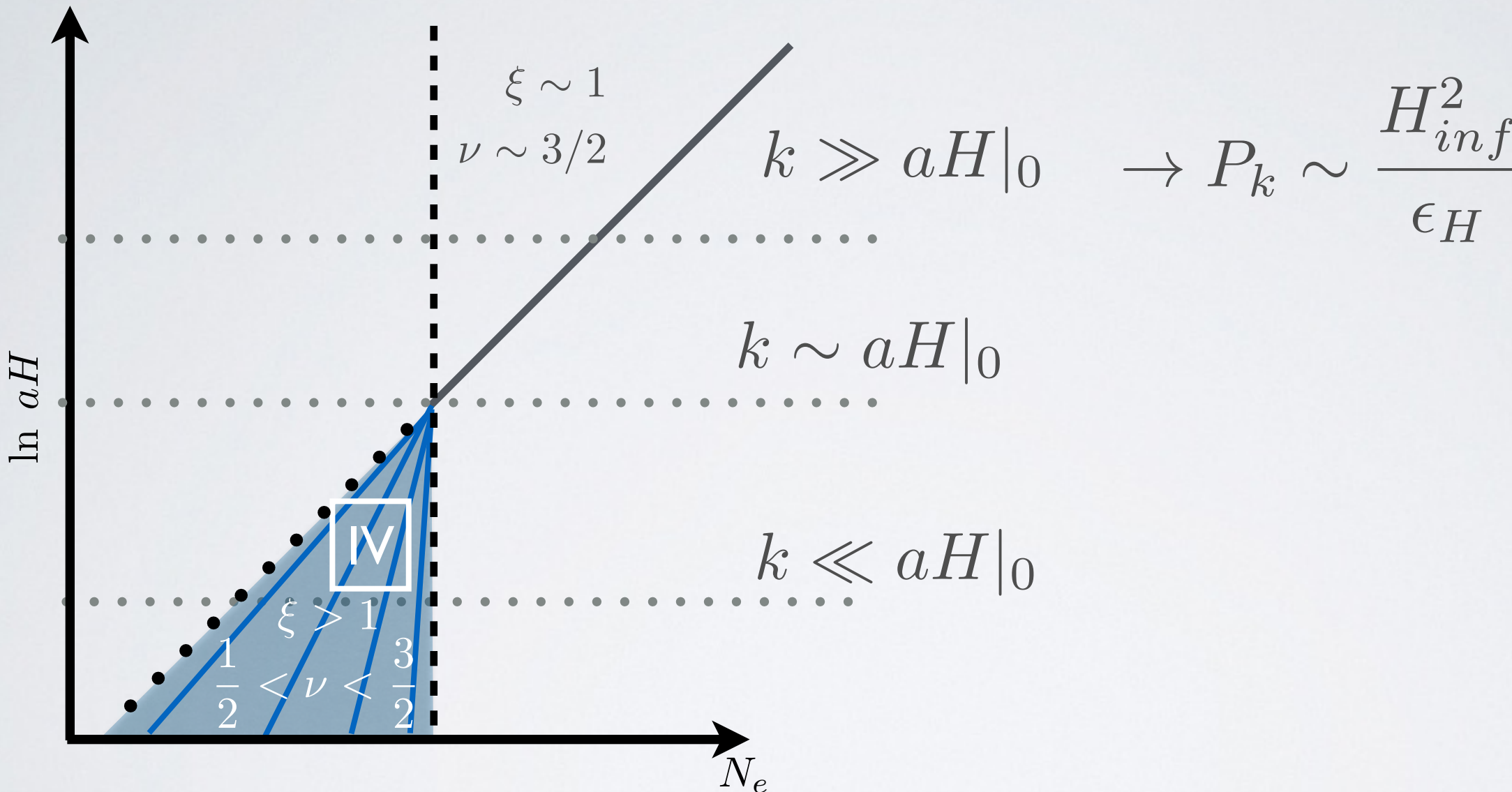
Large scale spectrum from pre-inf. subhorizon modes



# Type IV backgrounds

Accelerated expansion:  $H$  is growing     $H \propto e^{(\xi-1)N_e}$

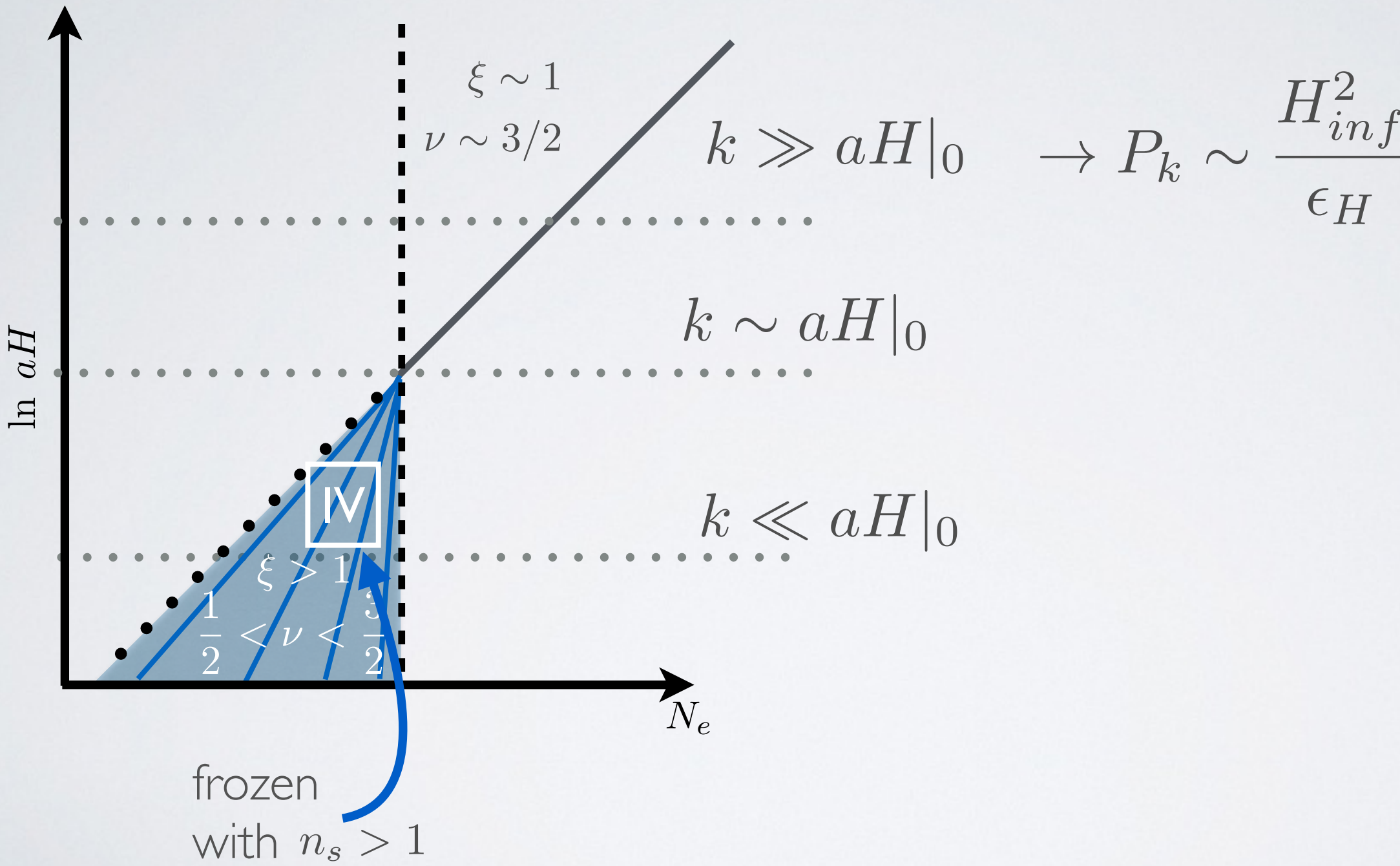
Large scale spectrum from pre-inf. subhorizon modes



# Type IV backgrounds

Accelerated expansion:  $H$  is growing     $H \propto e^{(\xi-1)N_e}$

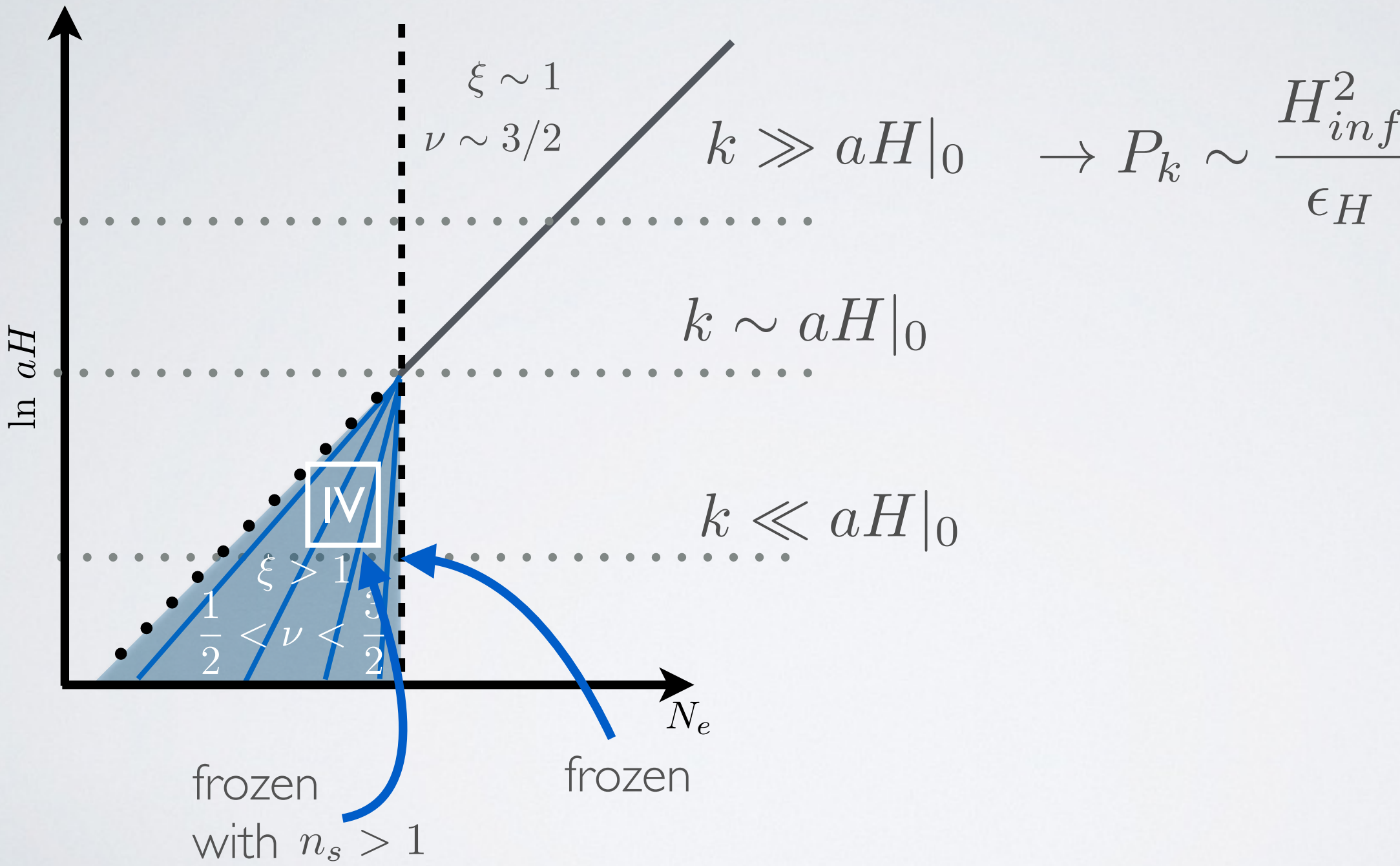
Large scale spectrum from pre-inf. subhorizon modes



# Type IV backgrounds

Accelerated expansion:  $H$  is growing     $H \propto e^{(\xi-1)N_e}$

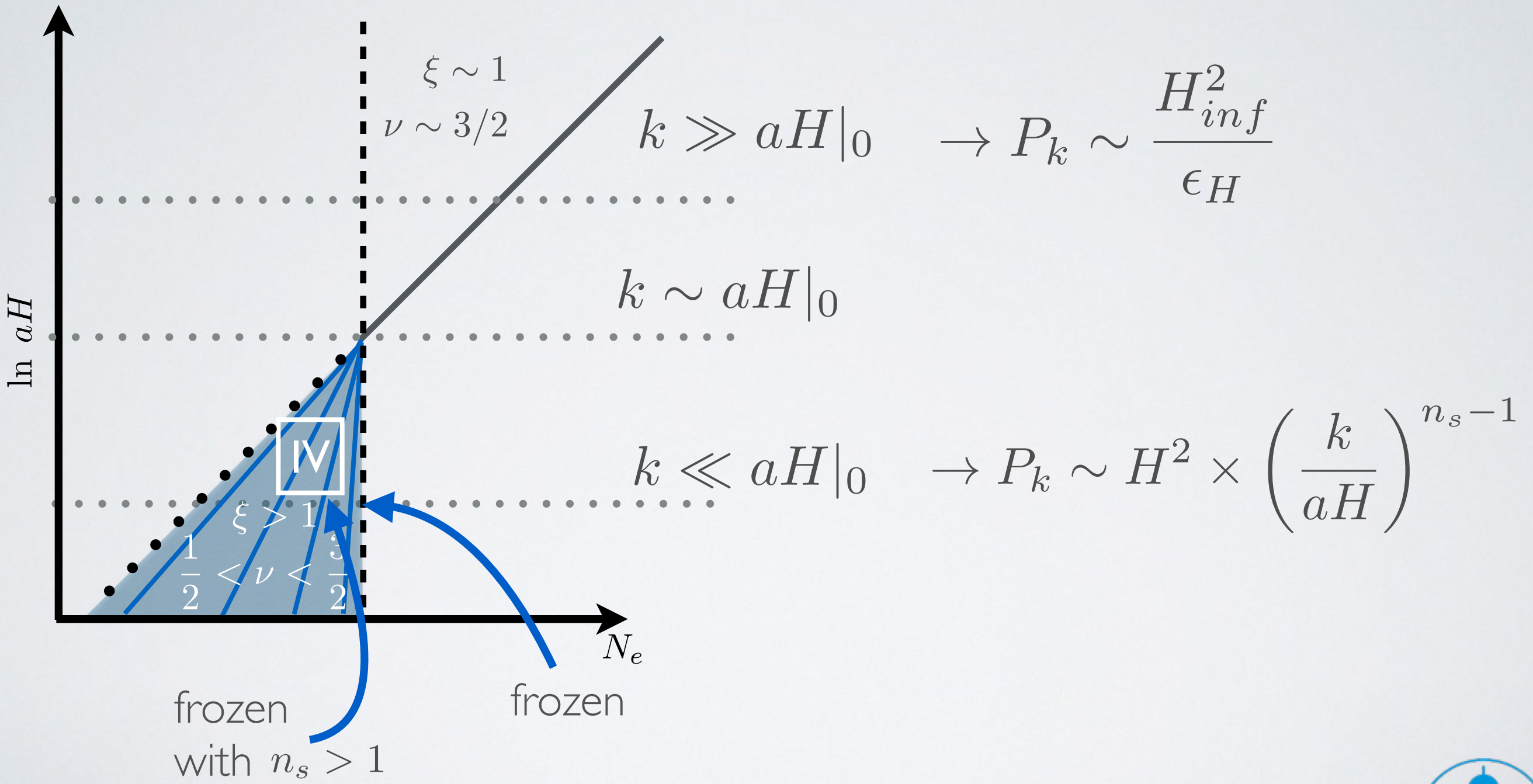
Large scale spectrum from pre-inf. subhorizon modes



# Type IV backgrounds

Accelerated expansion:  $H$  is growing     $H \propto e^{(\xi-1)N_e}$

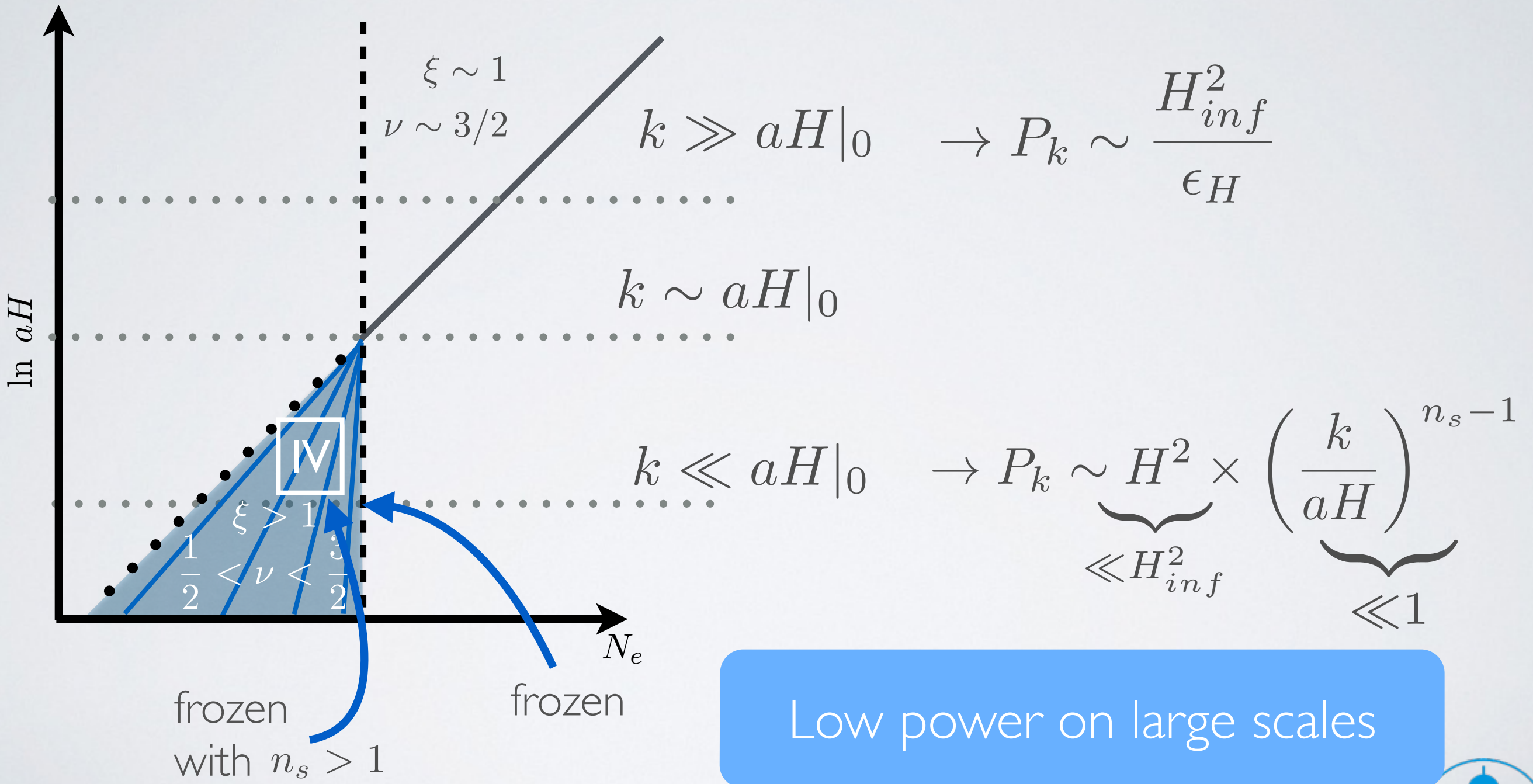
Large scale spectrum from pre-inf. subhorizon modes



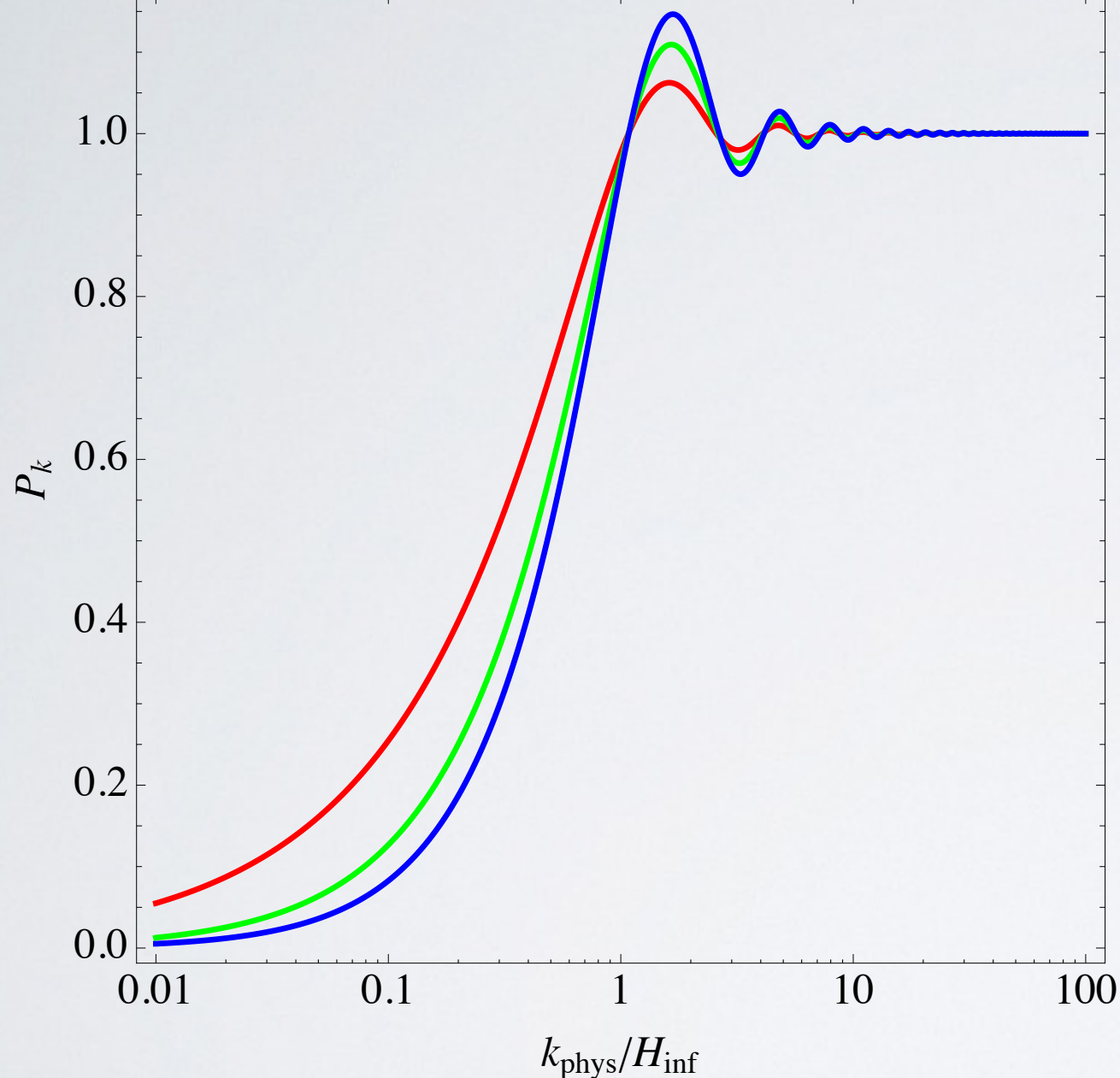
# Type IV backgrounds

Accelerated expansion:  $H$  is growing     $H \propto e^{(\xi-1)N_e}$

Large scale spectrum from pre-inf. subhorizon modes



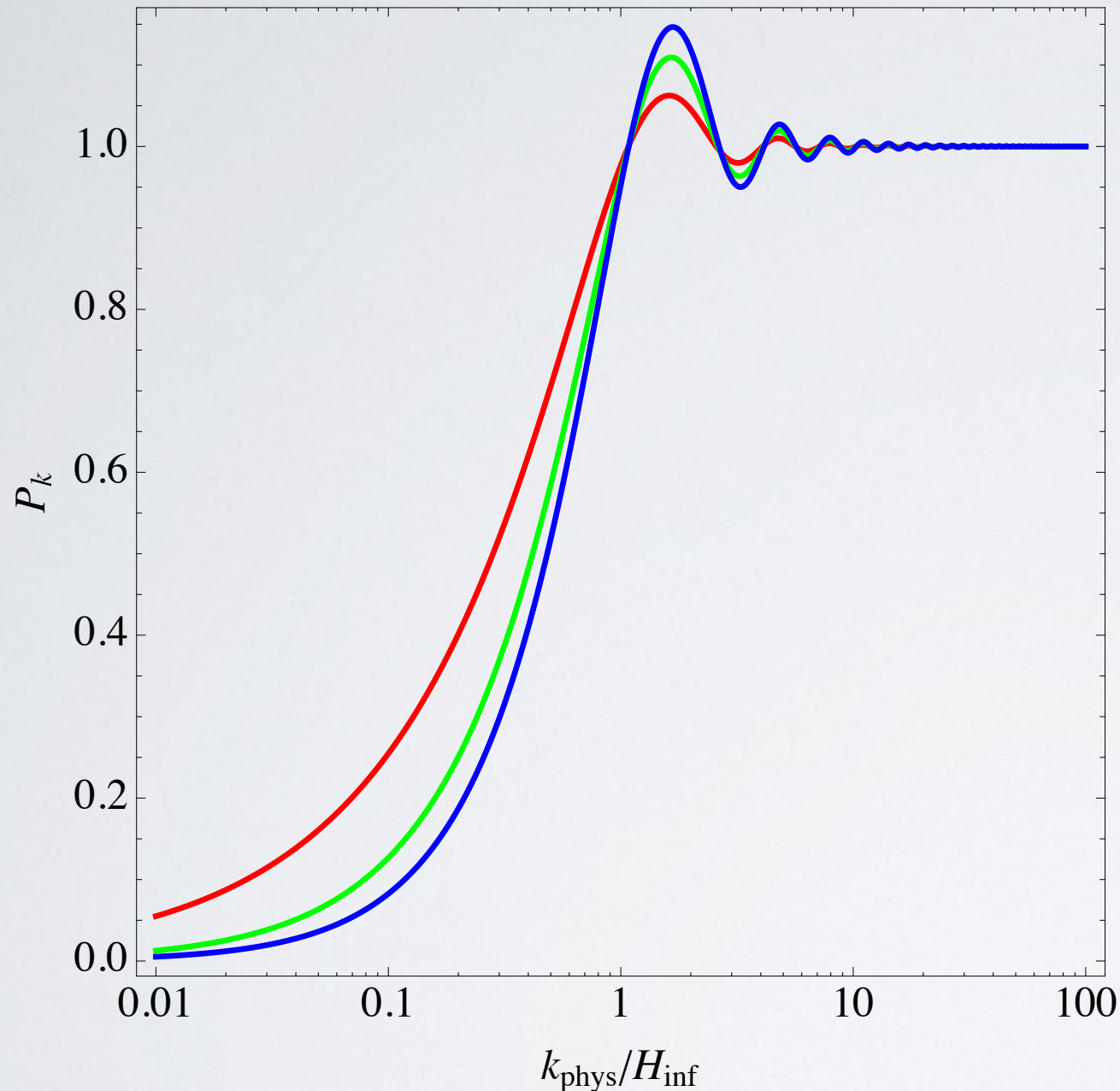
# Type IV backgrounds



red       $\xi = 3/2$   
green     $\xi = 2$   
blue      $\xi = 5/2$

background:  
super-inflation

# Type IV backgrounds

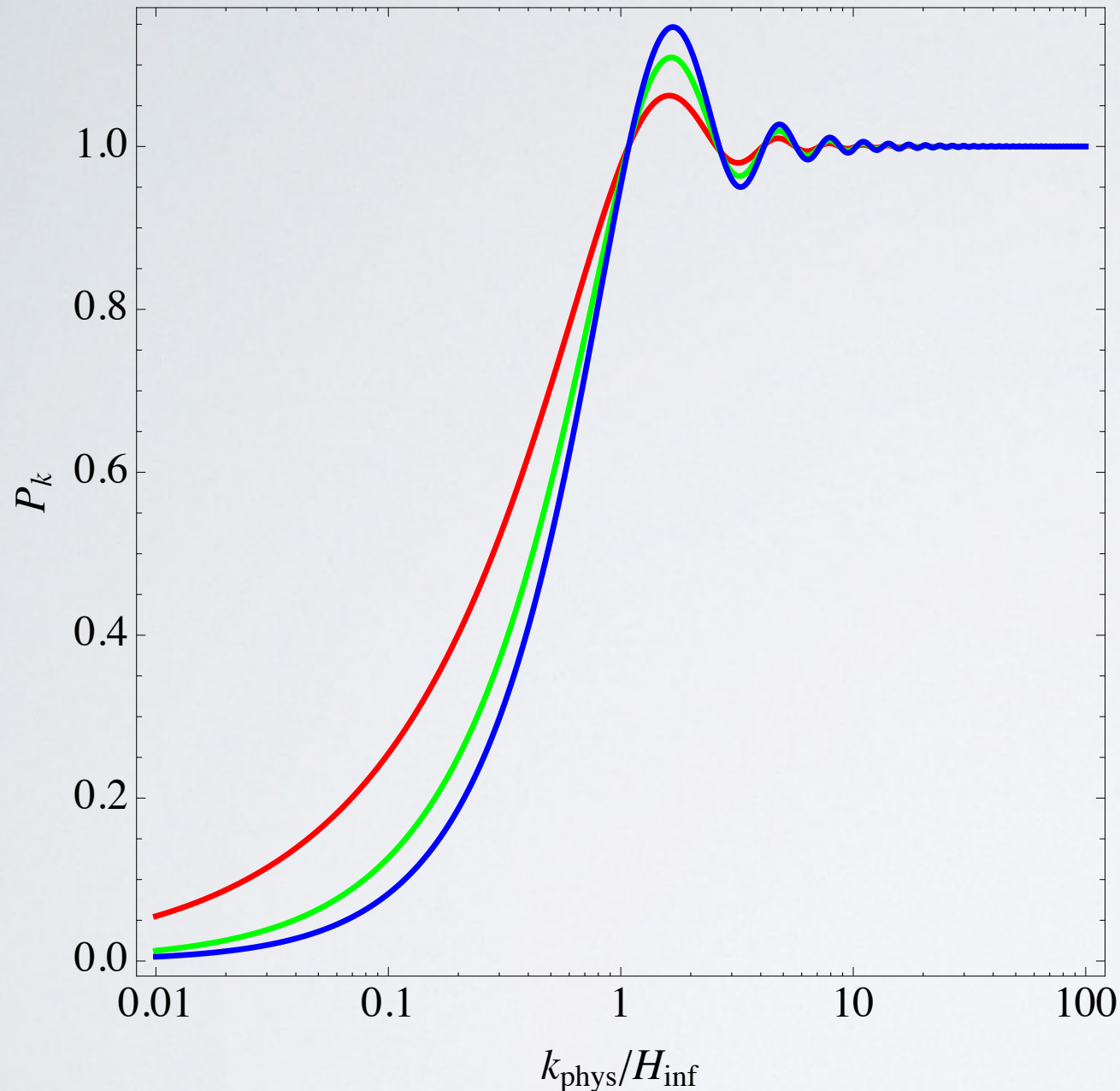


red       $\xi = 3/2$   
green     $\xi = 2$   
blue      $\xi = 5/2$

background:  
super-inflation

Different peak amplitude  
Different low-k fall-off

# Type IV backgrounds



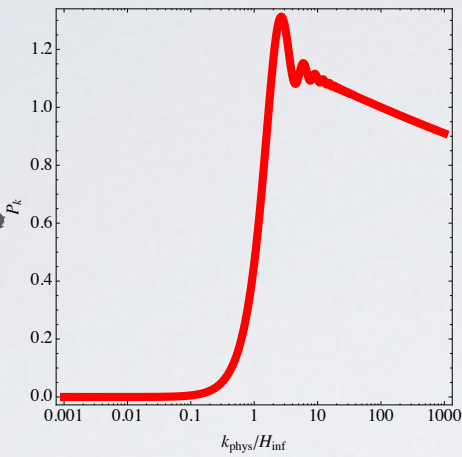
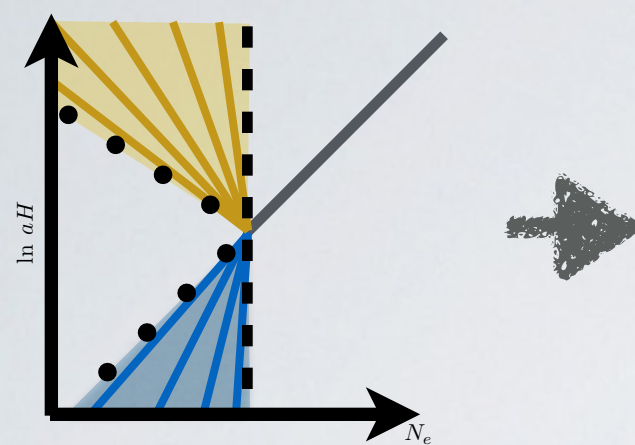
red       $\xi = 3/2$   
green     $\xi = 2$   
blue      $\xi = 5/2$

background:  
super-inflation

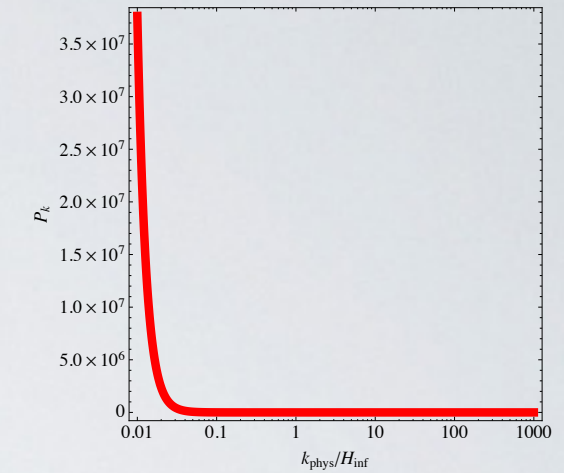
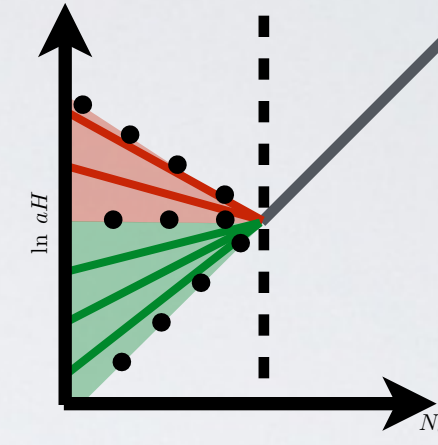
Different peak amplitude  
Different low- $k$  fall-off

Same broad features

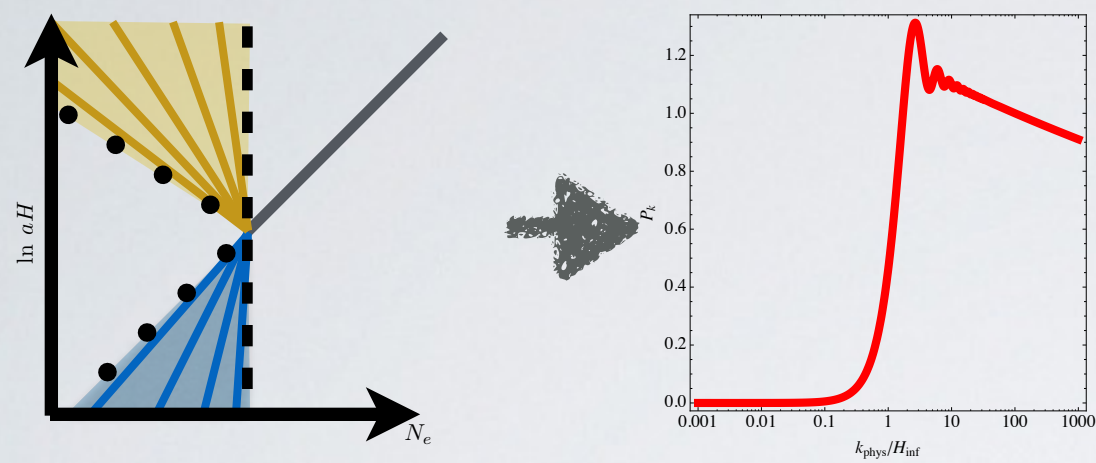
# Pre-inflation and power loss



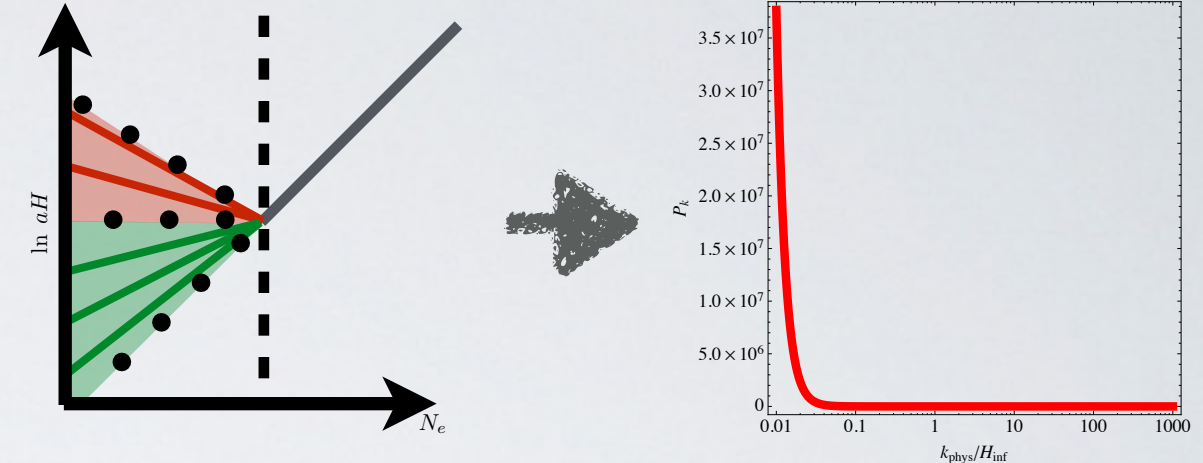
**vs.**



# Pre-inflation and power loss

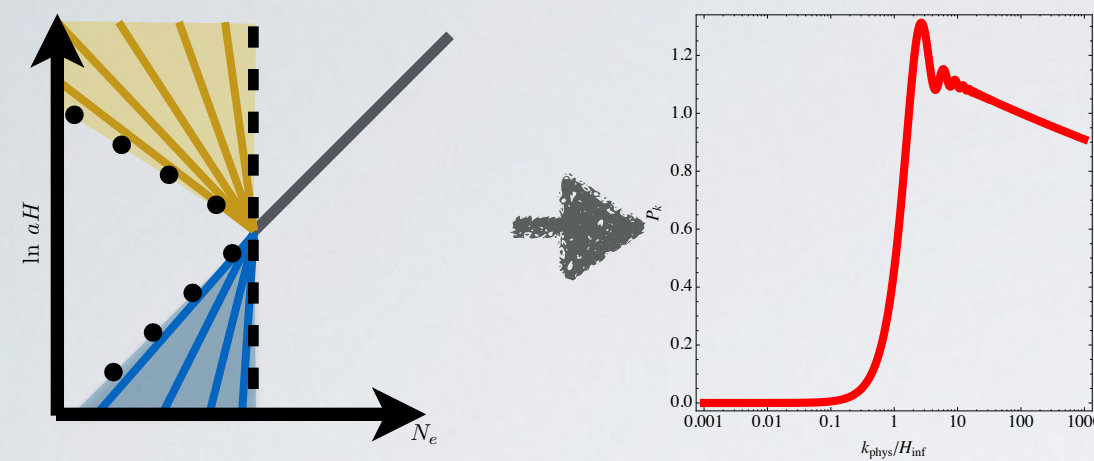


vs.

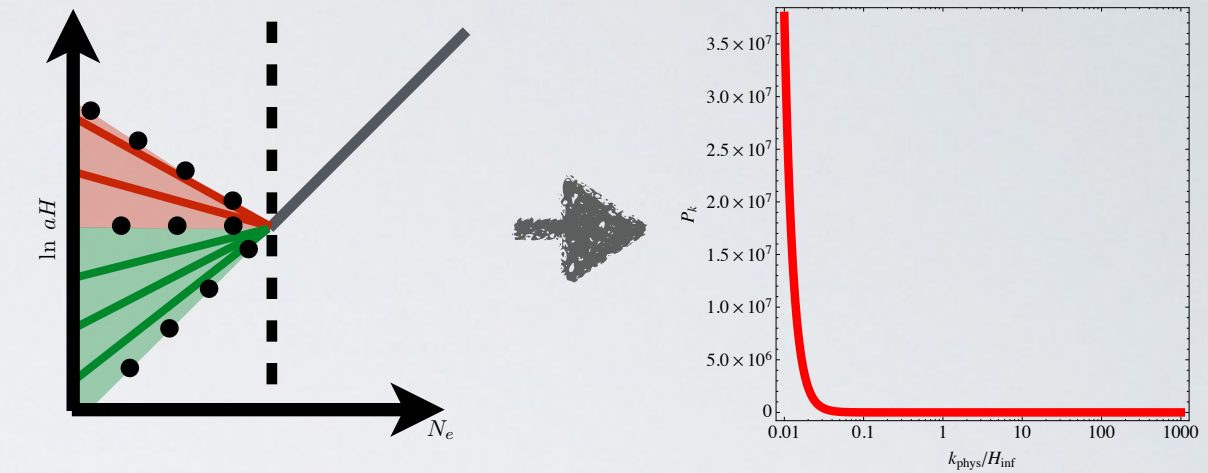


Degeneracy: 2 one-parameter families of primordial spectra

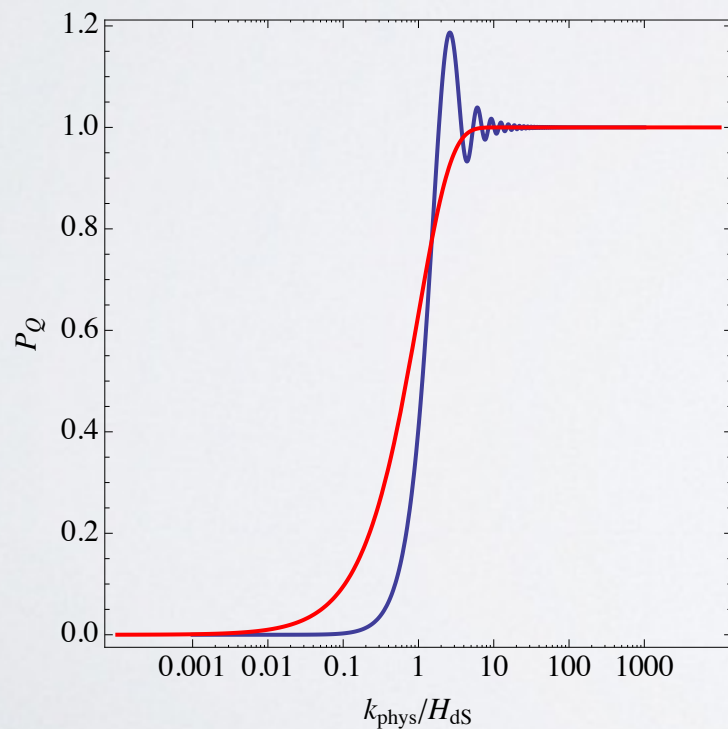
# Pre-inflation and power loss



vs.



Degeneracy: 2 one-parameter families of primordial spectra



Interesting hints:  
[1311.1599] & [1402.1418]

claim these spectra are better fits  
than simpler monotonic  
parametrization

# Summary

- ▶ Persistent hints from COBE / WMAP / PLANCK
- ▶ Short inflation modifies large scale/low-  $\ell$  power spectrum
- ▶ We might be seeing pre-inflationary phase
- ▶ Different ways to reduce power
- ▶ Degeneracy/universality in power loss
- ▶ Better understanding requires fit to the data